

Redefining the Role of p14ARF-p53 Wild Type Function in Breast Cancer

Diana Hamze Hatoum

MSc in Medical Biotechnology

Submitted in fulfilment of the requirements for the degree of Doctor of Philosophy from:

School of Life Sciences,

University of Technology Sydney

2018

Certificate of Original Authorship

I, Diana Hamze Hatoum, certify that the work in this thesis has not previously been submitted for a degree nor has it been submitted as part of requirements for a degree except as part of the collaborative doctoral degree and/or fully acknowledged within the text.

I also certify that the thesis has been written by me. Any help that I have received in my research work and the preparation of the thesis itself has been acknowledged. In addition, I certify that all information sources and literature used are indicated in the thesis.

This research is supported by the Australian Government Research Training Program.

Signature of Student:

Production Note:
Signature removed prior to publication.

Date: 28th October 2018

Acknowledgements

I would like to thank all the people who contributed to my PhD. Firstly, I would like to thank my supervisors, Dr Eileen McGowan and Dr Najah Nassif, for their patience, ongoing support and supervision. Without you, I would have never been in this position and our project would have not been successful.

Dr Eileen McGowan, I cannot thank you enough for helping me in everything experimental, academic and personal in the last five years. You have taught me to think critically about my work and you have provided me with lots of opportunities throughout these five years. I had many difficult (personal and academic) times through my PhD where I was about to give up, but you have gone out of your way to help me get through everything.

Thanks to Nikki Alling for making the MCF-7p14ARF cell lines and to Dr Daniel Yagoub for providing the original SILAC/MS proteomic dataset. Dr Matt Padula, Dr Alireza Ahadi and Prangwan Pateetin, thank you for helping with the proteomics and analysis of SILAC.

Thanks to Dr Sarah Bajan, Nahal Haddadi, David Moulder and all my PhD colleagues for their support. Thank you Diana Rose for your kindness and your scholarships and helping me achieve.

I would like to thank the examiners for reviewing this thesis. Also, thanks to the Australian Government Postgraduate Award Scholarship that I received in the first three and a half years of my PhD candidature.

Being a sole parent of two young children and a full-time PhD student, I struggled emotionally and financially so to my two children, Mariam and Ahmad, thank you so much for tolerating my stress and my time away from home during these five

years. To my family and to my children's adopted grandparents, John and Elizabeth, thank you so much for your support.

“If the facts don't fit the theory, change the facts.”

(Albert Einstein 1879 – 1955)

Table of Content

CERTIFICATE OF ORIGINAL AUTHORSHIP I

ACKNOWLEDGEMENTS II

LIST OF FIGURES IX

LIST OF TABLES X

PUBLICATIONS ARISING FROM THIS THESIS XI

ABSTRACT XVI

CHAPTER ONE 1

INTRODUCTION 1
1.1 Breast cancer 2
1.1.1 Breast cancer occurrence 2
1.1.2 Breast cancer risk factors 5
1.1.3 Breast cancer molecular subtypes 6
1.1.4 Breast cancer problems with treatments 7
1.2 P53 tumour suppressor gene 9
1.2.1 p53 – More than the Guardian of the genome 11
1.2.2 P53 – epigenomic (epigenetic) regulator 14
1.2.3 P53 and cancer metabolism 15
1.2.4 Overview of p53 in cancer 19
1.2.5 P53 and ERα 19
1.3 p14ARF – an upstream regulator of p53 21
1.3.1 p14ARF – structure and function 22
1.3.2 p14ARF in breast cancer 27
1.4 Importance of understanding p53 in breast cancer development, progression, recurrence and resistance 29
1.5 Aims of the project 29
1.6 Significance of the project 31

CHAPTER TWO 32

MATERIALS AND METHODS 32
2.1 MATERIALS 33
2.1.1 Protein lysates and Western blotting 35
2.1.2 RNA and DNA reagents 36

2.1.3 Antibodies 37
2.2 METHODS 40
2.2.1 Tissue culture 40
2.2.2 Cell counts 40
2.2.3 Cell lines and p14ARF-p53 inducible expression 41
2.2.4 Stable isotope labelling of amino acids in cell culture (SILAC) 43
2.2.5 Protein analysis 43
2.2.5.1 Western blotting 44
2.2.6 RNA extraction and Real-time quantitative polymerase chain reaction (RT-qPCR) 45
2.2.6.1 RNA extraction and quality control 45
2.2.6.2 cDNA Synthesis 46
2.2.6.3 Reference Gene Selection for Quantitative Reverse Transcription Polymerase Chain Reaction (RT-qPCR) Validation 46
2.2.7 Immunofluorescence and microscopy 47
2.2.7.1 Transformation and isolation of mito-GFP 47
2.2.7.2 Transient transfection of mito-GFP 48
2.2.7.3 Fixing and immunofluorescence staining 48
2.2.7.4 High Resolution OMX Microscopy 49
2.2.8 Data analysis 50
2.2.8.1 Cytoscape analysis 50

CHAPTER THREE 51

SNAPSHOTS OF THE P14ARF-P53 PROTEOME SWITCH IN BREAST CANCER 51

Abstract 52
3.1 Background & Summary 53
3.2 Methods 59
3.2.1 Cell Culture 59
3.2.2 SILAC labelling of breast cancer cells 59
3.2.3 Determining p14ARF-p53 proteome changes using SILAC triple labelling 63
3.2.3.1 Time course of induction of p14ARF in SILAC cell culture 63
3.2.3.2 LC-MS/MS sample preparation 63
3.2.3.3 Liquid chromatography-tandem mass spectrometry (LCMS/MS) acquisition 64
3.2.3.4 Quantification and MS/MS Data analysis 65
3.2.3.5 Protein analysis and western blotting 66
3.2.3.6 RNA extraction and Real-time quantitative polymerase chain reaction (RT-qPCR) 67
3.2.3.7 Immunofluorescence Microscopy 70
3.2.4 Statistical analysis 70
3.2.5 Data Records 71
3.2.6 Technical Validation 71
3.2.7 Usage Notes 72
3.3 Results and Discussion 73
3.3.1 SILAC/LC-MS/MS analysis of proteome changes in MCF-7 cells post p14ARF-p53 73
3.3.2 Validation of p14ARF-p53 differentially regulated proteins at the translational and transcriptional level 75
3.3.2.1 Confirmation of down-regulated protein 75
3.3.2.2 Confirmation of up-regulated proteins 76
3.3.3 Activation of p14ARF-p53 resulted in unique up- and down- regulated proteins 80

CHAPTER FOUR 85

ANNEXIN/S100A PROTEIN FAMILY REGULATION THROUGH P14ARF-P53 ACTIVATION: A ROLE IN CELL SURVIVAL AND PREDICTING TREATMENT OUTCOMES IN BREAST CANCER 85

Abstract **87**
4.1 Introduction 88
4.2 Materials and Methods 91
4.2.1 Cell lines and culture 91
4.2.2 SILAC and LC-MS/MS methodology 91
4.2.3 Data analysis 95
4.2.4 Protein analysis and western blot 95
4.2.5 Immunofluorescence microscopy 96
4.2.6 RT-qPCR analysis 96
4.3 Results 98
4.3.1 Differential regulation of the expression of the annexin/S100A protein family post p14ARF-p53-p21 activation 98
4.3.2 Annexin peptide sequences detected by SILAC LC-MS/MS map to unique N-terminal regions of annexin proteins 101
4.3.3 Differential regulation of annexin expression in MCF-7 cells post p14ARF-p53 activation occurs at the transcriptional level 104
4.3.4 Functional significance of alterations in the p53-p21-annexin network signaling 106
4.3.5 Predicted changes in cellular dynamics associated with annexin/S100A expression post p53 activation 109
4.3.6 Regulation of annexin expression is cell type specific 113
4.3.7 Association between p53 induced annexin-S100A overexpression and treatment outcomes in breast cancer: Analysis by individual protein expression status 116
4.4 Discussion 123
4.4.1 Annexins in normal physiology and breast cancer 124
4.4.2 The ER-p53-annexin expression profile and treatment outcomes 126

CHAPTER FIVE 128

P14ARF-P53-P21: REPROGRAMMING METABOLIC REGULATION AND FUNCTION IN BREAST CANCER 128
5.1 Introduction 129
5.1.1 Overview of the p14ARF-p53 pathway 129
5.1.2 Cancer metabolism and metabolic reprogramming 130
5.1.3 The role of p53 in cellular metabolism and metabolic switch 131
5.1.4 Mitochondrial Dynamics 132
5.2 Methods 136
5.2.1 Cell culture 136
5.2.2 Western blotting 136
5.2.3 RNA extraction and Real-time quantitative polymerase chain reaction (RT-qPCR) 137
5.2.3.1 RNA extraction and quality control 137
5.2.3.2 cDNA Synthesis 138
5.2.4 Immunofluorescence microscopy 139
5.2.4.1 Cell fixation and immunofluorescence staining 139
5.2.4.2 OMX microscopy and analysis 139
5.3 Results and Discussion 141
5.3.1 p14ARF upregulates TFAM but not Cytochrome C 141

5.3.2 Signalling pathways associated with metabolic reprogramming 143
5.3.2.1 Signalling pathways that are rapidly downregulated inhibit cell cycle progression, DNA repair and apoptosis 143
5.3.2.2 Signalling pathways that are upregulated are associated with metabolic functions 144
5.3.3 p53-mediated mitochondrial relocation/distribution and regulation of mitochondrial size and shape 147
5.4 Conclusion 153

CHAPTER SIX 155

CONCLUDING REMARKS AND FUTURE DIRECTIONS 155
Concluding Remarks 156
Future Directions 159
Supplementary Materials 160

REFERENCES 161

LIST OF FIGURES

FIGURE 1.1 WORLDWIDE BREAST CANCER RATES. 3
FIGURE 1.2. PREVALENCE OF DIFFERENT CANCER TYPES IN AUSTRALIA. 4
FIGURE 1.3. P53 CANONICAL AND NON-CANONICAL TUMOUR SUPPRESSOR ROLES OF P53 10
FIGURE 1.4. THE WARBURG EFFECT: CELLULAR BALANCE BETWEEN OXIDATIVE PHOSPHORYLATION AND GLYCOLYSIS. 17
FIGURE 1.5. THE INK4A/ARF LOCUS AND TRANSCRIPTION OF P14ARF. 24
FIGURE 1.6. FUNCTION OF P14ARF AND P16 INK4A IN CELL CYCLE ARREST. 26
FIGURE 1.7. P14ARF-P53-P21 PATHWAY IN MCF-7 BREAST CANCER CELLS. 28
FIGURE 2.1. P14ARF EXPRESSION USING THE LACSWITCH™ INDUCIBLE MAMMALIAN EXPRESSION SYSTEM. 42
FIGURE 3.1. P14ARF ACTIVATION OF THE P53 SIGNALLING PATHWAY. 57
FIGURE 3.2. SCHEMATIC ILLUSTRATION OF THE SILAC LC-MS/MS TRIPLE LABELLING PROTOCOL 61
FIGURE 3.3. COMPARATIVE ANALYSIS OF THE GLOBAL PROTEINS 24 AND 72 H POST P14ARF-P53 ACTIVATION. 74
FIGURE 3.4. VALIDATION OF P14ARF-P53 REGULATED PROTEINS. A. 78
FIGURE 4.1. TRIPLE LABELLING SILAC FOR PROTEOMIC ANALYSIS PRE- AND POST P14ARF-P53-P21 ACTIVATION. 93
FIGURE 4.2. LINEAR REGRESSION ANALYSIS OF ANNEXIN AND S100A PROTEIN EXPRESSION 24 H AND 72 H POST P14ARF-P53-P21 ACTIVATION. 100
FIGURE 4.3. ALIGNMENT OF ANNEXIN PEPTIDES IDENTIFIED BY MAXQUANT WITH THE ANNEXIN PROTEIN SEQUENCES. 103
FIGURE 4.4. DIFFERENTIAL REGULATION OF ANNEXIN A1, A2, A5 AND A6 EXPRESSION AT THE TRANSCRIPTIONAL LEVEL IN MCF-7 BREAST CANCER CELLS. 105
FIGURE 4.5. SCHEMATIC REPRESENTATION OF THE P53/P21/ANNEXIN/S100A INTERACTOME. 108
FIGURE 4.6. DIFFERENTIAL REGULATION OF ANNEXIN A1, A2, A5 BY P14ARF-P53 OCCURS IN MCF-7 BUT NOT IN U2OS OSTEOSARCOMA CELLS. 114
FIGURE 4.7. THE EFFECT OF P53 AND INDIVIDUAL UPREGULATED ANNEXINS ON PATIENT PROGNOSIS. 118
FIGURE 4.8. EFFECT OF P53 AND ALL UPREGULATED ANNEXINS AND S100A GENES (ANNEXIN EXPRESSION PROFILE) ON ER+ PATIENT PROGNOSIS. 121
FIGURE 5.1 THE MITOCHONDRIAL FISSION-FUSION CYCLE SUSTAINING MITOCHONDRIAL FUNCTION, NUMBER AND GENETIC HEALTH 134
FIGURE 5.2. INCREASE IN MITOCHONDRIA ACTIVITY, VIABILITY AND BIOMASS WITHOUT LOSS OF MEMBRANE POTENTIALITY POST P14ARF-P53 ACTIVATION 135
FIGURE 5.3. UPREGULATION OF MITOCHONDRIAL ASSOCIATED PROTEIN TFAM BUT NOT CYTOCHROME C POST P14ARF-P53 ACTIVATION. 142
FIGURE 5.4 GENE ONTOLOGY ANALYSIS OF THE TOP 50 DOWN-REGULATED PROTEINS POST P53 ACTIVATION IN MCF-7 CELLS. 145
FIGURE 5.5 GENE ONTOLOGY (GO) ANALYSIS OF THE TOP 50 UPREGULATED PROTEINS POST P53 ACTIVATION IN MCF-7 CELLS. 146
FIGURE 5.6. VISUALISATION OF MITOCHONDRIA IN NORMAL PROLIFERATING MCF-7 CELLS BEFORE P14ARF-P53 ACTIVATION 149
FIGURE 5.7. VISUALISATION OF MITOCHONDRIA IN NON-PROLIFERATING MCF-7 CELLS AFTER P14ARF-P53 ACTIVATION 150
FIGURE 5.8. MITOCHONDRIAL VOLUME AND SPHERICITY ARE INCREASED POST P14ARF ACTIVATION. 151
FIGURE 5.9. MITOCHONDRIA NUMBER AND DISTANCE FROM THE NUCLEUS ARE INCREASED POST P14ARF ACTIVATION 152

LIST OF TABLES

TABLE 1.1 SUMMARY OF MAJOR BREAST CANCER SUBTYPES AND THEIR PREVALENCE [9, 10, 13]..... 7
TABLE 2.1: BUFFERS, SOLUTIONS AND COMMERCIAL REAGENTS. 34
TABLE 3.1. SPECIFICATION TABLE.....58
TABLE 3.2. FUNCTIONS OF SIGNIFICANTLY REGULATED PROTEINS. 77
TABLE 4.1: SILAC DATA SHOWING DIFFERENTIAL EXPRESSION OF THE ANNEXINS AND ASSOCIATED S100A PROTEINS AT 24 AND 72 HOURS POST P14ARF INDUCTION. 102
TABLE 4.2. P53/P21/ANNEXIN/S100A INTERACTOME SCORES FOR THE PROTEIN TO PROTEIN INTERACTIONS FROM STRING DATABASE.....107
TABLE 4.3: ANNEXIN PROTEIN FUNCTION ANALYSED USING THE METSCAPE PLUGIN IN CYTOSCAPE. 111
TABLE 4.4: CYTOSCAPE (GENEMANIA) ANALYSIS OF OVEREXPRESSION OF ANNEXINS AND ASSOCIATED S100A PARTNERS DEFINING THE PHYSICAL INTERACTIONS; CO-LOCALIZATION AND GENETIC INTERACTIONS POST P14ARF INDUCTION. 112

Publications arising from this thesis

Journal original articles

1. **Hatoum D**, Yagoub D, Ahadi A, Nassif NT, McGowan EM (2017) Annexin/S100A Protein Family Regulation through p14ARF-p53 Activation: A Role in Cell Survival and Predicting Treatment Outcomes in Breast Cancer. *PLOS ONE* 12(1): e0169925. DOI: 10.1371/journal.pone.0169925.

2. Yagoub D, Wilkins MR, Lay AJ, Kaczorowski DC**, Hatoum D,** Bajan S, Hutvagner G, Lai JH, Wu W, Martiniello-Wilks R, Xia P, McGowan EM, (2014), Sphingosine kinase 1 isoform-specific interactions in breast cancer *Molecular Endocrinology* 28 (11). DOI: 10.1210/me.2013-1423.

Journal Reviews

3. Moulder DE, **Hatoum D**, Tay E, Lin Y, and McGowan EM**,** (2018), The Roles of p53 in Mitochondrial Dynamics and Cancer Metabolism: The Pendulum between Survival and Death in Breast Cancer? Special issue, "p53 and cancer", *Cancers*.10 (6). DOI: 10.3390/cancers10060189.

4. McGowan EM, Lin Y, **Hatoum D,** (2018) Good guy or bad guy? The dual roles of wild-type p53 in breast cancer origin, treatment resistance and recurrence, Special issue, "p53 and cancer", *Cancers* 10 (6). DOI: 10.3390/cancers10060172.

5. **Hatoum D**, Haddadi N, Lin Y, Nassif NT, McGowan EM (2017) Mammalian sphingosine kinase (SphK) isoenzymes and isoform expression: challenges for SphK as an oncotarget. *Oncotarget*. DOI: 10.18632/oncotarget.16370.

6. **Hatoum D,** McGowan EM, (2015), Recent advances in the use of metformin: Can treating diabetes prevent breast cancer? *Biomedical Research International.* DOI: 10.1155/2015/548436.

Published Abstracts

7. **Hatoum D,** Yagoub D, Brennan S, Nassif N, McGowan EM. P14ARF-p53-p21 alters the metabolic pathway in breast cancer a novel proteomic global approach. *Annals of Oncology– 26 (Supplement 3): iii10–iii14, 2015.*

8. **Hatoum D**, and McGowan EM. Activation of the p14ARF-p53 Pathway: A Role for p14ARF-p53 in the differential regulation of the Annexin family and S100-associated proteins. Endocrine Reviews 35: 3 (Mon-0292), 2014.

9. **Hatoum D,** Yagoub Y, Nassif N, Brennan S, Martiniello-Wilks R, McGowan EM. The misnomer of activating p14ARF-p53 for breast cancer therapy. *Journal of Gene Medicine 15: (8-9),* 333-334, 201.

Manuscripts in preparation

10. **Hatoum D**, Yagoub D, Ahadi A, Turnbull L, Whitchurch C, Nassif NT, McGowan EM., Dissecting the p14ARF-p53 pathway in breast cancer proliferation and breast function.

Conference presentations

11. **Hatoum** D, Yagoub D, Nassif N, Ahadi A, McGowan E, Turning p53 back on in breast cancer: predicted functions for p14ARF-p53 in cell cycle braking and pre-secretory differentiation through SILAC proteomic analysis*, 2017 NCRI Cancer Conference*, 5-8 November 2017, Liverpool, UK.

12. **Hatoum D**, Bok CF, Touw A, Nassif N, McGowan EM, 2015, Sphingosine Kinase 1 (SK1-43kDa) isoform expression may contribute to cancer aggressiveness, *New Horizons Conference 2015*, UTS.

13. **Hatoum D**, Yagoub D, Brennan S, Nassif N, McGowan EM, P14ARF-p53-p21: reprogramming metabolic regulation and function in breast cancer. *New Horizons Conference 2015,* UTS.

14. Moulder D*, Mitchell H*, **Hatoum D***, Bajan S, Hutvagner G, Johnson M, Mills K, Brennan S, Nassif N, McGowan EM, P14ARF-p53 plays a major

role in mitochondria dynamics in breast cancer cells, *New Horizons Conference 2015*, UTS. * Authors equal contribution.

15. **Hatoum D,** Yagoub D, Brennan S, Nassif N, McGowan EM, 2015, A Role for p14ARFp53 in Altering the Metabolic Pathway in Hormone-Dependent Breast Cancer. 2015 Innovations in Cancer Treatment and Care Conference.

16. **Hatoum D,** Nassif N, McGowan EM, 2015, A Role for p14ARF-p53 in Treatment Resistance and Recurrence in Hormone-dependent Breast Cancer, Sydney Vital Conference, May 2015, *Oral presentation.*

17. **Hatoum D**, Yagoub D, Brennan S, Nassif N, and McGowan EM, 2015, p14ARF-p53-p21 alters the metabolic pathway in breast cancer – a novel proteomic global approach, *IMPAKT Breast cancer conference*, Brussels May 6th-9th 2015 poster 37.

18. **Hatoum D,** Yagoub D, Brennan S, Nassif N, and McGowan EM, 2015, p14ARF-p53-p21 reversing the Warburg effect – a novel proteomic global approach, Australian Cancer and Metabolism Meeting, Garvan Institute of Medical Research, April 29th-1st May 2015.

19. **Hatoum D** and McGowan EM, 2014, Activation of the p14ARF-p53 Pathway: A Role for p14ARF-p53 in the Differential Regulation of the Annexin Family and S100-Associated Proteins, *ICE/ENDO,* Chicago June 21st-24th 2014.

20. **Hatoum D** and McGowan, 2012, Differential Regulation of Annexins Through the Activation of the p14-53 Pathway in Breast Cancer Cells**.** SRM, Kolling Institute Scientific Research Meeting.

List of Abbreviations

A1-A9: Annexins A1-9

ACTB: Beta-actin

ALDH4A1: Aldehyde dehydrogenase 4 family member A1

ARF: Alternate reading frame

ATP: Adenosine triphosphate

β2M: β2-microglobulin

DMEM: Dulbecco's modified eagle medium

DNAJC15: DnaJ heat shock protein family (Hsp40) Member C15

DNMT1: DNA (cytosine-5)-methytransferase 1

ERα: Estrogen Receptor Alpha

FCS: Foetal calf serum

GAPDH: Glyceraldehyde-3-phosphate dehydrogenase

GFP: Green fluorescent protein

GSN: Gelsolin

IPTG: Isopropyl-β-D-thiogalactopyranoside

MCM: Minichromosome maintenance complex

MDC1: Mediator of DNA damage checkpoint protein 1

PAPSS2: 3'-phosphoadenosine-5'-phosphosulfate synthase 2

PBS: Phosphate-buffered saline

PBST: Phosphate-buffered saline with Tween20

RT-qPCR: Quantitative real time polymerase chain reaction

SILAC: Stable isotope labelling with amino acids in cell culture

Rb: Retinoblastoma

RT: Room temperature

TNBC: Triple negative breast cancers

TRIS: Tris(hydroxymethyl)aminomethane

Abstract

Background: Breast cancer is endemic, ranking the number one cancer in women worldwide. About 80% of all breast cancers are late onset, arising in post-menopausal women, and are mainly estrogen receptor alpha (ERα) positive and p53 wild type. However, the function of p53 is compromised in many cancers due to constitutive degradation of p53 by the ubiquitin ligase human double 2 (hdm2). Degradation of p53 by hdm2 can by blocked by the p14ARF tumour suppressor protein; however p14ARF is frequently deleted in breast cancer. By re-introducing p14ARF into breast cancer cells p53 function can be restored. In this study, an inducible p14ARF ERα positive breast cancer model was used to determine the effects of reactivating p53 in hormone-dependent breast cancer. While the role of p53 in the breast cancer treatment is well recognised as a tumour suppressor, the evidence supporting an opposite action of p53 in treatment resistance and recurrence in breast cancer is emerging.

Aims of this thesis: The overall aim of this thesis was to define the role of p53 in ERα+ breast cancer cells. This aim was addressed by three specific aims, 1) to determine the global proteomic changes associated with p14ARF-p53 activation in breast cancer, 2) to characterise and validate novel p53 regulated proteins and associated signalling pathways, detected by the proteomic analysis, and 3) to examine the morphological and protein expression changes occurring in the cellular metabolism focusing on mitochondria dynamics post p53 activation.

Methods: Stable isotopic labelling in cell culture and mass spectrometry (LC-MS/MS) techniques were used for proteomic profiling of simultaneous global

protein changes in breast cancer cells post activation of the p14ARF-p53 signalling pathway. High resolution immunofluorescent microscopy, conventional Western blots and RT-qPCR and bioinformatics analyses were used for p14ARF-p53 signalling validation.

Results: 1) SILAC LC-MS/MS analyses identified a unique global differential profile of protein expression changes upon activation of the p14ARF-p53 pathway over a 24 h and 72 h period. Listings of the proteome changes have been deposited in the PRoteomics IDEntifications (PRIDE) archive with identification numbers PXD009334. Significantly downregulated proteins were associated with cell cycle arrest, DNA repair, and anti-apoptosis. Many of the upregulated proteins were specifically associated with modulation of the metabolic pathways in favour of oxidation and mitochondria regulation. 2) The tumour suppressor p53 is usually associated with the modulation of the calcium regulator protein annexin A5 to promote cell death or to permanently facilitate cell cycle arrest to prevent tumour growth. Due to the sequence similarity of the annexin family of proteins, it is difficult to determine how these multi-faceted proteins are regulated. Using unbiased, quantitative proteomics we identified p53-differential regulation of the annexin/S100A family through unique peptide recognition at the N-terminal regions. This report is the first to describe how p53 acts as the central orchestrator of these calcium regulators and its role in cell survival and function in breast cancer. 3) Changes in the mitochondria occurring after p53 activation were studied using immunofluorescence, visualising on the high resolution DeltaVision OMX Blaze™ microscope and analysing using IMARIS x64 software. Activation of the p14ARF-p53 pathway resulted in unique changes in cellular metabolism. Activation of this pathway had dramatic effects on the morphological,

activity and protein expression changes in the mitochondria, observed by an increase in mitochondrial biomass, activity, cellular distribution, sphericity and volume.

Summary: Overall, the work presented in this thesis provides a unique insight into the key proteins involved in the changing cell metabolism in hormone dependent breast cancer cells upon p53 activation and elucidates the role for p53 as a master regulator of cellular processes. Specific proteins and signalling pathways that are synchronised to rapidly hit the brakes on proliferation and coordinate metabolic cellular switching in breast cancer are discussed. These p53 proteome snapshots will provide valuable information on the duplicity of p53 in cell survival and its potential role in latency and resistance to treatment in breast cancer.

Chapter One

Introduction

1.1 Breast cancer

1.1.1 Breast cancer occurrence

Breast Cancer is the most commonly diagnosed cancer in the female population worldwide [1, 2]. Rates of prevalence are highest in Europe, Australia/New Zealand and North America (Fig. 1.1) [2]. In Australia, breast cancer is the most frequently diagnosed female cancer making up 43% of all new female cancer cases: with over 17500 breast cancer cases presenting in 2017 amounting to one in eight women diagnosed before the age of 85 [3]. In Australia, breast cancer, is the second highest cause of death, marginally after lung cancer, mortality estimated at 3087 females (1 in 41 risk of death) per year (Fig. 1.2) [3], unfortunately, this number is on the rise due to our aging population. Early diagnosis, mainly through the introduction of the mammographic screening program in 1991, has led to a perceived increased prevalence of breast cancer, however early diagnosis and better treatments (chemotherapy and hormonal therapies) have resulted in reduced overall mortality rates [4].

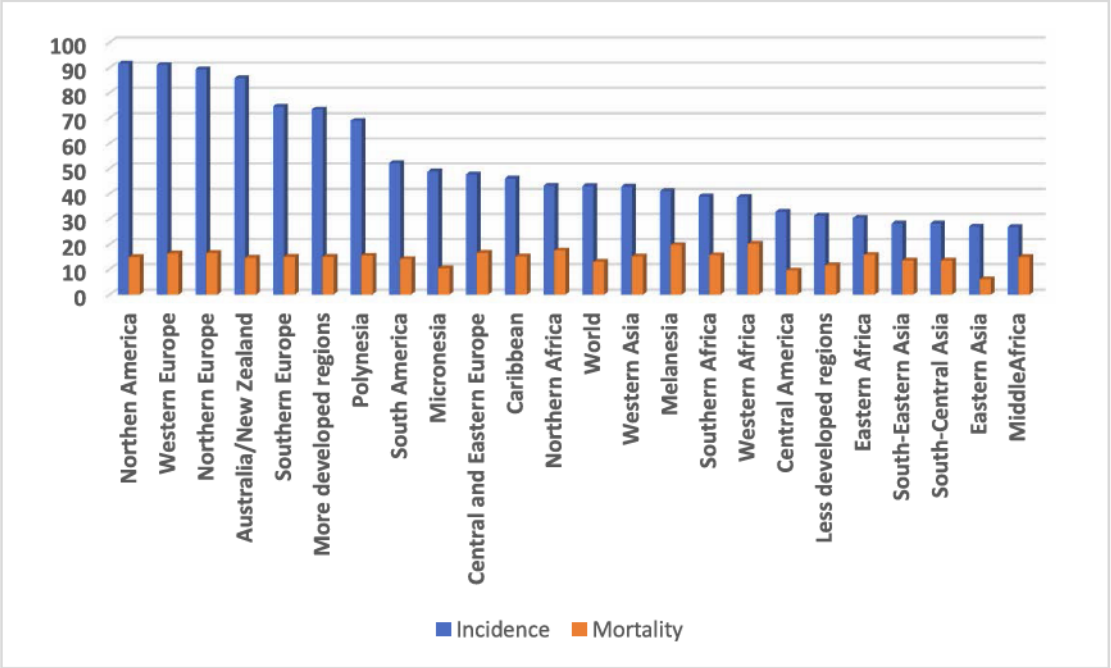


Figure 1.1 Worldwide Breast Cancer Rates.

Percentages of estimated incidence and mortality rates of breast cancer (per 100,000 population) in both males and females in different regions of the world in 2012 [5].

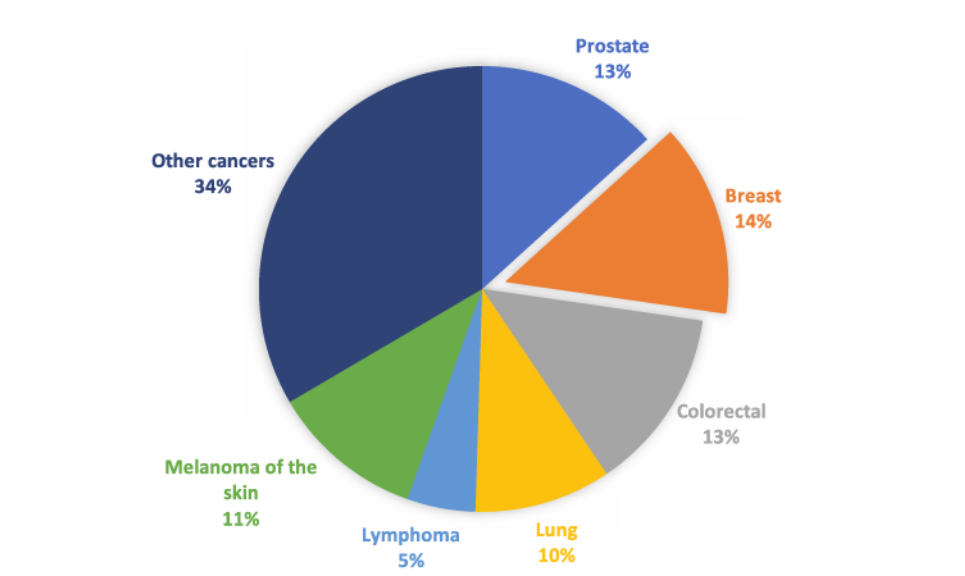


Figure 1.2. Prevalence of different cancer types in Australia. Percentages of new cases of the most diagnosed cancers in Australia in 2017 (statistics from AIHW, 2017) [3].

1.1.2 Breast cancer risk factors

Breast cancer can occur in males, however the primary breast cancer risk factor is being of the female gender, after which the risk increases with age [6]. Age is also an independent risk factor for breast cancer survival [7]. With a better understanding of this disease and more effective treatments, increased overall survival rates have been demonstrated in women between the ages of 40 – 69 [7]. Younger women who develop breast cancer usually have a strong familial or genetic history of breast cancer, whereas in older women breast cancer is mainly sporadic [6]. One of the major factors in later age of onset breast cancers is the fluctuation of the female hormones throughout a woman's lifetime. Early menarche, late menopause, lack of breast feeding, lack of, or late pregnancy, taking hormone replacement therapy, and taking the contraceptive pill are breast cancer risks factors, all associated with fluxes in the female hormones estrogen and progesterone [8]. Hormone responsive breast cancer can typically be treated successfully with anti-hormonal therapies. Early onset breast cancers are usually hormone receptor negative making these breast cancers harder to treat.

In addition, lifestyle factors such as obesity, alcohol consumption or smoking can lead to increased breast cancer risk [8]. Family history and genetic susceptibility, excess body fat and physical inactivity, occupational exposure, including exposure to chemicals, dust, radiation and industrial processes, diagnostic X-rays, air pollution, water and soil, and side effects of medical and pharmaceutical drugs can be added to the extended list of risk factors [3].

1.1.3 Breast cancer molecular subtypes

Breast cancer is a heterogeneous disease which can be clustered into five major molecular subtypes, namely (i) Triple negative / basal-like, (ii) Human epidermal growth factor receptor 2 (HER2) positive, (iii) Luminal A, (iv) Luminal B and (v) normal breast like [9, 10]. The characteristics and prevalence of these subtypes are summarised in Table 1.1. The majority (>70%) of all breast cancers are estrogen receptor positive and are treated with surgery, radiation therapy and anti-estrogen treatments [11, 12].

Table 1.1 Summary of major breast cancer subtypes and their prevalence [9, 10, 13].

Subtype	Characteristics	Prevalence
Luminal A	ER-positive and/or PR-positive, HER2-negative, low Ki67 expression	34%
Luminal B	ER-positive and/or PR-positive, HER2-positive (or HER2-negative with high Ki67 expression)	18%
Triple negative/basal-like	ER-negative, PR-negative, HER2-negative, CK 5/6-positive	25%
HER2	ER-negative, PR-negative, HER2-positive	18%
Breast Tissue Like / Unclassified	ER-negative, PR-negative, HER2-negative, CK 5/6-negative	5%

Abbreviations: ERα (estrogen receptor), PR (progesterone receptor), HER2 (human epidermal growth factor receptor 2, CK (cytokeratin).

1.1.4 Breast cancer problems with treatments

Given breast cancer is highly heterogeneous at the clinical and molecular levels the treatment of breast cancer is dependent on the cancer sub-type and characteristics of the breast cancer (i.e. stage, size, invasive/non-invasive nature of the breast cancer) and whether the cancer has spread beyond the breast to lymph nodes [9]. Conventional treatments include surgery, chemotherapy, radiotherapy, hormonal therapy and targeted therapies such as Herceptin (HER2 antibody), however treatments have many adverse effects such as pain, hair loss, hot flushes, fatigue, and acquired resistance to treatment [11, 12]. The most serious side effect would have to be acquired resistance leading to metastasis and increased mortality. Endocrine resistance, which is one of the most devastating problems facing the majority of hormone-related breast cancers, is difficult to predict and treat [14-19].

To this end, many of the recent clinical trials are using combinational treatments, combining conventional drugs in new regimes or, conventional drugs with new drugs coming onto the market for more efficacious treatment and to combat resistance, recurrence and metastasis. Approved treatment options include: switching endocrine agents, for example, sequential hormone therapy (switch the order and timing of anastrozole (estrogen blocker) with tamoxifen (ER blocker); endocrine therapy in combination with targeted therapy such as the cdk4/6 cyclin D1 complex; and using endocrine therapy with histone deacetylase (HDAC) inhibitors, reviewed in [16]. In Australia there are currently 72 breast cancer clinical trials registered with the National Institute of Health (NIH) Clinical Trials [20]. Of particular interest for this thesis is combinational treatments using anti-estrogen combinational therapy with Palbociclib, an inhibitor of the ckd/4 and cdk6 complex [21-25]. Currently, Palbociclib + endocrine therapy is showing some success in the ongoing clinical trials at the Royal North Shore Hospital in Sydney and is one of 88 clinical trial centres worldwide trialling this combinational therapy [26].

The cdk4/6 cyclin D complex is a direct downstream target in the p14 alternative reading frame (ARF)/p53 signalling pathway and the activity of cdk4/6/cyclin D1 is inhibited upon activation of p14ARF/p53 [27]. However, in hormone-dependent breast cancer cells, the downside of p53 activation is that cells can enter a senescent-like state (dormancy) with latent recurrence [27]. The main emphasis in this thesis is to explore the p14/ARF/p53 pathway in more detail to try to explain how this pathway is involved in resistance and recurrence in breast cancer.

In the following sections I will discuss the classical and emerging roles of p53 and more specifically the role of p53 in hormone-dependent breast cancer. Further, I

will discuss the role of a second tumour suppressor, p14ARF which is a major upstream regulator of p53. A full review of the dual role of p53 in breast cancer development has been recently published (June 2018) [28] in a special issue in Cancers.

1.2 P53 tumour suppressor gene

The p53 transcription factor is a tumour suppressor protein encoded by the TP53 gene located on chromosome 17p13 [29]. This gene is one of the most extensively studied proteins in the prevention of cancer development, deletion of this gene makes the cell more vulnerable to becoming cancerous [30-35]. Due to its well-characterised tumour suppressor functions p53 is often described as 'the guardian of the genome' [36]; stopping the cell cycle to repair DNA damage and deciding whether the cell lives or dies. However, the functions of p53 are very diverse, beyond the guardian of the genome. A summary of p53 well-characterised and emerging p53-functions, beyond the guardian of the genome are illustrated in Fig. 1.3. Unless otherwise stated, p53 wildtype is referred to as p53 in this thesis.

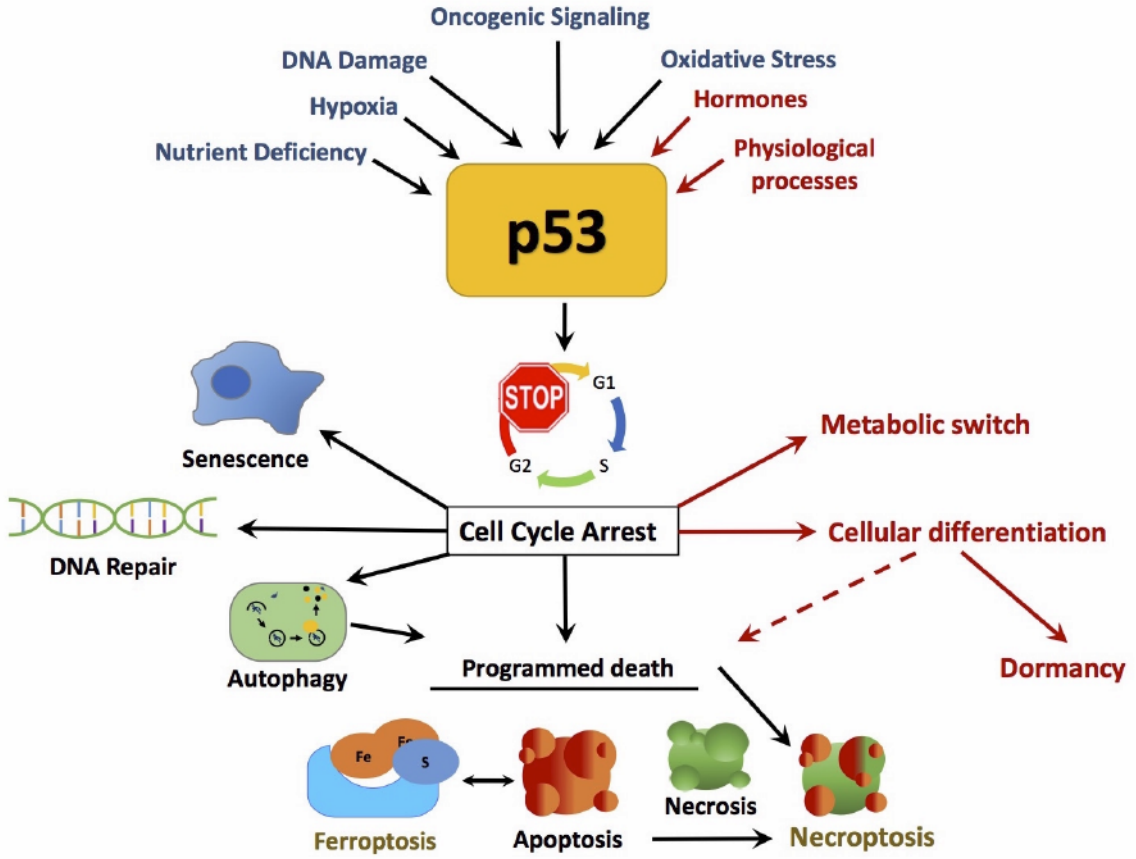


Figure 1.3. p53 canonical and non-canonical tumour suppressor roles of p53. P53 is activated by a range of cellular stress signals. These activators of p53 include: nutrient stress, hypoxic conditions, activation of oncogenes, DNA damage and oxidative stress from reactive oxygen species (ROS) and, as a result, increase the activity of p53. Classical, or canonical responses of p53 include, transcriptionally and translationally, cell cycle arrest, repair damage to DNA, place the cell in state of senescence or induce apoptosis. Non-canonical, controlled programmed cell death roles include autophagy pathways necrosis, necroptosis, and ferroptosis. Normal physiological processes such as hormone activation, can also lead to p53-induced cell cycle arrest and p53 acts as a switch in metabolic process involved in differentiation, redirecting specialised cell function [28].

1.2.1 p53 – More than the Guardian of the genome

The classical and most well-documented functions of p53 include induction of cell cycle arrest, apoptosis, cellular senescence, DNA repair and autophagy through the transcriptional and translational activation of genes in the p53 pathway [37] (Fig. 1.3). The p53 pathway can be activated by DNA damage, or through the loss of the upstream regulators such as the tumour suppressor protein p14ARF, or cytotoxic anti-tumour agents [38, 39]. When induced by cellular stress signals such as DNA damage, oxidative and nutrient stress, activation of oncogenes and hypoxic conditions, p53 maintains cell viability and regulates the cell cycle by functioning as a tumour suppressor gene stabilising within the nucleus and regulating genes involved in apoptosis, DNA repair, cell cycle arrest and senescence [34, 35, 40, 41]. These functions are mainly mediated in the nucleus through p53 binding to the promoter region of $p21^{Waf1}$ (alternatively known as $p21^{Cip1}$), a cyclin dependent kinase inhibitor that inhibits all cyclin/CDK complexes, upregulating the expression of p21. The p21 protein is important in dephosphorylation of the retinoblastoma (Rb) protein (also a tumour suppressor protein) leading to cell cycle arrest. A number of genes that function in the DNA damage repair pathway and/or inhibitors of angiogenesis and metastasis are activated and damaged DNA is repaired [38, 42-45]. Nuclear p53 transcriptionally regulates pro-apoptotic proteins Noxa and PUMA (p53-upregulated modulator of apoptosis) inducing apoptosis [46, 47]. Oda *et al.* (2000) have shown that blocking Noxa resulted in suppression of apoptosis, indicating that Noxa is a mediator of p53 dependent apoptosis [46]. p53 has also been shown to translocate to the mitochondria and activate Bax, a mitochondrial apoptotic regulator, thus contributing to apoptosis [48]. Alternatively, p53 can induce

cellular senescence, a state of irreversible cell cycle arrest [49-52], or mediate quiescence, a prolonged cell cycle arrest [53-55]. Senescence and quiescence lead to a state of dormancy, which unfortunately is not well understood and in the context of breast cancer may partly explain recurrence [56] .

p53-mediated Autophagy - The definition of autophagy from ancient Greek is 'self-devouring', a process of cell degradation of proteins and cell organelles and their conversion to building blocks that fuel metabolic processes [57]. Autophagy is associated with both pro-survival, providing energy for cells by recycling of proteins and organelles, and cell death [58-60]. Under normal physiological conditions, cytosolic p53 inhibits autophagy whereas under conditions of cellular stress (low nutrient content, growth factor, ATP and oxygen depletion; high ER stress, and DNA damage) p53 translocates to the nucleus where it transcriptionally activates pro-autophagy genes [61]. Cytoplasmic p53 has also promote mitochondrial-mediated cell death [62]. On the other hand, autophagy is associated with breast cancer survival and resistance to conventional therapies including anti-estrogens [58, 59].

p53-mediated Necrosis – Less well characterised p53-mediated programmed cell death functions include necrosis (programmed necrosis, and necroptosis); Once regarded as uncontrolled or 'accidental' cell death. This idea has been superseded whereby necrosis is now regarded as a process of irreversible programmed once regarded as uncontrolled or 'accidental' cell death. cell death where apoptosis has failed, and this process can also be triggered by p53 [63-66]. The terms of necrosis have extended to include programmed necrosis, regulated necrosis and necroptosis [67, 68]. *Necroptosis* is a relatively new concept, which is a combination of, necrosis and apoptosis-mediated p53 cell

death and contributes to immune system regulation, contributing to managing cells during inflammation, tissue injury and other organismal stresses such pathogen infection [67-69].

P53-mediated Ferroptosis. Ferroptosis, a novel non-apoptotic form of cell death, characterised by lethal iron-dependent accumulation of lipid ROS, in a caspase-independent manner. Morphologically, cells undergoing ferroptosis cell death are distinguished by small mitochondria with condensed membrane density. p53 associated energy metabolism and ROS functions have been demonstrated as disconnected from the conventional cell cycle arrest and death mechanisms [70]. Specific p53 target genes have been identified as important in p53-directed ferroptosis including solute carrier family 7 member 11 (SLC7A11), a cysteine-glutamate exchanger, glutamase 2 (GLS2), prostaglandin-endoperoxide synthase 2 (PTGS2), and spermidine/spermine N1-acetytransferase1 (SAT1) [71]. This unique form of cell death is implicated in multiple disease states including cancer [72, 73].

P53-mediated Cellular senescence or quiescence or dormancy. P53 is a decision maker in cellular senescence, quiescence, or dormancy. Senescence is defined as a state of irreversible cell cycle arrest in which cells display an inability to proliferate or respond to growth factors [50, 52, 74, 75]. *In vivo* studies highlight the pivotal role that p53-induced senescence plays in tumour suppression [52, 74]. Quiescence, a prolonged cell cycle arrest and attenuated cellular activity at the G0-G1 phase, is also mediated by p53 [54, 76]. Alternatively, dormancy is not unheard of in terms of breast cancer recurrence, with 20-50% of all breast cancers recurring from years to decades post treatment [77, 78]. A common attempt to explain dormancy arises from models of both senescence and

quiescence, both mediated by p53. However, understanding the paradox of how these potentially overlapping, and supposedly anti-tumorigenic functions facilitate dormancy, and lead to recurrence remains incomplete [79]. One potentially unidentified area to be investigated, involves the effects of p53 within cancer metabolism throughout and leading up to the point of recurrence.

In summary, mitochondria are core powerhouses for metabolic reactions which drive cellular reprogramming through diverse pathways and mechanisms as outlined above. Classical roads in p53 tumour suppression lead to mitochondrial de-regulation or inactivity, whether it be for cell destruction or temporary/permanent inactivation, respectively. However, in cancer, p53-regulated mitochondrial-cell death programs can be diverted and enhance cell survival.

1.2.2 P53 – epigenomic (epigenetic) regulator

One of the less characterised functions of p53 is as an epigenetic regulator. Epigenetic regulation (DNA methylation, chromatin remodelling, and histone modification) is an important process in development, and provides a lasting genetic imprint restricting gene expression patterns for many years after the modification effector has been removed [80]. The p53 gene is an effector of epigenetic modification and is itself a prime target for epigenetic alterations. p53 protein regulates p53 transcriptional programs, in the repair of genetic alterations and also by preventing epigenetic abnormalities [81, 82]. Tovy and colleagues showed that p53 was important in balancing DNA methylation in embryonic stem cells, maintaining the DNA homeostasis, however loss of p53 responded poorly to differentiation signals [83]. These observations were important given the

growing evidence that one of the drivers of cancer is epigenetic aberration. It has been suggested that p53 participates in chromatin remodelling initiating epigenetic reprogramming of during pregnancy [84]. Specific chromatin alterations in the mammary glands of parous rodents have been associated with the persistent increase in p53 activity [84]. Parous breast cells contain high levels of heterochromatin compared to predominantly euchromatin found in the nucleus of breast cells in nulliparous postmenopausal women. The suggestion being that as the nulliparous breast cells did not reach full differentiation they were more susceptible to transformation and insult from carcinogenic agents. As a consequence, latent breast cancer cells retain the ability to re-acquire the potential to self-renew [85]. Remodelling of the chromatin during pregnancy has been proposed as a decisive step in protection against breast cancer latency in post-menopausal years [85].

1.2.3 P53 and cancer metabolism

Aberrant cellular metabolism is now considered as one of the key hallmarks of cancer. Recently, p53 has been implicated as a master regulator, or mediator in the process of oxidative phosphorylation to glycolysis [86-90], and an interesting target for cancer treatment. The concept of cancer hijacking the cellular mechanism is not new, and was first introduced by Otto Warburg in 1930, whereby he predicted cancer cells hijack the glycolytic pathway even under the presence of oxygen [91-93]. This shift in cellular metabolism from oxidative respiration to a dominant glycolytic state, which preferentially metabolises glucose as a form of energy is anti-intuitive as it is less energy efficient (Fig. 1.4) [91-93]. Most cancer cells have a ‘sweet’ tooth and become addicted to glucose,

and in the absence of glucose, in treatments such as metformin, which reduces glucose production (used in diabetic treatment), do not survive [94].

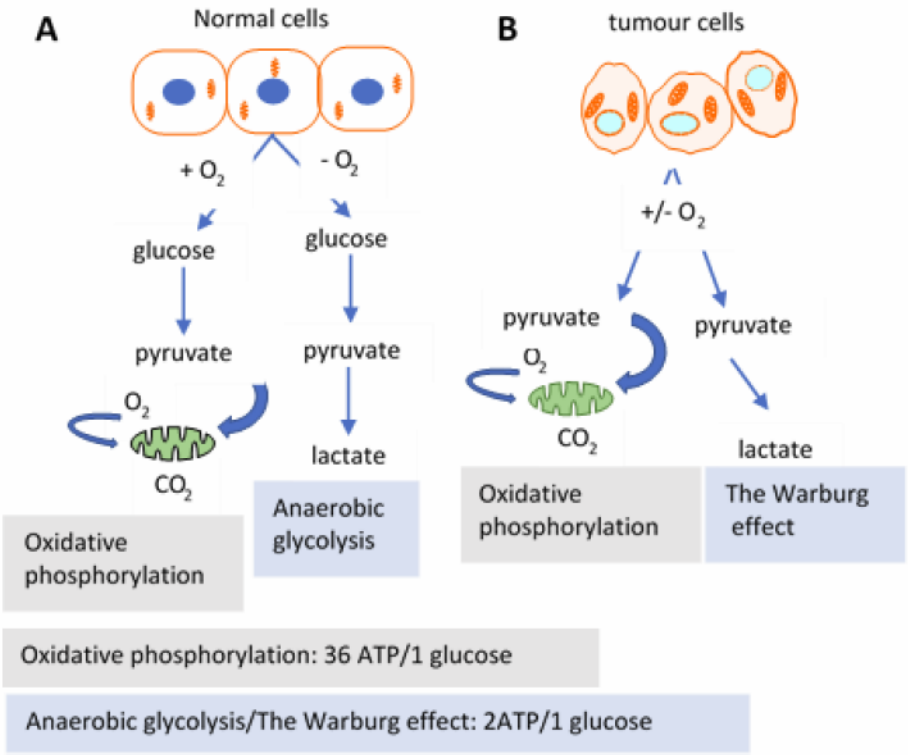


Figure 1.4. The Warburg effect: Cellular balance between Oxidative phosphorylation and Glycolysis. A) Within normal tissue, a homeostatic balance between glycolysis and mitochondrial respiration/oxidative phosphorylation (OXPHOS) is present. B) However, many cancers consume glucose at greatly higher rates than the surrounding tissue, due to a shift to a state of glycolytic dominance. Irrespective of the presence or absence of oxygen (O_2), cancers still preferentially utilize glycolysis as a means to support cancer growth and proliferation known as the Warburg effect [91-93].

Previous publications from our laboratory support the link between p53 activation and mitochondrial architecture changes, and metabolic reprogramming within a common epithelial breast cancer cell line (MCF-7) [27, 95, 96]. These include increases in mitochondrial biomass, membrane potentiality, as well as metabolic and cellular morphological changes. This data suggests p53 activation may activate major metabolic re-programming events, possibly triggering metabolic and morphological phenotypic changes within the cells. However, further investigation must be carried out. The association between p53 and metabolism is discussed in more detail in Chapter 5.

We are now realising is that the actions of p53 are more broad than protection of the genome and it has been described as the guardian of the proteome [97], guardian of homeostasis [98], guardian of maternal reproduction [99] and guardian of cellular respiration and metabolism [86, 89, 100-108], and a negative regulator of pluripotency and positive regulator of de-differentiation [109].

1.2.4 Overview of p53 in cancer

P53 is mutated in more than 50 % of human cancers with different p53 mutations shown to have different effects on the ability of a cell to maintain genetic stability [110, 111]. Interestingly, given the importance of p53 mutations and deletions in most cancers, in the breast p53 mutations and deletions only account for approximately 20% of all breast cancer patients [112]. Over 70-80 per cent of breast cancers retain functional p53, especially in the post-menopausal patients [113, 114]. The 20-30% of patients with p53 mutations have a worse patient survival (2005) [115], where p53 mutations have been found, in the main, to have a negative effect on patient resistance to treatment [115, 116]. Inactivation of p53 through loss of upstream regulatory factors plays a major role in p53 loss of function and underpins the development of many breast cancers [112]. Deregulation of p53 has also been associated with p53 isoform expression, which may suppress p53 function [117]. However, this thesis focuses on a key upstream regulator of p53 is the p14ARF tumour suppressor protein which is frequently deleted in breast cancers. Restoring and characterizing the p14ARF/p53 pathway in breast cancer is the key pathway described in this thesis.

1.2.5 P53 and ERα

Latent breast cancers in post-menopausal women are usually less aggressive and growing more slowly than early onset breast cancers (pre-menopause). Post-menopausal breast cancers are predominantly ERα and p53 positive [118]. Overexpression of p53 by immunohistochemistry, used as a surrogate for mutation status, is strongly linked to both early and late recurrence of ERα-

positive breast cancer in postmenopausal patients after treatment with aromatase inhibitors, which is commonly used as an adjuvant endocrine therapy [119].

There have been several articles that have provided mechanisms indicating a strong interaction between ERα and p53 associated with the prevention of cell death [112, 120]. Liu et al. (2006) reported that ERα suppressed p53 function via direct binding and this suppression was achieved by the activation of the ERα function-2 domain and the C-terminal regulatory domain of p53 [121]. ERα has been shown to bind to p53 and inhibit its transcriptional repression of anti-apoptotic genes, thus contributing to the ERα anti-apoptotic function in ERα positive breast cancer cells [112]. ERα positive breast cancer with wild-type (WT) p53 is more responsive to anti-estrogens than ERα positive breast cancer with mutated p53 not only due to blocking estrogen from binding to ERα and inhibiting ERα transcription, but also due to the reactivation of p53 by disrupting the p53-ERα complex [120]. In addition, it is suggested by Liu et al (2009) that radiation therapy can be combined with hormonal therapy as it has an inhibitory effect on ERα-p53 complex thus activating p53 [122].

ERα is activated by estrogen [123], and high levels of estrogen in ER positive breast cancers has been shown to correlate with high levels of p53 [124]. Berger et al. (2012) showed estrogen enhanced p53 activation by ERα whereas, anti-estrogens reduced p53 activation [125]. Our laboratory has demonstrated that combination of increased p53 via p14ARF activation and anti-estrogen treatment is more effective in reduction of recurrence in cell culture assays [27, 95]. In 2012, Myles Brown's group at Harvard University, Cambridge MA, provided supportive evidence suggesting this avenue of combinational therapy, using antagonists that block ERα inhibition of p53 entirely along with drugs that activate p53 mediated

cell death [126]. The evidence strongly implies that the interaction between p53 and ERα provides a protective mechanism against the cancer cells undergoing apoptosis and cell death and blocking this interaction may restore the p53 apoptotic pathway.

Breast cancer cells also express ERβ in most breast cancers [127]. Since the completion of the experimental work in this thesis, recent evidence has also shown that p53 binds to ERβ which has a contrasting regulatory action on cell survival and proliferation [127]. Competitive binding of ERβ antagonizes the transcription regulation of p53-ERα [127].

1.3 p14ARF – an upstream regulator of p53

As mentioned earlier, p14ARF is an endogenous upstream regulator of p53. P14ARF is well recognized as an upstream activator of p53 under adverse environmental conditions, however its mouse homolog p19ARF it has also been shown to respond to hormonal signals in mammary glands [128]. In this thesis, reactivation of p14ARF under favourable physiological conditions is used to explore p53 function in breast cancer cells.

Hormonal Activation of P19ARF-p53 in Mammary Development and cancer

In support of the role of p53 function in normal mammary development, deletion of the upstream p53 regulator p19 alternative reading frame (p19ARF), the homolog of the human p14ARF protein, led to immortalization of mammary epithelial cells [128]. p19ARF was shown to be regulated during pregnancy by progesterone, and activation of the p19ARF-p53 pathway was necessary for

normal proliferation and cell death during mammary gland development in pregnancy. Activation of the p19ARF/p14ARF-p53 pathway has been shown to block cells in both the G1 and G2 phases of the cell cycle, initiating a rapid cell cycle arrest in breast cancer cells [27, 95, 129]. The cell cycle is dynamic and, depending on the phase of cell cycle arrest (G1, G2, or S phase), different genes We proteins are be switch on or off, hence activating distinct molecular signalling pathways[130]. In speculate that discordance in p53 regulation of the cell cycle pathways could, in part, have negative repercussions in p53-associated differentiation and de-differentiation of breast cells during development. Using reactivation of p14ARF in breast cancer therapy may therefore have longer term consequences for breast cancer recurrence. This thesis furthers our understanding of reactivation of p14ARF-p53 in breast cancer biology and the potential problems raised in using p14ARF based therapies for breast cancer.

1.3.1 p14ARF – structure and function

The p14ARF gene is transcribed from the INK4a/ARF locus, located on chromosome 9p21-22, which encodes two overlapping but distinct tumour suppressor proteins: p14ARF and p16INK4A [131, 132] (Fig. 1.5). Despite their different structures, both p16INK4a and p14ARF act as negative regulators of the cell cycle through the retinoblastoma (Rb) and p53-p21 pathways (Fig. 1.6) [131]. Shan et al. (2013) found that the diverse roles of p16 INK4A and p53 are dependent on the subtype of breast cancer. p53 is important in the triple negative (negative for ERs and PRs [133]) subtypes of breast cancer, whereas p16 INK4A is more important in the luminal (expressing ERs [133]) breast cancer subtypes [134].

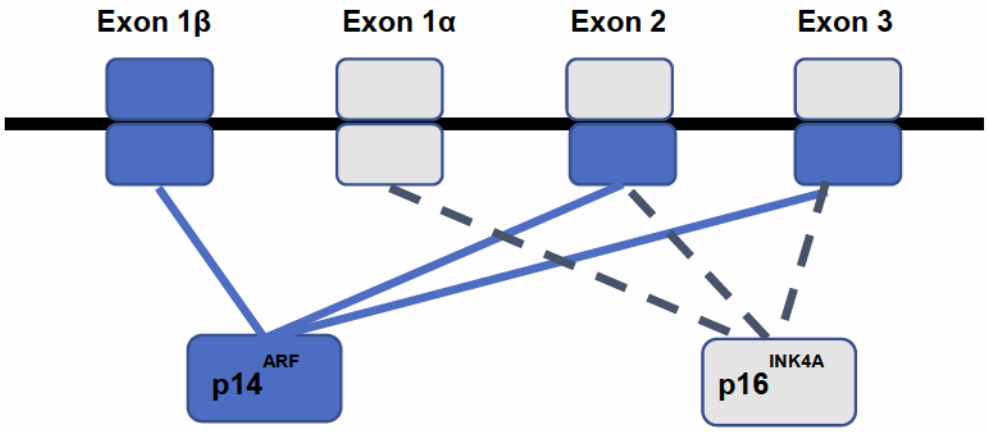


Figure 1.5. The INK4A/ARF locus and transcription of p14ARF. The INK4A/ARF locus, located on chromosome 9p21-22, encodes two overlapping but distinct tumour suppressor proteins: p14ARF and p16INK4A. p14ARF is an alternatively spliced gene which encompasses exon 1β, exon 2 and exon 3. It transcribes a completely different gene to p16INK4A. Although both are suppressor genes, they act differently in the cell and have different functions.

The p14ARF protein activates p53 by blocking HDM2 (homologue of mouse MDM2), a ubiquitin ligase that binds and degrades p53. The p14ARF protein blocks the interaction of HDM2 and p53 by directly binding to HDM2 and/or sequestering it to the nucleolus [131, 135], thus preventing degradation of p53 (Fig. 1.7) [136]. p53 then binds to the promoter region of p21 and upregulates p21 at the transcriptional level and, in turn, dephosphorylates the retinoblastoma (Rb) protein leading to cell cycle arrest, senescence or apoptosis [137].

In addition, the ubiquitous nature of aberrant splicing in the ARF/MDM2/P53 pathway has significant impact on the functions of p53 (reviewed in [138] however due to the constraints of this thesis we only refer to the conventional p14ARF/p53 pathway.

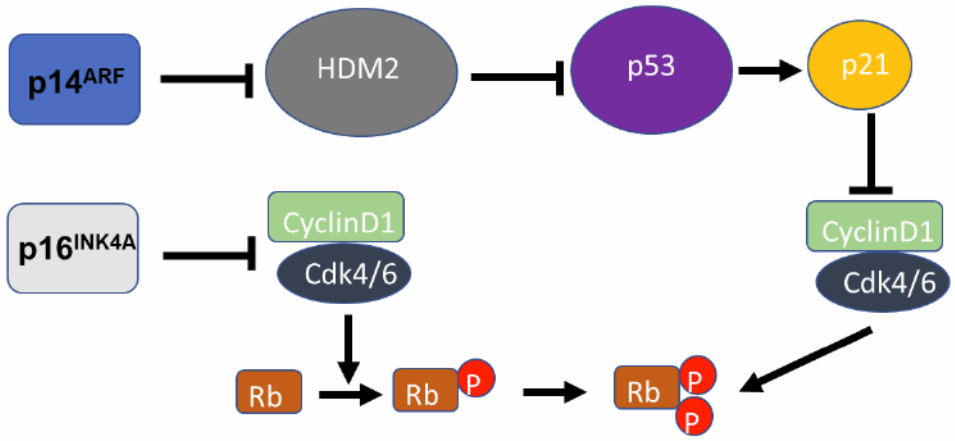


Figure 1.6. Function of p14ARF and p16 INK4A in cell cycle arrest. Upon exposure to environmental stresses, p14ARF and p16INK4A inhibit the phosphorylation of Rb.

1.3.2 p14ARF in breast cancer

Activation of the tumour suppressor gene p14ARF is one of the major mechanisms driving p53 to initiate cell cycle arrest as a protective response against uncontrolled cell proliferation (i.e. protective against cancer development) [139]. Although there have been a number of reports describing p14ARF functions that are independent of p53 [140-142], this thesis focuses on the p14ARF-p53 pathway due to its implication in p53-dependent endocrine resistance.

p14ARF is induced by chemotherapy or radiation treatments in cancer and it is mutated, deleted or hypermethylated in most breast cancers [143]. Due to the intrinsic role of p14ARF as a tumour suppressor, mimics such as nutlin-3a are currently in clinical trial for cancer treatment [95, 144-147]. Nutlin-3a activates p53 and suppresses p21-induced senescence [148]. Nutlin-3a was efficient in reactivating the p14ARF-p53 pathway in both *in vivo* and *in vitro* models including ovarian and breast cancers [144, 145]. McGowan et al. (2012) proposed a role for p14ARF-p53 in ER positive breast cancers resistance to treatment [27]. This theory was supported by a more recent report by Bailey et al. (2012) who indicated that the expression of both p53 and ER are associated with poor breast cancer patient outcome resulting from the development of apoptosis resistance [126]. Therefore, it is questionable whether reactivating the p14ARF-p53 pathway alone is a good therapy for ER positive breast cancer.

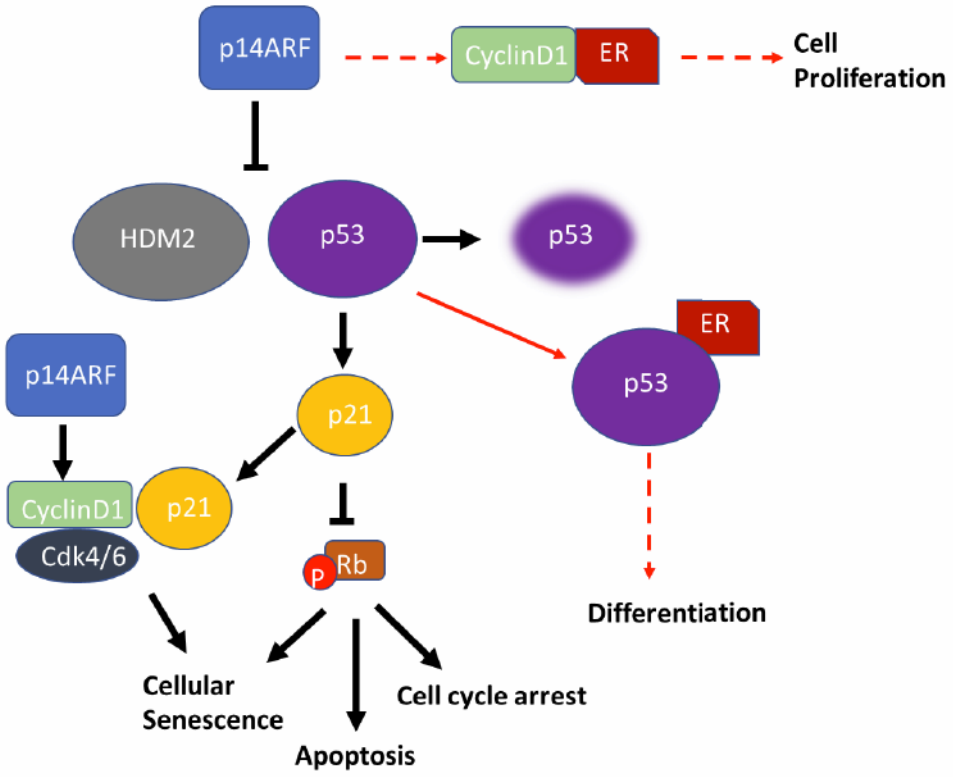


Figure 1.7. p14ARF-p53-p21 pathway in MCF-7 breast cancer cells.

p14ARF binds HDM2 and sequesters it to the nucleolus which prevents HDM2 from inhibiting p53. p53 binds to the promoter region of p21 and upregulates p21. p21 which dephosphorylates and downregulates the retinoblastoma protein (Rb). This pathway leads to cellular senescence, cell cycle arrest or apoptosis [27]. The binding of ER-p53 could potentially be important in differentiation. Additionally, ER may also bind to cyclin D1 and enhances cell proliferation.

In summary, in ER positive breast cancer, the p14ARF-p53 pathway has two major effects: (1) a positive effect, when there is DNA damage, by arresting the cell cycle and blocking the estrogen pathway, and (2) a negative effect whereby this pathway can potentially be important in cell differentiation.

1.4 Importance of understanding p53 in breast cancer development, progression, recurrence and resistance

Approximately 80% of all breast cancer are late onset, ERα and PR positive and p53 positive cancers arising from the luminal epithelial cells of postmenopausal women [1, 118]. Currently, these breast cancers are effectively treated with radiation, chemotherapy and anti-estrogen therapy [1]. Regrettably, many ERα positive breast cancers become resistant to treatment and recur. Mortality is usually associated with resistance to treatment and recurrence after treatment [14, 149]. WT p53 is associated with both cell death and cancer cell survival (as discussed in this introduction). In ERα+ breast cancers p53 is associated with cell survival. Thus, investigating the mechanisms underlying the contribution of p53 to breast cancer cell survival in ERα positive breast cancer will help in developing novel avenues for breast cancer treatment.

1.5 Aims of the project

The overall aim of this project is to define the role of p53 in estrogen responsive breast cancer cells. This will be completed through the following specific experimental aims.

Aim 1: To determine the global proteomic changes associated with p14ARF-p53 activation in breast cancer using a well characterised MCF-7 breast cancer luminal epithelial cell model.

Aim 2: To characterise and validate novel p53 regulated proteins and associated signalling pathways, detected by the proteomic analysis.

Aim 3: To examine the morphological and protein expression changes occurring in the mitochondria post p53 activation.

This thesis is composed of three main results sections namely chapters 3, 4 and 5.

Chapter 3 addresses Aim 1 and describes the global proteomics changes in breast cancer cells that occur upon activation of the p14ARF-p53 pathway. Using stable isotopic amino acid labelling (SILAC) in cell culture we identified global proteome changes post p14ARF-p53 activation in an ERα positive MCF-7 breast cancer luminal epithelial cell line. Listings of the proteome changes have been deposited in the PRoteomics IDEntifications (PRIDE) archive with identification numbers PXD009334. (**Hatoum D**, Ahadi A, Pateetin P, Padulla M, Whitchurch C, Yagoub D, McGowan EM (2018) Snapshots of the p14ARF-p53 proteome switch in breast cancer. *submitted to Nature Scientific Data, under revision).*

Chapter 4 addresses Aim 2. Using the proteomics data from Chapter 3, a sub-set of proteins belonging to the annexin family and associated S100 family were found to be differentially regulated post p14ARF-p53 activation. This section describes: 1) verification of differential regulation of the annexin proteins identified using conventional western blot analysis and RT-qPCR. 2) Use of the Kaplan-Meier plot database (kmplot.com) has revealed how the differential regulation of the annexin proteins may be used to influence breast cancer treatment. (*This work has been published:* **Hatoum D**, et al (2017) Annexin/S100A Protein Family Regulation through p14ARF-p53 Activation: A

Role in Cell Survival and Predicting Treatment Outcomes in Breast Cancer. *PLOS ONE* 12(1): e0169925. DOI: 10.1371/journal.pone.0169925).

Chapter 5 addresses Aim 3. A major finding from the global proteomic profiling described in chapter 3 was that activation of the p14ARF-p53 pathway resulted in unique changes in cellular metabolism. This chapter describes novel insights into the role of p53 changes that occur in breast cancer metabolism, focusing on mitochondrial protein changes which may be specific to breast cancer cells and breast function.

1.6 Significance of the project

This thesis provides a unique insight into the key proteins involved in the changing cell metabolism in breast cancer cells upon p53 activation and refines a role for p53 as a master regulator of cellular processes. This thesis identifies unique changes in the proteome of ER positive breast cancer cells post p14ARF-p53 activation, identifying specific proteins and signalling pathways that are synchronised to rapidly hit the brakes on proliferation and coordinate metabolic cellular switching in breast cancer. These p53 proteome snapshots will provide valuable information on the duplicity of p53 potential latency and resistance to treatment in breast cancer.

Chapter Two

MATERIALS AND METHODS

This materials and methods section describe general materials and methods used throughout the thesis. Specific methods relevant to individual Chapters will be described within the methods section of each Chapter.

2.1 MATERIALS

General tissue culture reagents and molecular reagents were supplied by Thermo Fisher Scientific (Australia), Life Technologies, Sigma-Aldrich (Australia), Sigma Chemical Co. (USA), GE Healthcare Life Sciences (Australia), VWR International (Australia), BD Biosciences (Australia), Sapphire Bioscience and Abcam. An extensive reagent supplier summary is provided in table 2.1.

Table 2.1: Buffers, solutions and commercial reagents.

Reagents	Abbreviation	Catalogue number	Stock concentration
Foetal bovine Serum (FBS, HI)	FBS	Thermo: 161140071	
Dulbecco's Modified Eagle Medium supplemented with 4.5g/L D-Glucose, L-Glutamine, 25mM HEPES	DMEM	Thermo: 12430062	
Penicillin / Streptavidin	P/S	Thermo: 15140122	10X
TryPLE™ (trypsin)	Trypsin	Thermo: A1217701	
DMEM media for SILAC	SILAC medium	Thermo: 89985	1X
SILAC amino acids		Silantes, Germany	
Isopropyl-β-D-thiogalactopyranoside	IPTG	Sigma: I6758	1M in sterile PBS
Bovine serum albumin	BSA	Sigma: A9418	
Geneticin (G418-sulfate)	G418	Thermo: 11811031	
Hygromycin B	HB	Sigma: H3274	
Insulin, human recombinant, zinc solution	Insulin	Thermo: 12585014	
Commercial kits			
MycoAlert™ Mycoplasma Detection kit	MycoAlert	LT07 (Lonza)	

2.1.1 *Protein lysates and Western blotting*

- Blocking solution: 5 % (w/v) skim milk powder in dH_2O.
- ECL Prime western blotting Detection Reagent, Amersham: Solution A (Luminol enhancer solution) and solution B (Peroxide solution) (GE Healthcare Life Sciences, Australia) (Cat # RPN2232)
- HiMark Prestained Protein standard (Cat # LC5800)
- NuPAGE MES SDS Running Buffer (20x) (Cat # NP0002): 1M MES, 1M Tris base, 69.3mM SDS, 20.5 mM EDTA, pH 7.3 stored at 4^0C
- NuPAGE Transfer Buffer (20x) (Cat # NP0006): Bicine, Bis-Tris (free base), EDTA, pH 7.2
- NuPage Sample Reducing Agent (10x) (Cat # NP0009)
- NuPage Antioxidant (Cat # NP0005)
- NuPage LDS sample buffer (4x) (Cat # NP0007)
- NuPage Novex, 4-12% Bis-Tris Gels (Cat # NP0322BOX)
- Protein extraction lysis buffer: 10mM Tris, 0.45M NaCl, 1% Triton-X100, pH 7.4, cOmplete Protease inhibitor cocktail tablet (Sigma-Aldrich, Australia) (Cat # 4693132001).
- Phosphate buffered saline (PBS)
- PBST: PBS and 1% Tween 20
- Polyvinylidene fluoride (PVDF) blotting membranes (Cat # LC2002)

- Quick Start Bradford kit 2 (Bio-Rad Life Science) (Cat # 500-0202)
- Stripping Buffer: 0.1 M Glycine at pH 2 diluted to 100 mM glycine
- Western blot Transfer Buffer: 5% NuPAGE Transfer Buffer (20x), 10% Methanol, 1% NuPAGE Antioxidant and 84% dH_2O

2.1.2 *RNA and DNA reagents*

- 4-bromoanisole (BAN) (Molecular Research Centre Inc., Cincinnati, OH, USA) (Cat # BN 191)
- High Capacity cDNA Reverse Transcription kit (Thermo Fisher) (Cat # 4374966)
- 2-Propanol (Isopropanol) (Sigma Aldrich) (Cat # I9516)
- MicroAmp Fast Optical 96-Well Reaction Plates (Cat # 4346907)
- MicroAmp Optical Adhesive Film (Cat # 4313663)
- RNAzol®RT I (Sigma-Aldrich, Australia) (Cat # R4533)
- RNase Inhibitor (Cat # N8080119)
- TaqMan Fast Advanced Master Mix (Cat # 4444556)

Taqman Probes:

- ACTB - Hs01060665_g1 (Cat # 4331182)
- ALDH4A1 - Hs01013142_m1 (Cat # 4453320)
- ANAX2 - Hs01561520_m1 (Cat # 4453320)
- ANXA1 - Hs00167549_m1 (Cat # 4453320)

- ANXA5 - Hs00996187_m1 (Cat # 4453320)
- ANXA6 - Hs01049082_m1 (Cat # 4453320)
- ARG2 - Hs00982833_m1 (Cat # 4453320)
- β2M - Hs00187842_m1 (Cat # 4331182)
- CTDSPL2 - Hs00931978_m1 (Cat # 4453320)
- DNAJC15 - Hs01098150_m1 (Cat # 4453320)
- DNMT1 - Hs00154749_m1 (Cat # 4453320)
- GAPDH - Hs02758991_g1 (Cat # 4331182)
- GSN - Hs00609272_m1 (Cat # 4453320)
- HSPA4L - Hs00204675_m1 (Cat #4331182)
- MDC1 - Hs00206182_m1 (Cat # 4453320)
- MKI67 - Hs01032443_m1 (Cat # 4453320)
- PAPSS2 - Hs00989928_m1 (Cat # 4453320)

2.1.3 *Antibodies*

All antibodies were diluted with PBS and stored at optimal conditions according to the manufactures (-20 ^{0}C or 4 ^{0}C).

Primary Antibodies

- ALDH4A1 Rabbit Polyclonal IgG (Thermo Fisher) (Cat # PIEP A5-29119)
- Annexin I human (1:10 000) (from book1)
- Annexin II human (1:10 000) (from book 1)

- Cytochrome C Rabbit Polyclonal IgG (Thermo Fisher) (Cat # PIEP A5-28856)
- Ferredoxin Reductase Rabbit Polyclonal IgG (Thermo Fisher) (Cat # PIEP A5-28018)
- Gelsolin Rabbit Polyclonal IgG (cat # (Thermo Fisher) (Cat # PIEP A5-27350)
- MDC1 Rabbit Polyclonal IgG (Thermo Fisher) (Cat # PIEP A5-27757)
- MCM4 Rabbit Polyclonal IgG (Thermo Fisher) (Cat # PIEP A5-29039)
- mtTFA Rabbit Polyclonal IgG (Thermo Fisher) (Cat # PIEP A5-27865)
- PAPSS2 Rabbit Polyclonal IgG (Thermo Fisher) (Cat # PIEP A5-29104)
- p21 (c-19, Santa Cruz)
- p53 (DO-7, Dako, CA, USA)
- RNA polymerase II CTD repeat YSPTSPS (phospho S5) (Sapphire Bioscience) (cat # ab5131)
- RNA polymerase II CTD repeat YSPTSPS (phoshpo S2) (Sapphire Bioscience) (cat # ab5095)
- RNA polymerase II CTD repeat YSPTSPS (cat # ab5408) (Sapphire Bioscience)
- RNA polymerase II CTD, unphosphorylated CTD (VWR International) (Cat # CHTK1C7TS)
- α-Tubulin (Invitrogen)

Secondary Antibodies

- α mouse HRP secondary antibody (BD Biosciences)
- α Rabbit HRP secondary antibody (BD Biosciences)
- β-actin conjugated antibody (BD Biosciences)
- GFP booster (Chromotek)
- Alexa fluro 488 (Invitrogen)
- Alexa fluro 568 (Invitrogen)
- Hoechst 33342 (Invitrogen)

2.2 METHODS

2.2.1 *Tissue culture*

Cancer cell lines were routinely cultured in DMEM (4.5 g/L D-Glucose, L-Glutamine, 25 mM HEPES) supplemented with 10% FCS (DMEM 10 N), 1% (v/v) penicillin / Streptomycin (P/S). Cells were passaged upon reaching 70% - 80% confluence by removing the medium and washing the cells with warm (37 ^{0}C) PBS, followed by the addition of 2 mL TryPLE™ per 75 cm flask. Cells were incubated at 37 ^{0}C for 3 min and fresh culture medium added to deactivate the trypsin. Cells were counted using a haemocytometer and 1x 10^{6} cells transferred to a new T75 flask containing fresh medium. All cell lines routinely tested negative for mycoplasma contamination using the MycoAlert™ Mycoplasma detection kit.

2.2.2 *Cell counts*

Cells were harvested and counted in technical triplicates using a haemocytometer. Cell viability and proliferation rates for the two cell lines were estimated by calculating the mean generation (doubling) time using the following formula:

$$T2 = t (\ln 2) / \ln (N2/N1)$$

Where: N1 = initial cell number (seeding density)

N2 = final cell number

T2 = doubling time

t = time interval in hours

2.2.3 *Cell lines and p14ARF-p53 inducible expression*

P14ARF inducible cell lines: MCF-7 BCa epithelial cells (ATCC HTB-22) are a well-characterised cell line used extensively to study the role of the ER in BCa [150]. U2OS osteosarcoma cells (ATCC HTB-96) are derived from a moderately differentiated sarcoma of the tibia [151]. U2OS cells are ER negative and express functional p53.

MCF-7 breast cancer cell lines and U2OS osteosarcoma cells stably (inducible) transfected with p14ARF have been described previously [95, 152-154]. In brief, cells were transfected with p14ARF using the LacSwitch™ inducible mammalian expression system (Fig. 2.1). Transfected cells were selected and maintained in geneticin (G418-sulfate) and hygromycin B (hB). G418 and hB were resuspended in sterile calcium and magnesium free phosphate saline (PBS), and used at a final concentration of 400 μg/ml for selection and 200 μg/ml for maintenance.

Induction of p14ARF expression – MCF-7p14ARF and U2OSp14ARF cells were induced to express p14ARF by the addition of 5 mM IPTG 24 h post seeding. In all experiments, controls were cells treated with PBS in place of IPTG.

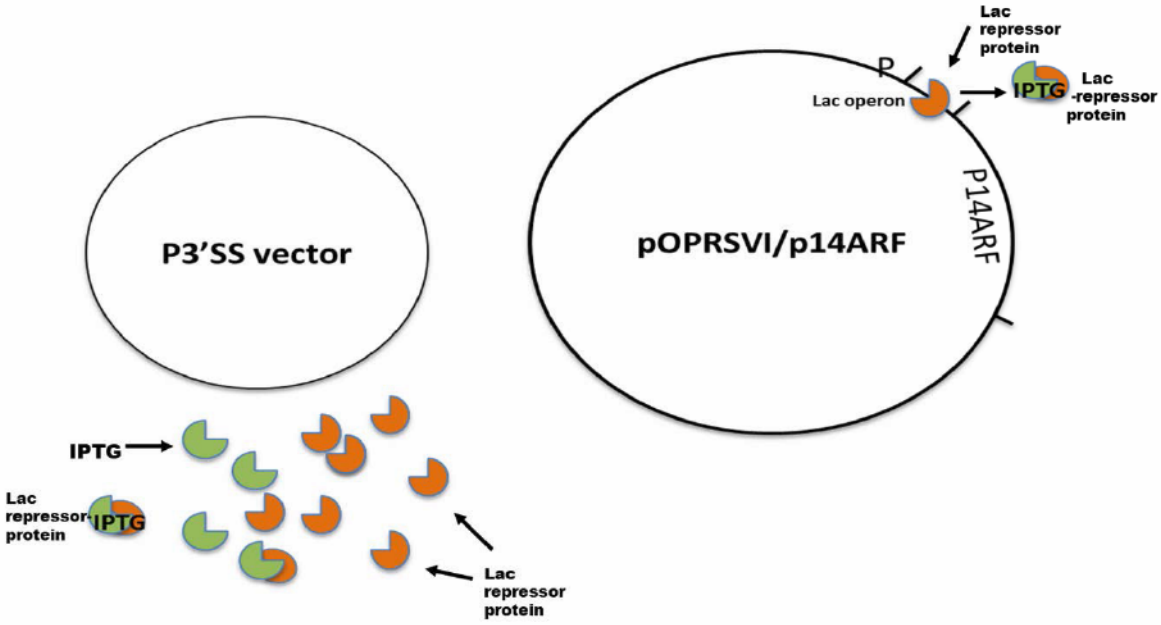


Figure 2.1. p14ARF expression using the LacSwitch™ inducible mammalian expression system. The LacSwitch™ system consists of two plasmids: (1) the p3'SS, which constitutively expresses the lac repressor protein and (2) the pOPRSV1 plasmid (Stratagene). p14ARF was inserted into the pOPRSV1 plasmid downstream of the promoter and the lac operon region. In the absence of IPTG, the lac repressor protein (orange) binds to the lac operon and blocks p14ARF transcription. IPTG (green) has a high affinity for the lac repressor protein. The lac repressor protein preferentially binds to IPTG and inducing p14ARF expression.

2.2.4 *Stable isotope labelling of amino acids in cell culture (SILAC)*

Stable isotope labelling by amino acids in cell culture (SILAC) and mass spectrometry (MS) – based quantitative proteomics [155] were used to determine changes in protein expression pre- and post- p14ARF-p53 expression in MCF-7 and U2OS cells. Proteins were metabolically labelled with 'light' (arginine 0 and Lysine 0), 'medium' (lysine-4 and arginine-6) or 'heavy' (arginine 10 and lysine 8) isotopically-labelled amino acids (Fig. 2.2). Cells were cultured for a minimum of 6 cell passages to allow incorporation of the labelled amino acid analogues into all the newly synthesised proteins in the cell instead of the natural amino acids. Cells were induced to express p14ARF by the addition of 5 mM IPTG for 72 h or equivalent volume of phosphate buffered saline (PBS) in the case of the control cells. SILAC MS/MS analysis was performed by Daniel Yagoub.

2.2.5 *Protein analysis*

Cells were seeded at 2.0 x 10^5 cells/mL in DMEM for 24 h. IPTG (5mM) and PBS (control) were added to cells respectively for 24 h and 72 h. Cells were harvested by washing twice in cold PBS followed by the addition of 150 µL of lysis buffer with protease inhibitors (PI) for 3 mins. The cell monolayers were collected by scraping and transferred to 1.5 mL Eppendorf tubes. Cell lysates were centrifuged for 10 min and the supernatant transferred to new Eppendorf tubes. The cells were centrifuged (12000 g, 4 ^{0}C) and samples kept on ice. After protein extraction, the protein concentration was determined using the Quick Start™ Bradford Kit 2 according to the manufacturer's instructions. Protein was stored at -80 ^{0}C until ready for use.

2.2.5.1 Western blotting

Denaturing electrophoresis was performed using 10 µg of total protein to which was added 2.5 µL of 25% (v/v) NuPAGE® LDS Sample Buffer (4x), 1 µL of 10% (v/v) NuPAGE® Reducing Agent (10x) and dH_2O to a final volume of 10 µL. The samples were then incubated at 85 ^{0}C for 3 min and centrifugated for 2 min. Proteins were separated on NuPAGE® Novex® Bis-Tris gels with MES SDS Running Buffer and SeeBlue® Plus2 Pre-Stained Standard as a reference protein ladder. Proteins were electrophoresed for 45 min at 170 V. Separated proteins were then transferred onto PVDF membranes for 1 h in Western blot transfer buffer using the Invitrogen Western blot transfer system. Protein transfer was verified by staining the membrane with Ponceau S. PVDF membranes were soaked in blocking solution for 2 h (with gentle agitation) at room temperature and washed twice. PVDF membranes were incubated in the appropriate primary antibody for 2 h on a MACSmix^{TM} tube rotator at room temperature then washed. The membranes were incubated with secondary α mouse HRP for 1 h at room temperature then washed every 10 min for 1 h. The membranes were visualised using Amersham ECL reagents (1:1 ratio) and protein abundance quantified by image analysis using the Kodak image station 4000 MM. To prepare the loading control, PVDF membranes were stripped by placing in boiled stripping buffer for 7 min, repeating three times with fresh stripping buffer each time, then washed three times by incubating for 10 min each time followed by blocking with 0.2% (v/v) FCS in PBST for 2 h. Membranes were probed with mouse β-actin secondary conjugated antibody for 1 h then visualised as described above. PBST was used in all washing steps.

2.2.6 *RNA extraction and Real-time quantitative polymerase chain reaction (RT-qPCR)*

MCF-7p14ARF and U2OSp14ARF cells were seeded at 2.0 x 10^5 cells/mL in DMEM for 24 h. Test cells and control cells were then treated with either 5 mM IPTG or PBS respectively for 6 h and 15 h. Centrifugation at all steps was performed at 12000 g at 4 ^{0}C and samples were always kept on ice.

2.2.6.1 RNA extraction and quality control

RNA was harvested by washing cells with cold PBS, adding RNAzol®RT, at 500 mL per well and scraping cells before pipetting into an Eppendorf tube. Cells in RNAzol®RT were stored frozen at -20 ^{0}C. RNA was extracted by adding 40% (v/v) RNase/DNase free water to the lysate, centrifuging at 12000 g for 15 min and transferring 75% of the supernatant into a fresh vial. 0.5% (v/v) of 4-bromoanisole (BAN) was added to the supernatant, shaking the mixture for 15 s and storing for 3-5 min at room temperature followed by centrifuging at 12000 g for 10 min to clear off any residual DNA, proteins and polysaccharide. The RNA-containing supernatant was transferred to a new vial and 75% (v/v) Isopropanol was added to supernatant and incubated overnight at -20 ^{0}C to increase the RNA yield.

RNA was collected as a precipitate after centrifugation (15 min, 12000 g) and washed twice with 75% (v/v) ethanol. The RNA pellet was dried at 37 ^{0}C and resuspended in 20 µL RNase/DNase free water and then heated at 55 ^{0}C for no more than 5 min and stored at -80 ^{0}C.

The quality of RNA was assessed, and total RNA concentration was measured at 260 nm using a NanoDrop 1000 Spectrophotometer (Thermo Scientific, DE, USA).

2.2.6.2 cDNA Synthesis

RNA (400ng) was reverse transcribed using the High Capacity cDNA Reverse Transcription kit according to the manufacturer's instructions. The following reagents were used to prepare Reverse Transcriptase (RT) master mix per reaction: 2.0 µL of 10 x RT Buffer, 0.8 µL of 100 mM dNTP, 1.0 µL of RNase Inhibitor, 2.0 µL of 10 x RT Random Primers, 0.5 µL of MultiScribe™ RT and 9.7 µL RNase/DNase free water. 4 µL of pure RNA (400ng) was added to 16 µL of RT master mix and centrifuged briefly. Reverse transcription was carried out at 37 ^{0}C for 120 min. As soon as reverse transcription was completed, cDNA was diluted (1:4) in RNase/DNase free water and stored at -20 ^{0}C until used.

2.2.6.3 Reference Gene Selection for Quantitative Reverse Transcription Polymerase Chain Reaction (RT-qPCR) Validation

In order to normalise target gene expression data, a reference gene, stably expressed across both cell lines under all experimental conditions, was sought. Three reference genes were tested: β-actin (ACTB), β2-microglobulin (β2M) and glyceraldehyde-3-phosphate dehydrogenase (GAPDH). A fourth control gene, HSPA4L, was also assessed as it was found to have a 1:1 ratio in SILAC analysis across all experimental conditions. RT-qPCR was performed on ANXA1, ANXA2, ANXA5, ANXA6, CTDSPL2, ARG2, DNAJC15, PAPSS2, ALDH4A1, DNMT1, MKI67 and MDC1.

For RT-qPCR, 5 µL Taqman fast master mix was mixed with 0.5 µL of Taqman probe (GAPDH, ANXA1, ANXA2, ANXA5, ANXA6, CTDSPL2, ARG2, DNAJC15, PAPSS2, ALDH4A1, DNMT1, MKI67 or MDC1 (FAM)) were mixed with 1 µL of cDNA and 3.5 µL of RNAse/DNAse free water and the solution was centrifuged. Samples were transferred, in triplicate, into a MicroAmp® Fast Optical 96-Well Reaction Plate. The plate was sealed, centrifuged for 6 min at 1400 RPM, and placed into the QuantStudio™ 12K Flex System (Applied Biosystems). Fold change in expression was calculated by the $2^{-\Delta\Delta Ct}$ method [156].

2.2.7 *Immunofluorescence and microscopy*

2.2.7.1 Transformation and isolation of mito-GFP

Mito-GFP was obtained from Evrogen pTagGFP2-mito, a mammalian expression vector, courtesy of Dr Kate Mills, Millennium Institute in Westmead. 0.5 µL of Mito-GFP plasmid (10 ng) was transformed into 50 µL of competent Escherichia Coli (*E.coli*) DH5α by incubation on ice for 30 minutes then heat shocked for 30 seconds at 42 ^{0}C and placed on ice. 250 µL of Luria broth (LB) broth was added and samples incubated for 1 hour at 37 ^{0}C on a shaker. Transformed mito-GFP-DH5α colonies were selected on kanamycin (50 µg/mL) agarose plates. Colonies were selected from the kanamycin positive agar plates, subcultured then suspended into 5mL of LB containing kanamycin (50 µg/mL) followed by overnight incubation at 37 ^{0}C on a shaker at 180 RPM. Samples were centrifuged at 3500 x g for 15 minutes, supernatant was discarded and the pellet containing the mito-GFP plasmid was purified using PureLink Quick plasmid DNA mini prep kit as per the manufacturers protocol (Invitrogen). DNA concentration was obtained using a nano-spectrophotometer at 260 nm. A single and double

restriction enzyme (RE) digests of 1 µg of mito-GFP plasmid DNA were performed using the two enzymes BAMH1 and NOT1-HF (20,000 U/mL of each enzyme, NEB 4 buffer and 20mg/mL of BSA) and incubated for 1 h at 37 ^{0}C. DNA RE digests (10 µL per sample) were analysed using gel electrophoresis (1% agarose with 5 µL of loading dye) at 100 V for 45 minutes and the size of the insert was determined using 10 kbp and 100 bp standard markers (Biorad).

2.2.7.2 Transient transfection of mito-GFP

MCF-7p14ARF cells were transfected with mito-GFP (0.507 µg/µL) using Lipofectamine 2000 DNA Transfection reagent protocol (Life Technologies). The protocol was performed in a 10 cm^2 plate. Mito-GFP DNA solution containing Optimum and Lipofectamine 2000 was added to the plate containing p/s free medium and incubated for 4-6 hours at 37 ^{0}C. Cells were then washed in warm PBS and incubated overnight in medium containing p/s at 37 ^{0}C.

2.2.7.3 Fixing and immunofluorescence staining

Transfected MCF-7p14ARF cells were seeded at 1x10^5 cells on glass coverslips in 6-well plates for 24 h, in a 37 ^{0}C, 5% CO_2 incubator. Following seeding, 5 mM IPTG was added to induce p14ARF and PBS (vehicle) added to control wells for 24 h and 72 h. Cells were fixed by washing three times in warm PBS, 1 mL of freshly thawed 4% paraformaldehyde (PFA) was gently added and incubated at 37 ^{0}C for 30 min at RT. Following incubation, cells were washed with warm PBS then permeabilised with 0.2% Triton for 10 min at RT. Cells were washed with PBS and blocked with 2% (v/v) BSA in 0.1% (v/v) Triton for 1 hour at RT. Cells were washed with PBS and incubated with tubulin primary antibody (1:50) in 1% BSA plus Tween 20 overnight at 4 ^{0}C. Cells were washed three times in PBS

leaving the first wash for 1 h. Secondary antibodies (1:500) conjugated to Alexa fluor 568, Alexa fluor 488, plus GFP booster (1:500) and Hoechst 33342 (trihydrochloride trihydrate 10mg/mL solution in water) (1:1000) containing 1% BSA plus Tween 20 (0.25 v/v) were incubated at RT for 1 h. Coverslips containing the cells were washed three times with PBS and mounted by adding n-propyl-gallate (npg). Slides were placed onto coverslips cells side down then sealed with nail polish. Slides were then viewed on Nikon confocal microscope. Objective specifications were: 60x, oil planApo, 1.40 N/A Perfect Focus System and Differential Interference Contrast (DIC). DAPI (EX 340-380nm), GFP-HQ (EX 420-440nm) and Texas Red (EX 542-580nm) fluorescent filter cubes were used.

2.2.7.4 High Resolution OMX Microscopy

3D Structured Illumination imaging was performed on the prepared sample using a DeltaVision OMX SR imaging system (GE Healthcare, Issaquah, WA, USA). Solid-state lasers provided wide-field illumination and images were captured using a × 60 1.4 numerical aperture UPlanSApo objective (Olympus, Toyko, Japan), standard filter sets and three scientific CMOS 512 × 512 pixel 15-bit cameras (pco.edge, PCO AG, Kelheim, Germany). Interference patterns were generated by interfering light beams [157] and samples were sectioned using a 125 nm Z-step size. Raw 3-phase images were then reconstructed to extract finer detail using the Gustafsson algorithms [158, 159]. Images were captured and processed using AcquireSR and SoftWorX software (GE Healthcare). Light sources used were 405 and 488 nm lasers and emission Filters used were DAPI (405 EX / 419-465 EM) and EGFP (488 EX / 500-550 EM).

IMARIS x64 (9.0.0) was used to find the number of mitochondria per cell using the 'Surface' module by thresholding for DAPI to find surface 1 (nucleus) and EGFP signal to find surface 2 (mitochondria) then the number of detected surfaces was counted in the selected region of interest.

2.2.8 *Data analysis*

2.2.8.1 Cytoscape analysis

To further define the proteomic interactive network changes relevant to p14ARF-p53 expression and action, the software program of choice was the Cytoscape Bioinformatics Platform. Cytoscape is an open source bioinformatics software platform that allows the visualisation of molecular interaction networks and biological pathways that protein targets of interest may be involved in. The ClueGO Plugin for Cytoscape is a tool that can be used to analyse protein interactions and their biological effects. A query in ClueGO from cytoscape 3.0 provided the molecular network interactions between the query proteins and most related proteins and their biological processes. These are predicted functions drawn from known interactions from curated databases or have been experimentally determined. In addition, the STRING database (v10.0) and the Cytoscape MIMI Plugin were also used to find the signalling molecular network interactions. In the query, specific proteins of interest were added and MIMI Plugin generated there interacting neighbouring proteins. Furthermore, protein function was analysed using the MetScape Plugin and physical interactions, co-localization and genetic interaction analysis was completed using GenMANIA plugin.

Chapter three

Snapshots of the p14ARF-p53 proteome switch in breast cancer

The dataset from this Chapter is presented as a manuscript submitted to Nature Scientific data and is currently under review.

Abstract

The tumour suppressor TP53 (p53 protein) is one of the most studied and attractive targets for cancer therapeutics, however in breast cancer there is still a conundrum regarding its role in 'prevention of, protection from and latent progression' of cancers. This report records and details snapshots of proteomic changes occurring in breast cancer cells post p53 stabilisation and activation by the induction of CDKN2A (p14ARF), a tumour suppressor that inhibits the ubiquitination and degradation of p53 to orchestrate consequent cellular changes and outcomes. Using stable isotope labelling by amino acids in cell culture (SILAC), the cellular proteome, before the induction of p14ARF expression, was directly compared at 24 h and 72 h post induction p14ARF expression. The unique dataset generated can be used to identify specific p53-dependent proteins and signalling pathways that are synchronised to rapidly hit the brakes on proliferation and coordinate metabolic cellular switching in breast cancer. Data are available through ProteomeXchange with identifier PXD009334. These p53-dependent proteome snapshots will provide valuable information on the duplicitous role of p53 in potential latency and resistance to treatment in breast cancer.

3.1 Background & Summary

The p53 (TP53) transcription factor is one of the most extensively studied proteins, well characterised for its canonical role as a tumour suppressor in the prevention of cancer development [30-34, 40, 86, 160, 161]. As a transcriptional regulator, p53 is stabilized within the nucleus upon DNA damage or oncogenic signalling regulating genes involved in cell cycle progression, either temporarily to facilitate repair of the DNA, or more permanently to induce apoptosis or senescence to prevent aberrant cell proliferation [33] (Fig. 3.1). Although TP53 mutations are common in most cancers, in breast cancer only 28.3% are associated with TP53 mutations or deletions leaving the remaining 71.7% with WT p53 [162], which makes reactivation of p53 in breast cancer an attractive target for breast cancer treatment [163]. This is particularly relevant for hormone responsive breast cancers where a large majority of tumours harbour p53 [113, 114]. In addition, p53 has been identified as a potential hormone-inducible protein, in part, responsible for the hormone-refractory phenotype [164], and activation of p53 blocks apoptosis in estrogen receptor positive cells [27, 126]. A targeted protein for p53 reactivation is the p14 alternative reading frame (ARF): p14ARF (transcribed from CDKN2A) blocks the ubiquitination of p53 by deactivating the ubiquitin-protein ligase human double minute2 (hdm2) [165], preventing p53 degradation and thus stabilizing p53 expression, in turn, p53 activates p21 (CDKN1A) and consequently blocks cell cycle progression[166-168]. Under the pressure of an unfavourable environment, p14ARF is activated to stabilize p53 (Fig. 3.1). Most studies designed to activate the p14ARF pathway are stress-induced, using chemotherapy or ultraviolet (UV) radiation, which are

core cancer therapies. Activation of p53 under favourable physiological conditions is less well explored. This report describes the switching of p53 “back on” in MCF-7 cells by inducible expression of the p14ARF gene, thus reactivating p53-p21 in a mitogen rich, stress free environment.

The MCF-7 cell line is a hormone responsive human breast cancer cell line [150, 169] that has retained many of the properties expressed by luminal breast epithelium *in vivo*, making it a good model to study breast cancer cells *in vitro* [170]. This cell line is one of the most well-characterised cell models for basic breast cancer research studies [171]. MCF-7 cells retain p53, however they lack the upstream p14ARF regulator such that p53 is continuously being degraded. Thus, an inducible p14ARF MCF-7 cell model, to explore p14ARF-p53 activation, was developed for this study [27, 95, 96]. In this model system p14ARF-p53 is activated by the addition of 5mM Isopropyl β-D-1-thiogalactopyranoside (IPTG) into the culture medium. Prior to any experimentation, we determined whether IPTG had any overt effects on the MCF-7 parental cells and found no obvious morphological changes or changes in any of the well characterised p53-downstream proteins, providing confidence in the developed p14ARF-p53 model system [95]. This study employed a global proteomic approach, using SILAC and mass spectrometry coupled with liquid chromatography (LC-MS/MS), to explore the proteomic and functional changes occurring post p14ARF-p53 activation.

To generate a high confidence list of comparative protein changes, a triple isotopic labelling strategy we designed and is represented in Fig. 3.2. After identifications at the 1% false discovery rate (FDR) threshold of the data generated by MaxQuant software, the proteins were further filtered to include only proteins present in biological replicates (PRIDE ID PXD009334). A heat map was

generated to compare the 24 h and 72 h proteomic changes pre- and post-p14ARF activation (Fig. 3.3A). Significant changes (p-value <0.05) are represented as volcano plots in Fig. 3.3B (24 h) and Fig. 3.3C (72 h). Western blotting detection of p53-p21 expression was performed in each experiment to confirm activation of the p14ARF-p53-p21 signalling pathway (inset). The integrity of this dataset has recently been verified by demonstrating differential regulation of the annexins by p14ARF-p53 by mapping peptide sequences from the SILAC dataset to unique N-terminal regions of individual annexin proteins [96] (Chapter 4 of this thesis). Additional validation is presented in Fig. 3.4 where we document p14ARF-p53 activation dependent downstream changes, at the transcriptional and translational level, of representatives of the most prominent up- and down- regulated proteins in the SILAC dataset. Using the interactive REACTOME pathway database, we highlight how this dataset can be used to analyse specific p53-signal transduction pathway changes that occur in DNA processes, metabolic pathways, and cell morphology, as represented in Fig. 3.6A and Fig. 3.6B. Revisiting p14ARF-p53 signalling in these defined conditions can be used to identify specific proteins and coordinated signalling pathways adding valuable information on p53-dependent metabolic reprogramming events in breast cancer cells. This data, which is publicly available in the PRoteomics IDEntifications (PRIDE) archive, proteomics data repository [172], will also complement and add to the existing knowledge of p14ARF-p53 in the duplicity of roles of p53 in acquired resistance to treatment in breast cancer. We have updated the p14ARF-p53 SILAC experiment in PRIDE (identifier: PXD009334). The reviewers can access this data through PRIDE using the following Reviewer account details:

Experiment 1 - Username: reviewer53474@ebi.ac.uk Password: LtuZKaUx.

PRIDE identifier: PXD009334.

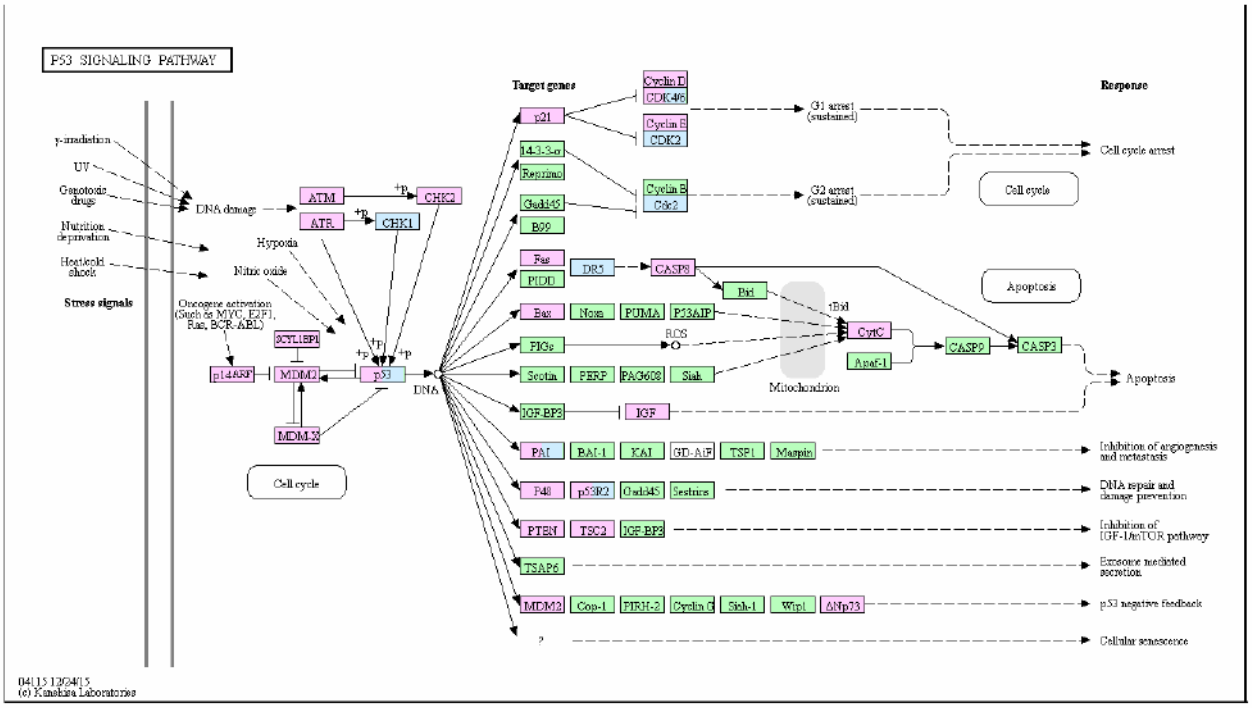


Figure 3.1. p14ARF activation of the P53 Signalling pathway. The KEGG (Kyoto encyclopaedia of genes and genomes) database was utilised to analyse the p14ARF-p53 pathway activation. Traditionally the p14ARF-p53 pathway is most commonly induced by a number of stress signals, including DNA damage, oxidative stress and activated oncogenes. The p53 protein is employed as a transcriptional activator of p53-regulated genes. This results in three possible cellular consequences: (i) cell cycle arrest, (ii) cellular senescence or (iii) apoptosis. Other p53-regulated gene functions communicate with adjacent cells, repair damaged DNA or set up positive and negative feedback loops that enhance or attenuate the functions of the p53 protein and integrate these stress responses with other signal transduction pathways. Legend: Pink refers to known genes involved in disease, the blue refers to the drug targets.

Table 3.1. Specification table

Subject area	Biology
More specific subject area	Proteomics – p53 regulation in breast cancer
Type of data	Mass spectrometry
How data was acquired	MS data was acquired on an Orbitrap Velos ETD (Thermo Electron) mass spectrometer.
Data format	Mascot and Peaks Studio
Experimental factors	MCF-7 cells were stably transfected with inducible p14ARF using the LacSwitch™ lac repressor system. SILAC was used to quantify protein regulation pre- and post p14ARF-p53-p21 activation. Cells were cultured in light (unlabelled lysine and arginine), medium ($^{2}H_4$-lysine and $^{13}C_6$-L-arginine) and heavy ($^{13}C_6$ $^{15}N_2$-L-lysine and $^{13}C_6$ $^{15}N_4$-L-arginine). Light was treated with phosphate buffered saline (PBS) while medium and heavy were treated with 5 mM Isopropyl β-D-1-thiogalactopyranoside (IPTG) for 24 h and 72 h respectively to induce p14ARF.
Experimental features	After treatment cells were lysed and the lysates were fractionated using nuclear/cytosol fractionation kits (BioVision) then separated by electrophoresis and in-gel tryptic digestion was carried out. Peptides were separated by nano-LC using Ultimate 3000 HPLC and autosampler system (Dionex) and analysed by high-resolution mass spectrometry.

3.2 Methods

The specifications for the experimental protocol are outlined in Table 3.1.

3.2.1 Cell Culture

MCF-7 breast cancer epithelial cells (ATCC:HTB-22) were stably transfected with p14ARF (CDKN2A) [171] using the LacSwitch™ II inducible expression system. The LacSwitch™ II methodology has been described in detail in McGowan et al, 1999 [95]. In brief, two plasmids were transfected into MCF-7 cells: the p3'SS lac repressor producing plasmid and the POPRSVI/MCS (lac-operator vector) containing the p14ARF insert. To maintain p14ARF inducibility selectively, cell culture medium was supplemented with geneticin (200 µg/ml) and hygromycin B ((200 µg/ml). p14ARF expression was induced with 5 mM Isopropyl β-D-1thiogalactopyranoside (IPTG) (Promega) dissolved in phosphate buffered saline (PBS) from a 1 M stock solution. MCF-7p14ARF cells were routinely cultured in Dulbecco's Modified Eagle Medium (DMEM, high glucose) with 10% (v/v) foetal bovine serum (FBS). All cell lines were mycoplasma free, as demonstrated through routine testing for mycoplasma using the Lonza MycoAlert mycoplasma assay.

3.2.2 SILAC labelling of breast cancer cells

Lysine- and arginine-free DMEM medium (SILAC-DMEM), dialyzed foetal calf serum (dFCS), and isotopic labelled and unlabelled amino acids were purchased from Silantes GmbH (Germany). The triple-labelling of MCF-7p14ARF cells was performed by splitting and culturing MCF-7p14ARF cells into three different formulations of labelled SILAC-DMEM+10% dFCS supplemented with either: (1) normal or 'light' (L), unlabelled lysine (146mg/L) and arginine (84mg/L); (2)

'medium' (M) lysine-4 (lysine-4 ($^{2}H_4$-lysine) (150 mg/L) and arginine-6 ($^{13}C_6$-L-arginine) (86 mg/L); or (3) 'heavy' (H) lysine-8 ($^{13}C_6$ $^{15}N_6$L-lysine) (152 mg/L) and arginine-10 ($^{13}C_6$ $^{15}N_4$-L-arginine) (88 mg/L) (Fig. 3.2). Cells were passaged by rinsing with sterile PBS and incubation for 5 min at 37 ^{0}C with pre-warmed cell dissociation buffer (Invitrogen). Cell dissociation buffer was neutralized with 10 ml of SILAC wash (SILAC-DMEM containing 5% (v/v) dialyzed FBS with no amino acid supplements) and centrifugation for 5 min at 1000 rpm. Cell pellets were resuspended in 'light', 'medium' and 'heavy' medium respectively. To achieve complete isotopic amino acid incorporation, MCF-7p14ARF cells were cultured in labelling medium for a minimum of 6 doubling times. SILAC quantification depends on near completion of incorporation of isotopically labelled amino acid; therefore, stable amino acid incorporation was verified by LC-MS/MS and demonstrated approximately 96% incorporation.

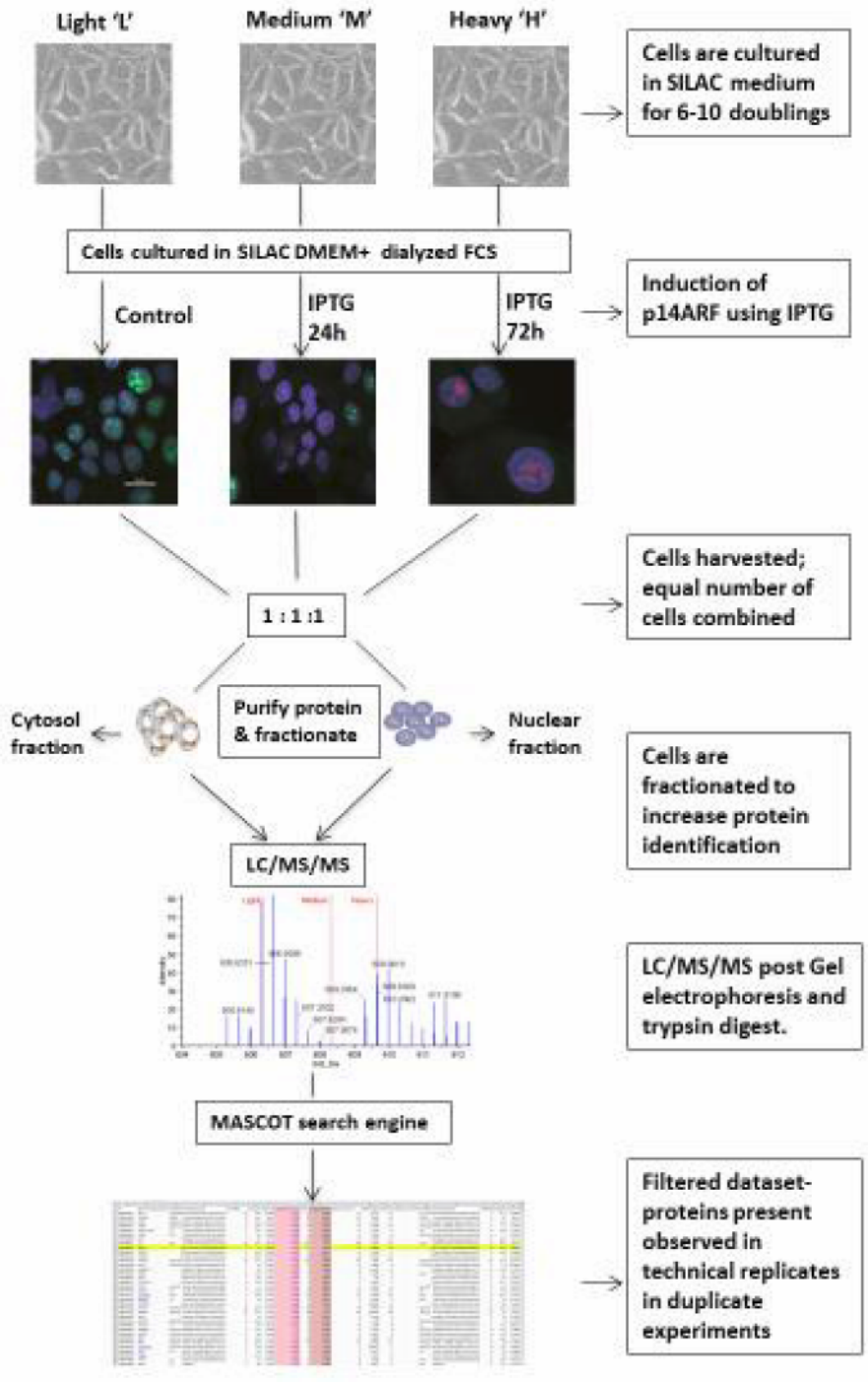


Figure 3.2. Schematic illustration of the SILAC LC-MS/MS triple labelling protocol. MCF-7 cells were stably transfected with inducible p14ARF using the Lac Switch™ system. Equal numbers of cells were cultured in Light 'L', Medium 'M', and Heavy 'H' SILAC medium for a minimum of 6 doubling times. Labelled

stable isotope amino acid incorporation was measure by LC/MS/MS. SILAC cultured cells in 'M' and 'H' medium were treated with 5 mM IPTG for 24 h and 72 h respectively. Immunofluorescence images demonstrates the induction of p14ARF; blue – DAPI; red – p14ARF; green – Ki67. Cells cultured in 'L' medium were vehicle (PBS) treated. Cells were counted and equal numbers of cells from 'L', 'M' and 'H' cultures were pooled (1:1:1). Subcellular fractionation (cytosol and nucleus) was conducted and proteins were analysed by LC-MS/MS. The Mascot search engine was used for protein identification from the mass spectrometric data.

3.2.3 Determining p14ARF-p53 proteome changes using SILAC triple labelling

3.2.3.1 Time course of induction of p14ARF in SILAC cell culture

Labelled cells were split and cultured into the three SILAC DMEM formulations until 40-50% confluent. Fresh medium was added to the three conditions as follows: on day 0, cells cultured in 'L' SILAC DMEM were treated with vehicle (PBS), and cells cultured in 'H' SILAC DMEM were treated with 5mM IPTG (diluted in PBS). On day 2, cells cultured in 'M' SILAC DMEM were treated with 5mM IPTG. All cells were harvested on day 3 to eliminate any potential effects of the PBS (vehicle) treatment (Fig 3.2). Cells were visualized under the microscope to confirm morphological changes at 24 h and 72 h post IPTG treatment. Cells were harvested by incubation with pre-warmed cell dissociation buffer for 5 min, neutralized with SILAC wash medium and washed twice with PBS. On harvesting, treated cells were counted and equal numbers of cells from the different SILAC labelled cells were combined in a 1:1:1 ratio. The SILAC experiment was repeated to provide 2 biological replicate experiments, comparing control (PBS) with p14ARF (IPTG) at 24 h and 72 h.

3.2.3.2 LC-MS/MS sample preparation

For better peptide coverage, nuclear and cytosolic fractions were separated using nuclear/cytosol fractionation kits (BioVision). Fractionated protein lysates (nuclear and cytosolic) were electrophoresed on 1-D SDS-PAGE gels and stained with blue silver. Peptide extraction by in-gel tryptic digestion prior to analysis by high-resolution mass spectrometry, was performed using the method described by Shevechenko and colleagues [155]. Gel lanes containing

electrophoresed proteins were cut into 20 pieces (10 from the nuclear protein lane and 10 from the cytosolic protein lane) and the gel fragments were reduced (dehydrated) in acetonitrile. Acetonitrile was removed, and the fragments dried using a vacuum centrifuge. The dried gel pieces were covered in Dithiotreitol (DTT) (10 mM) in 100 mM NH_4HCO_3 and proteins reduced for 60 min at 56 ^{0}C. the gel pieces were cooled to room temperature (RT) and the DTT was replaced with 55 mM iodoacetamide in 100 mM NH_4HCO_3 and left in the dark at RT, with occasional vortexing, for 45 min prior to washing for a further 10 min with approximately 100 µL of 100 mM NH_4HCO_3. The gel samples were further dehydrated with acetronile, rehydrated with 100 mM NH_4HCO_3 and dehydrated with acetronile. All liquid was removed and the gel pieces were dried in a vacuum centrifuge. Gel pieces underwent tryptic digestion using 12.5 ng/µL trypsin in tryptic digestion buffer (50 mM NH_4HCO_3/5 mM $CaCl_2$) on ice, for 45 min. Supernatant was then replaced with tryptic digestion buffer to ensure gel pieces remained wet during overnight enzymatic cleavage at 37 ^{0}C. The peptides were extracted from the gel with one wash using 20 mM NH_4HCO_3, and three washes with 5% formic acid in 50% acetronile (RT) and dried.

3.2.3.3 Liquid chromatography-tandem mass spectrometry (LCMS/MS) acquisition

Nano LC technology (Ultimate 3000 HPLC and autosampler system - Dionex) was used to separate the extracted protein peptides, of which 2.975 µL of sample was placed into a micro-C18 pre-column containing: 500µm × 2mm [155]; Michrom Bioresources; and H_2O-CH_3CN [98:2 (vol/vol), 0.1% trifluoroacetic acid], at 15 µL/min to desalt and concentrate the peptides. The peptides were washed for 4 min. The pre-column was transferred to a Valco 10 port valve (Dionex) into

line with a fritless nanocolumn (75µ x -10cm). The column contained C18 media (5 µm, 200 Å Magic; Michrom), which was manufactured according to Gatlin and colleagues (1998) [173]. Using a linear gradient, composed of H_2O-CH_3CN [98:2 (vol/vol), 0.1% formic acid] to H_2O-CH_3CN [64:36 (vol/vol), 0.1% formic acid], set at 250 nL/min, the peptides were eluted over 30 min. An Orbitrap Velos ETD (Thermo Electron) mass spectrometer was used to sequentially isolate and fragment the ten most abundant ions (>5000 counts). The Orbitrap was operated in a data-dependent acquisition setting: 2000 volts was applied to the low volume tee (Upchurch Scientific) with the column tip positioned 0.5 cm from the heated capillary (275 ^{0}C) and positive ions were generated by electrospray. The Orbitrap acquired a 350–1750 survey scan mass to charge ratio (m/z). Sequential isolation and fragmentation of the ten most abundant ions with charge states of +2 or greater within the linear ion trap was performed. A target value of 30 000 ions was chosen after collision-induced dissociation with an activation q = 0.25 and activation time of 30 milliseconds. Dynamic exclusion for 30 seconds of the m/z ratios selected for tandem mass spectrometry was applied.

3.2.3.4 Quantification and MS/MS Data analysis

To generate a high confidence list of proteins, biological duplicate experiments were performed with the triple labelling strategy, with each biological replicate subsequently being subjected to mass spectrometric analysis. Mass spectrometric data was processed using MaxQuant software (version 1.0.13.13). MS/MS spectra were searched with the MASCOT search engine against the decoy IPI-human database (forward and reverse sequences). Search parameters were as follows: variable modifications of N-terminal acetylation and methionine oxidation, fixed modification of cysteine carbamidomethylation, peptides of

minimum six or more amino acids, maximum of two missed cleavages, minimum two razor peptides for quantitation, and peptide and protein FDR of 0.01 [155]. MS/MS data files were searched using Peaks Studio (version 8.5) against the Human Proteome database and a database of common contaminants with the following parameter settings. Fixed modifications: none. Variable modifications: propionamide, oxidized methionine, deamidated asparagine. Enzyme: semi-trypsin. Number of allowed missed cleavages:3. Peptide mass tolerance: 30 ppm. MS/MS mass tolerance: 0.1 Da. Charge state: 2+, 3+ and 4+. The results of the search were then filtered to include peptides with a $-\log_{10}P$ score that was determined by the FDR of <1%, the score being that where decoy database search matches <1% of the total matches.

3.2.3.5 Protein analysis and western blotting

MCF-7p14ARF cells were seeded at 2.0 x 10^5 cells/mL in DMEM in 6-well plates for 24 h. PBS (control) (3 wells) were added. 48 h later 5 mM IPTG was added to a further 3 wells. Cells were harvested 24 h later, by washing twice in cold PBS then adding 150µL of lysis buffer (10 mM Tris, 0.45 M NaCl, 1% Triton-X100, pH 7.4, cOmplete Protease inhibitor cocktail table (Sigma-Aldrich) for 3 mins. Cells were scraped off the monolayer and transferred to a 1.5 mL Eppendorf tube. Cell lysates were centrifuged at 12000 g at 4 ^{0}C for 10 min and the supernatant transferred to a new Eppendorf tube and samples were always kept on ice. Protein was quantitated using QuickStar™ Bradford Kit 2 according to the manufacturer's instructions. Protein was stored at -80 ^{0}C until ready for use.

Denaturing electrophoresis was performed by adding 10 µg of total protein to 25% (v/v) NuPAGE® LDS Sample Buffer (4x), 10% (v/v) NuPAGE® Reducing

Agent (10x) and dH_2O, then incubating at 95 ^{0}C for 10min and centrifuged for 2 min. Proteins were separated on NuPAGE® Novex® Bis-Tris gel with NuPAGE® MES SDS Running Buffer and SeeBlue® Plus2 Pre-Stained Standard as a reference ladder (Invitrogen). The proteins were then transferred onto PVDF membranes for 1 h at 30 V in Western blot transfer buffer using the Invitrogen Western blot transfer system. Protein transfer was verified by staining the membrane with Ponceau S then washing with dH_2O, PBS and PBS + 0.2% Tween20 (v/v). PVDF membranes were soaked in 5% skim milk/PBST (w/v) blocking solution overnight (with gentle agitation) at 4 ^{0}C then washed three times. PVDF membranes were incubated in the appropriate primary antibodies (β-actin (SantaCruz), GAPDH, A2, ALDH4A1, Ferredoxin reductase, Gelsolin, p53, PAPSS2 and MCM4 (ThermoFisher)) overnight at 4 ^{0}C then washed. The membranes were incubated with secondary HRP-conjugated goat anti-mouse and HRP conjugated donkey anti-rabbit (Jackson Immuno-research) (1:10,000) for one hour at RT then washed every 20 min for a total of one hour. The membranes were visualized using Amersham ECL reagents (1:1 ratio) and protein abundance quantified by image analysis using the Amersham Imager 600 (GE Life Sciences). PBST was used in all washing steps.

3.2.3.6 RNA extraction and Real-time quantitative polymerase chain reaction (RT-qPCR)

MCF-7p14ARF cells were seeded at 2.0 x 10^5 cells/mL in DMEM for 24 h. Test cells and control cells were then treated by 5 mM IPTG and PBS respectively for 15 h. RNA was harvested by washing cells with cold PBS, adding RNAzol®RT (Molecular Research Centre Inc., Cincinnati, OH, USA) at 500 µL per well and scraping cells before pipetting into an Eppendorf tube. Cells in RNAzol®RT were

frozen at -20 ^{0}C until required for RNA extraction. RNA was extracted by adding 40% (v/v) RNase/DNase free water to the lysate, centrifuging at 12000g for 15 min and transferring 75% of the supernatant into a fresh vial. 0.5% (v/v) of 4-bromoanisole (BAN) was added to supernatant, shaking the mixture for 15 seconds and storing for 3-5 min at room temperature followed by centrifuging at 12000 g for 10 min to clear off any residual DNA, proteins and polysaccharide. The RNA-containing supernatant was transferred to a new vial and 75% (v/v) Isopropanol was then added to the supernatant and incubated overnight at -20 ^{0}C to increase the RNA yield.

The RNA pellet was collected by centrifugation for 15 min and washed twice with 75% (v/v) ethanol. The pellet was dried at 37 ^{0}C until it became clear and resuspended in 20 µL RNase/DNase free water and stored at -80 ^{0}C until required.

The quality of RNA was assessed, and total RNA concentration was measured at 260 nm using the NanoDrop 1000 Spectrophotometer (Thermo Fisher Scientific, DE, USA). RNA (400 ng) was reverse transcribed using the High Capacity cDNA Reverse Transcription kit (Life Technologies) according to the manufacturer's instructions. The following reagents were used to prepare the Reverse Transcriptase (RT) master mix per reaction: 2.0 µL of 10 x RT Buffer, 0.8 µL of 100 mM dNTP, 1.0 µL of RNase Inhibitor, 2.0 µL of 10 x RT Random Primers, 0.5 µL of MultiScribe RT and 9.7 µL RNase/DNase free water. 4 µL of pure RNA (400 ng) was added to 16 µL of RT master mix and centrifuged briefly. The tubes were loaded into the Eppendorf vapo.protect thermal cycler that performed reverse transcription at 37 ^{0}C for 120 min. As soon as reverse

transcription was completed, cDNA was diluted (1:4) in RNase/DNase free water and stored at -20 ^{0}C until used.

Quantitative RT-PCR reactions were performed in triplicate. 5 µL Taqman fast master mix was mixed with 0.5 µL of Taqman probe and 3.5 µL of RNAse/DNAse free water and the solution was centrifuged. 1 µL of cDNA was pipetted into each well of a MicroAmp® Fast Optical 96-Well Reaction Plate (Applied Biosciences). The plate was mixed then sealed, centrifuged for 6 min at 1400 RPM, and placed into the QuantStudio™ 12K Flex System (Applied Biosystems). Taqman Gene Expression Assays used were as follows (protein names are shown in brackets):

ALDH4A1, Hs01013142_m1 (Aldehyde dehydrogenase 4 family member A1); ANAX2, Hs01561520_m1 (Annexin A2); ANXA1, Hs00167549_m1 (Annexin A1); ANXA5, Hs00996187_m1 (Annexin A5); ANXA6, Hs01049082_m1 (AnnexinA6); MCM4, Hs00907398_m1 (Minichromosome Maintenance Complex Component 4); DNAJC15, Hs01098150_m1 (DnaJ heat shock protein family member C15); PAPSS2, Hs00989928_m1(3'-Phosphoadenosine 5'-Phosphosulfate Synthase 2); GSN, Hs00609272_m1 (Gelsolin); MDC1, Hs00206182_m1 (Mediator of DNA damage checkpoint protein 1); MKI67, Hs01032443_m1 (Marker Of Proliferation Ki-6); DNMT1, Hs00154749_m1 (DNA (cytosine-5)-methyltransferase 1) and normalised to GAPDH (Hs02758991_g1) (glyceraldehyde-3-phosphate dehydrogenase) expression.

Mean CT values and standard deviations were used in the $\Delta\Delta C_T$ calculations. Samples were analysed in triplicates. GAPDH was used as a reference gene. The mean C_T of GAPDH was subtracted from the mean C_T of each of the genes (control and IPTG treated) then the mean C_T of control (PBS) was subtracted

from the mean C_T of the IPTG treated $2^{-\Delta\Delta CT}$. Fold change in expression was calculated by the $2^{-\Delta\Delta CT}$ method [156].

3.2.3.7 Immunofluorescence Microscopy

MCF-7p14ARF and U2OSp14ARF cells were cultured on glass coverslips in 6well plates then treated with 5 mM IPTG for 72 h. Cells were fixed in freshly thawed 4% paraformaldehyde for 10 min at 37 ^{0}C. Cells were then washed with PBS and permeabilized by adding cold acetone for 3-5 min at -20 ^{0}C, blocked with 2% (v/v) BSA and 0.1% (v/v) PBS for 1 h at RT and labelled with primary antibodies overnight including Ki67 (1:400, Abcam, Sapphire), and p14ARF (1:300, Zymed-DKSH). Secondary antibodies were Alexa fluor 568 conjugated anti-mouse IgG (1:500, Invitrogen), Alexa fluor 488 conjugated anti-mouse IgG (1:500, Invitrogen) and Hoechst 33342 (trihydrochloride trihydrate 10mg/mL solution in water) (1:1000, Invitrogen) staining (1 h at RT) was used to visualize the nucleus. Slides were viewed on a Nikon A1 scanning confocal microscope. Objective specifications were: 60x, oil planApo, 1.40 N/A Perfect Focus System and Differential Interference Contrast (DIC). DAPI (EX 340-380nm), GFP-HQ (EX 420-440nm) and Texas Red (EX 542-580nm) fluorescent filter cubes were used.

3.2.4 Statistical analysis

Mass spectrometric data was processed using MaxQuant software (version1.0.13.13). SILAC LC-MS/MS analysis is presented in excel format. The hierarchal clustering was performed using the R programming package 3.2.3. The p53 signalling pathway analysis was performed using the KEGG pathway database. Statistical analysis was performed using the Perseus software platform

with two sample T-Test, P-value 0.05. Western blot images were analysed using a Bio-Rad imager.

3.2.5 Data Records

MCF-7 luminal breast epithelial cells (ATCC:HTB-22) were stably transfected with the tumour suppressor gene p14 alternative reading frame (p14ARF) using the LacSwitch™II inducible expression system and the methodology and validation of these cell lines is published in detail in [95, 171]. The SILAC/LC/MS/MS technology underlying the methodological design is schematically represented in Fig. 3.2. Mass spectrometric data was processed using MaxQuant software (version 1.0.13.13). The MS/MS data files were searched using Peaks Studio (version 8.5) against the Human Proteome database. The mass spectrometry proteomics data have been deposited to the ProteomeXchange Consortium via the PRIDE [174] partner repository with the dataset identifiers: SILAC triple-label accession PXD009334.

3.2.6 Technical Validation

Stable amino acid incorporation was verified by LC-MS/MS and demonstrated approximately 96% incorporation. All SILAC experiments were performed in duplicates at three time points (24 h and 72 h post p14ARF-p53 activation compared to vehicle control, PBS) and analysed using MaxQuant and the Perseus software platform. To validate the integrity of the datasets a heatmap was generated to compare the 24 h and 72 h proteomic changes pre- and post-p14ARF activation (Fig. 3.3A). The heat map shows high similarity of proteomic changes occurring at 24 h and 72 h. To generate a high confidence list of proteins, the identified proteins were further filtered to include only proteins present in

duplicate biological experiments. This filtered dataset is available in Suppl. Table 3.1 and a direct comparison of proteins expressed at 24 h and 72 h post p14ARF-p53 is graphically represented in suppl. Fig. 3.1. Volcano plots showing significant comparative changes are presented in Fig. 3.3B and 3.3C. Western blots of p53-p21 expression was performed in each experiment to confirm activation of the p14ARF-p53-p21 signalling pathway (Fig. 3.3 inset). Representative Western blots and immunofluorescence upregulated and downregulated proteins to validate the integrity of the SILAC protein expression are presented in Fig. 3.4. RT-qPCR was performed to further validate regulation and is presented in Fig. 3.4. Quantitative RT-PCR reactions were performed in triplicate and normalised to GAPDH expression. Fold change in expression was calculated by the $2^{-\Delta\Delta CT}$ method [156].

3.2.7 Usage Notes

Visual presentation of the workflow for this manuscript is schematically outlined in Fig. 3.2 and the data has been deposited in a centralized, standard compliant, and public repository. Data are available via ProteomeXchange with identifier: PXD009334 data. Gene Ontology (GO) software packages may be used to analyse biological functions post p14ARF-p53 activation. Suggested GO software includes the GO stats package in Bioconductor (http//www.bioconductor.org) and Cytoscape (http//www.cytoscape

.org).

3.3 Results and Discussion

3.3.1 SILAC/LC-MS/MS analysis of proteome changes in MCF-7 cells post p14ARF-p53

Here we explored p53-induced metabolic changes in breast cancer cells through activation of p14ARF-p53 by stably inducing the p14ARF gene in favourable cell culture conditions (DMEM containing 10% FCS). Snapshots of the proteome changes occurring at 24 h and 72 h post p14ARF-p53 activation by addition of 5mM IPTG were compared with control (no IPTG). The SILAC/LC/MS/MS technology underlying the methodological design is schematically represented in Fig. 3.2. After identifications at the 1% false FDR threshold the data generated by MaxQuant software was deposited into the PRIDE database [155]. To validate the integrity of the datasets a heat map was generated to compare the 24 h and 72 h proteomic changes pre- and post- p14ARF activation (Fig. 3.3A). The heat map shows high similarity of proteomic changes occurring at 24 h and 72 h. The identified proteins were further filtered to include only proteins present in both sets of biological replicates and observed in technical replicates in duplicate experiments. This filtered dataset is available in Suppl. Table 3.1 and a direct comparison of proteins expressed at 24 h and 72 h post p14ARF-p53 is graphically represented as volcano blots in Fig. 3.3B and 3.3C. The 30 most prominent downregulated and 50 upregulated proteins were analysed Cytoscape 3.0 software. A query in ClueGO from cytoscape 3.0 provided the molecular network interactions between the query proteins and most related proteins.

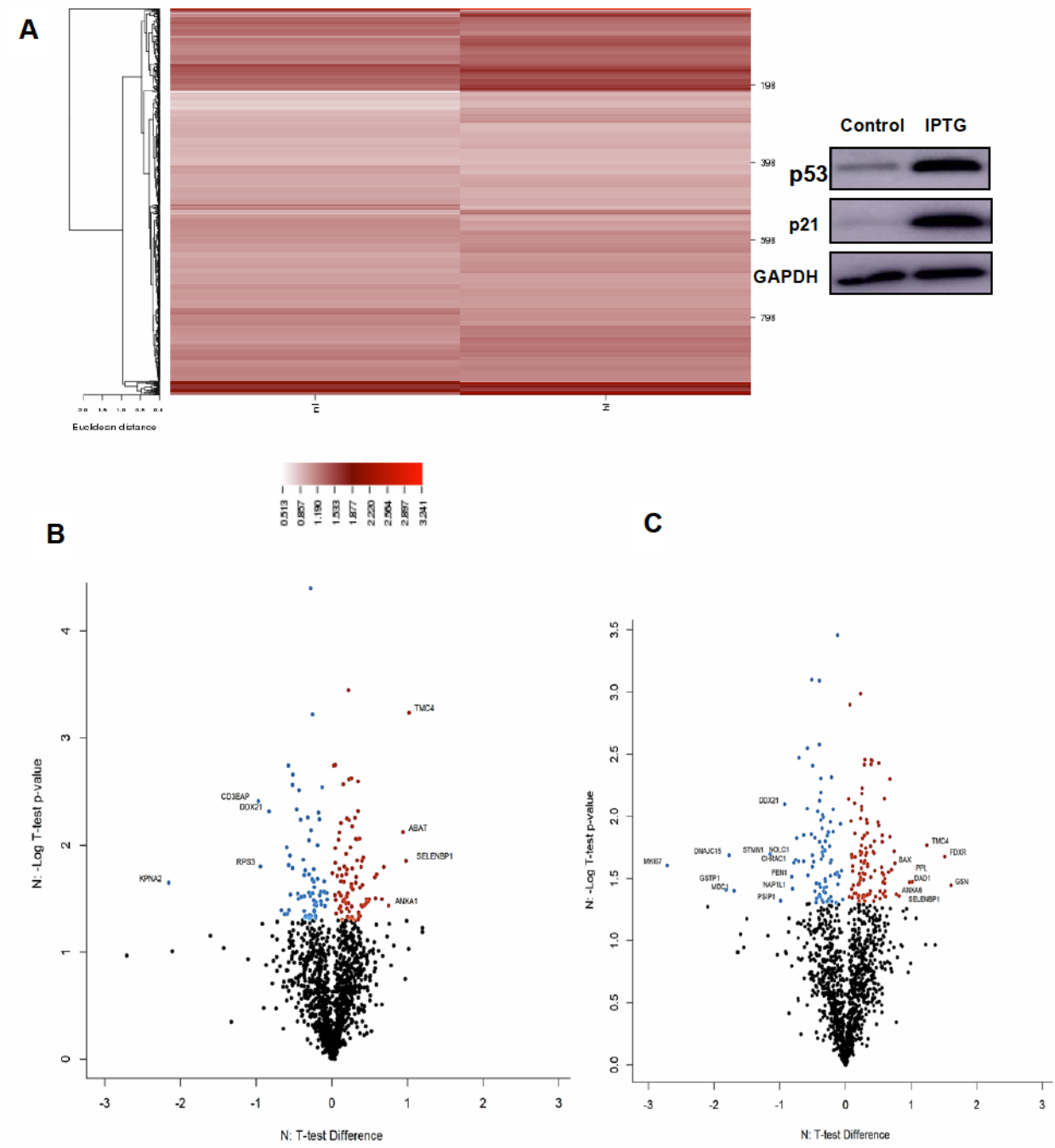


Figure 3.3. Comparative analysis of the global proteins 24 and 72 h post P14ARF-P53 activation. A. A heatmap was generated of hierarchal clustering of protein expression 24 h and 72 h post p14ARF induction in MCF-7 cells. **B.** and **C.** Volcano plots show significant changes in 5 mM IPTG (24 h) and 5 mM IPTG (72 h) respectively compared to control (PBS) (significant p-value <0.05). Blue and red dots are represented of proteins that were identified as significance and show down-regulation or up-regulation respectively. **Inset:** a representative Western blot showing p53-p21 comparative protein levels 24 h post p14ARF induction: GAPDH control.

3.3.2 Validation of p14ARF-p53 differentially regulated proteins at the translational and transcriptional level

Proteins identified as up- and down- regulated by SILAC-LC-MS/MS analysis were validated by immunofluorescence and Western blot in independent biological experiments at 24 h and 72 h post IPTG (p14ARF) activation. To determine if these proteins were regulated at the transcriptional level, RT-qPCR was also performed on the same treated cells at an earlier time-point, 15h post IPTG activation of p14ARF. Note: RT-qPCR was performed at the earlier timepoint of 15h to determine that transcriptional regulation preceded translation. Table 3.2 summarizes the main functions of the proteins validated in this section and referenced.

3.3.2.1 Confirmation of down-regulated protein

In this dataset Ki67, a marker for proliferation (used in breast cancer diagnosis) was validified by immunofluorescence at 24 h. As shown in Fig. 3.4A, induction of p14ARF using IPTG (red) correlated with downregulation of Ki67 (green), clearly indicating, after p14ARF induction, cells stopped proliferating. Downregulation of Ki67 was also verified at the transcriptional level by RT-qPCR (Fig. 4B). In the SILAC LC-MS/MS dataset, members of the minichromosome maintenance complex (MCM) proteins necessary for DNA replication were significantly downregulated. A representative of this family of MCM proteins, MCM4, was validated as downregulated at both 24 h and 72 h post p14ARF activation by Western blot (Fig. 3.4B). Downregulation of MCM4 was also observed at the transcriptional level by RT-qPCR (Fig. 3.4B). Due to antibody

availability and cost, only RT-qPCR was performed on A5 (annexin A5), DNA (cytosine-5)-methytransferase 1 (DNMT1), DnaJ heat shock protein family (Hsp40) Member C15 (DNAJC15) and mediator of DNA damage checkpoint protein 1 (MDC1) (Fig. 3.4B). Annexin A5, a marker of apoptosis did not change at the transcriptional level supporting the SILAC data where A5 at the protein level remained unchanged. Fig. 3.4B also confirmed transcriptional downregulation of DNMT1, associated with DNA methylation, DNAJC15, associated with negative regulation of mitochondrial respiration, MDC1, associated with DNA repair checkpoint.

3.3.2.2 Confirmation of up-regulated proteins

Similarly, confirmation of SILAC upregulated proteins was performed using Western blots and at the transcription level by RT-qPCR. The following proteins were upregulated at both the translational level and transcriptional level (Fig. 4C, D respectively) (Table 3.2): Gelsolin (GSN), associated with regulation of actin filament assembly; 3'-phosphoadenosine-5'-phosphosulfate synthase 2 (PAPSS2), a sulfation enzyme; Aldehyde dehydrogenase 4 family member A1 (ALDH4A1), a mitochondrial enzyme which oxidises pyrroline-5-carboxylate to glutamate; Members of the annexin family of proteins (Annexins A1, A2, A6), calcium regulators (see Table 3.2 for references). Ferredoxin reductase (FDXR), an iron sulfur protein that mediates $NADP^+$ oxidoreductase, was verified as upregulated at the protein level only (Fig.3.4C).

Table 3.2. Functions of significantly regulated proteins.

Protein	Key functions	Reference
ALDH4A1	Oxidises pyrroline-5-carboxylate to glutamate (mitochondrial)	[175]
PAPSS2	Sulfation enzyme	[176]
FDXR	Associated with the oxidative metabolism in the cell (mitochondrial)	[177]
GSN	Key regulator of actin filament assembly and disassembly	[178]
MCM4	Initiation of DNA replication	[179]
MKI67	Marker for proliferation used in breast cancer prognosis	[180]
DMT1	Maintenance of DNA methylation i.e. replication	[181]
MDC1	Checkpoint mediated cell cycle arrest in response to DNA damage within both the S phase and G2/M phases of the cell cycle	[182]
DNAJC15	Negative regulator of the mitochondrial respiratory chain.	[183]

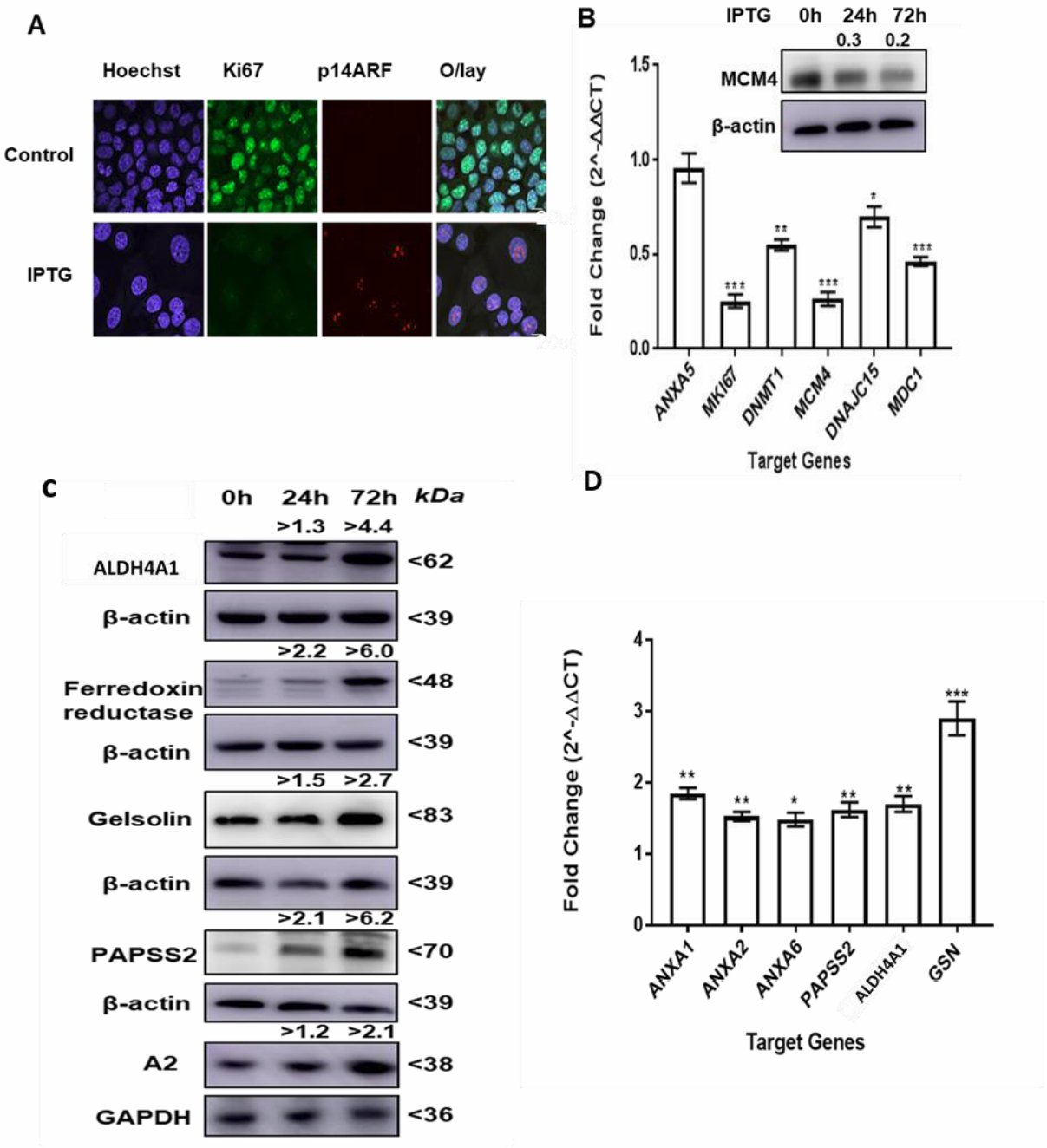


Figure 3.4. Validation of p14ARF-p53 regulated proteins. A. P14ARF activation correlates with Ki67 inactivation. Blue – DAPI nuclear staining, green – Ki-67, red – p14ARF, O/lay – overlay demonstrating discordance between p14ARF and Ki67. **B.** Graph represents Taqman RT-qPCR results for 5 downregulated genes (Ki67, DNMT1, MCM4, DNAJC15, and MDC1). **Inset:** Western blot shows validation of MCM4 at the protein level. Error bars show mean and sd+/- (*P<0.05). **C.** Validation of proteins overexpressed in the p14ARF-p53 signalling pathway, β-actin and GAPDH were used as loading

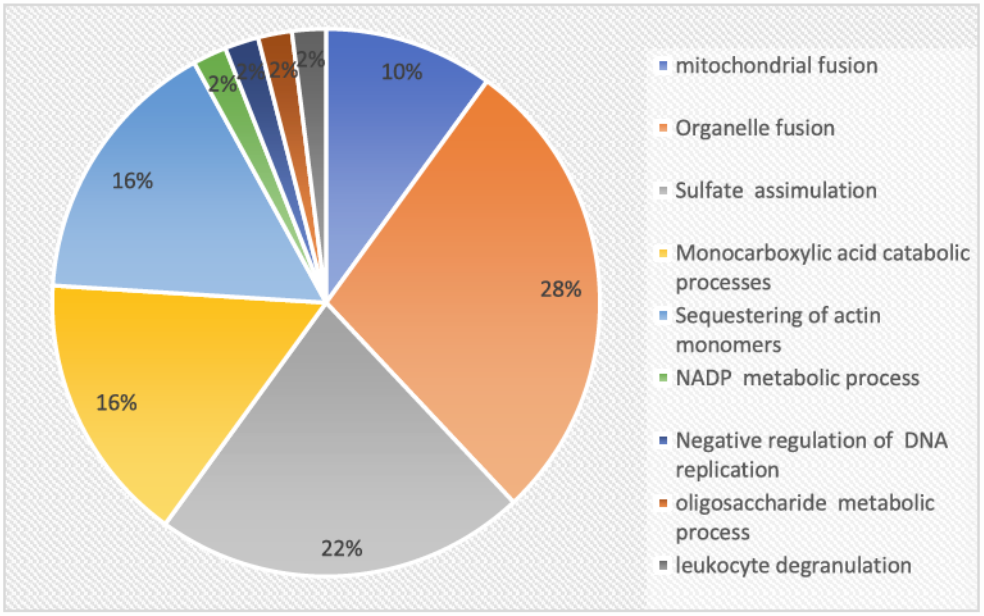
controls. The numbers on top of the blots are representative of fold changes with p-values <0.05. **D.** Graph represents Taqman RT-QPCR results for 6 genes (ANXA A1, A2, A6, PAPSS2, ALDH1A, and GSN) significantly upregulated in the p14ARF-p53 signalling pathway. The graph represents the fold-change in mRNA in IPTG-treated cells compared to cells treated with PBS. Error bars show mean and sd+/- (*P<0.05). These experiments were performed in biological replicates.

3.3.3 Activation of p14ARF-p53 resulted in unique up- and down- regulated proteins

Gene Ontology (GO) analysis based on the top 50 upregulated proteins from the SILAC dataset and the bottom 30 significantly downregulated proteins is illustrated in Fig. 3.5A and Fig. 3.5B, respectively. Some of top downregulated proteins have been previously identified but we found unique significantly downregulated proteins which were associated cell cycle arrest, DNA regulation and anti-apoptotic pathways (3.5A). Unique significantly upregulated proteins were associated with changing metabolic processes in the cell (3.5B). In this dataset members of the annexin family and associated members were identified as being differentially regulated by activation of the p14ARF-p53 pathway and these were further investigated and form Chapter 4 of this thesis.

In addition, the REACTOME pathway database was used to analyse signalling pathways associated with p14ARF-p53 activation, Fig. 3.6. A further indication of how re-introducing one gene, p14ARF to activate p53, can enforce global changes in cell signalling and cell function in breast cancer cells. We have previously published a series of (knockdown) KD experiments in our laboratory where KD of p53 results in no effect on p21. KD of p21 reverts the p53 effects on cell proliferation and cell morphology. P53 is essential for p21 induction in MCF-7 cells [27].

A



B

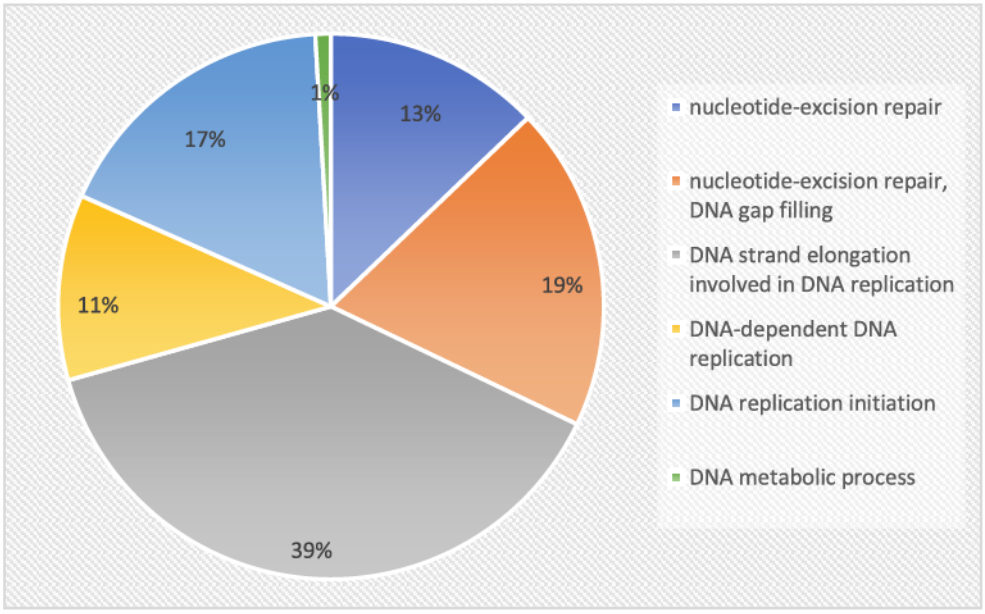


Figure 3.5. Cytoscape 3.0 analysis of p14ARF-p53 regulated proteins using ClueGO. A) Pie graph of biological processes identified for the bottom 30 downregulated proteins. The functions of the bottom 30 downregulated proteins included DNA replication, DNA repair and nucleotide excision repair. B) Pie graph identified relevant biological processes of the top 50 upregulated proteins. The functions of these top 50 upregulated proteins included mitochondrial fusion, organelle fusion, sulphate assimilation, monocarboxylic acid catabolic processes, sequestering of actin monomers and other metabolic processes.

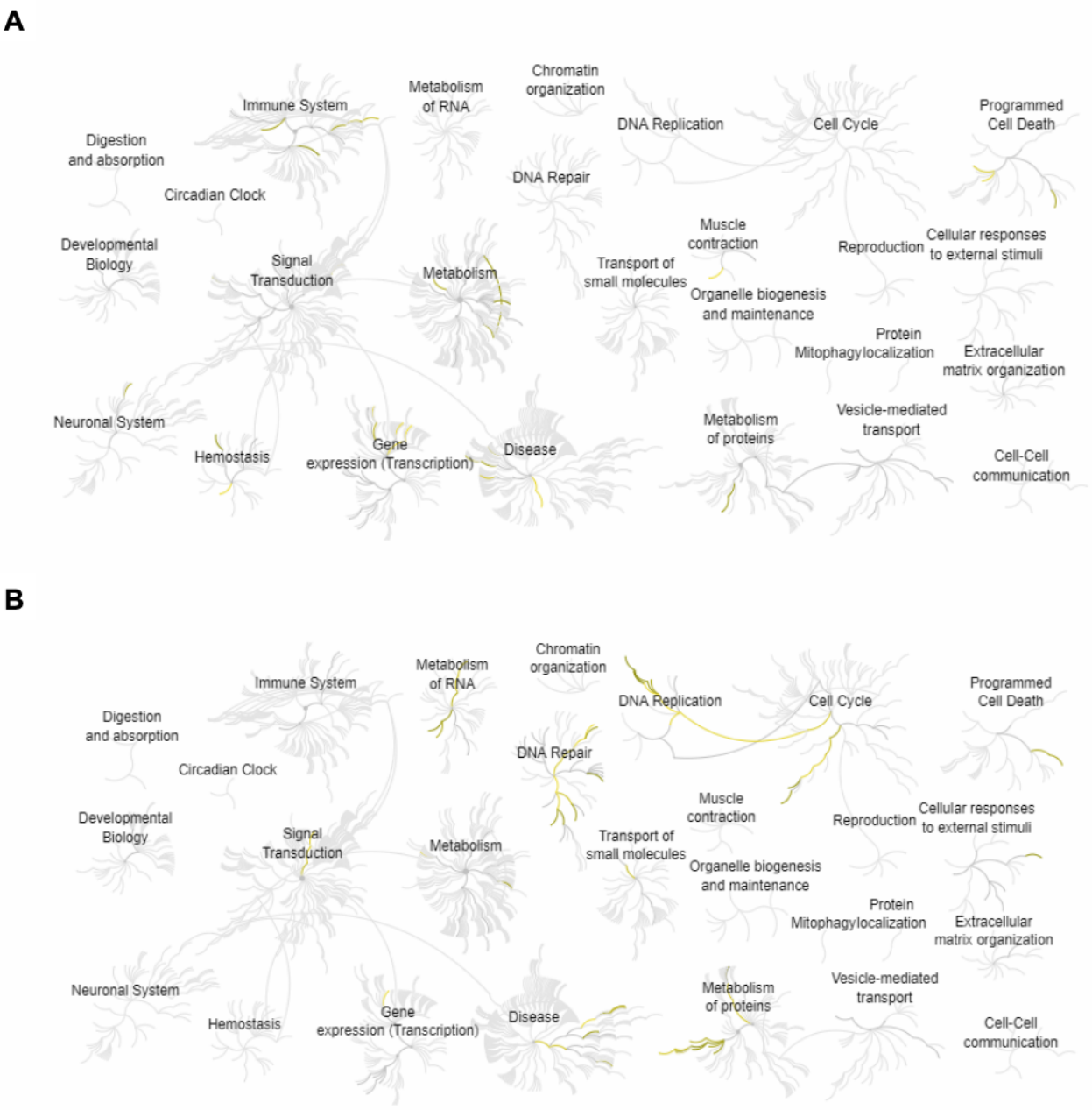


Figure 3.6. Differential regulation of signalling pathways post p14ARFp53 activation in breast cancer cells. The REACTOME pathway database was utilised to reconstruct the p14ARF-p53 signalling pathways as determined by proteomic changes induced in our p14ARF-p53 cell model. The top 50 up regulated **A.** and the bottom 50 down regulated proteins **B.** were used to determine significant changes in p14ARF-p53 cell signalling. Each colour represents different pathways. There are distinct non-overlapping signalling pathways between the pathways initiated by proteins overexpressed **A.** and proteins downregulated **B.** in the p14ARF-p53 dataset. To determine pathways

that are activated post p14ARF-p53 activation these can be visualized by going through the link then on the coloured nodes.

In conclusion, using SILAC and LC-MS/MS proteomics Specific downregulated proteins were associated with cell cycle arrest, DNA repair, and anti-apoptosis whereas, specific upregulated proteins were associated with differentiation and changes in cell metabolism after reactivation of p14ARF-p53 in ER+ breast cancer cells.

Acknowledgement: The SILAC LC-MS/MS was generated with the help of Daniel Yagoub. Data analysis, verification of the data (Western blots and imaging) was performed by Diana Hatoum. Design and editing of the manuscript was mainly compiled by Diana Hatoum as part of this thesis. I would like to thank A.A. for help with the statistical analysis.

Author contributions

Diana Hatoum – first author, performed repeat experiments and wrote and edited the paper.

Daniel Yagoub – performed preliminary experiments.

Alireza Ahadi – consultation.

Eileen McGowan – conceived and edited the paper.

Chapter Four

Annexin/S100A Protein Family Regulation through p14ARF-p53 Activation: A Role in Cell Survival and Predicting Treatment Outcomes in Breast Cancer

Certificate of authorship and originality

This paper was published in PLOS ONE Journal. I certify that the work present in this chapter has not previously been submitted as part of the requirements for a degree. I also certify that I carried out the majority of the work presented in this paper.

Principal supervisor

Dr Najah Nassif

Production Note:
Signature removed
prior to publication.

Date: 05-06-2018

Diana Hatoum

Production Note:
Signature removed
prior to publication.

Date: 05-06-2018

Abstract

The annexin family and S100A associated proteins are important regulators of diverse calcium-dependent cellular processes including cell division, growth regulation and apoptosis. Dysfunction of individual annexin and S100A proteins is associated with cancer progression, metastasis and cancer drug resistance. This manuscript describes the novel finding of differential regulation of the annexin and S100A family of proteins by activation of p53 in breast cancer cells. Additionally, the observed differential regulation is found to be beneficial to the survival of breast cancer cells and to influence treatment efficacy. We have used unbiased, quantitative proteomics to determine the proteomic changes occurring post p14ARF-p53 activation in estrogen receptor (ER) breast cancer cells. In this report we identified differential regulation of the annexin/S100A family, through unique peptide recognition at the N-terminal regions; demonstrating p14ARF-p53 is a central orchestrator of the annexin/S100A family of calcium regulators in favour of pro-survival functions in the breast cancer cell. This regulation was found to be cell-type specific. Retrospective human breast cancer studies have demonstrated that tumours with functional p53 respond poorly to some chemotherapy agents compared to tumours with a non-functional p53. Given that modulation of calcium signalling has been demonstrated to change sensitivity of chemotherapeutic agents to apoptotic signals, in principle, we explored the paradigm of how p53 modulation of calcium regulators in ER+ breast cancer patients impacts and influences therapeutic outcomes.

4.1 Introduction

Breast cancer sub-types are defined by their molecular heterogeneity and pathological profiles and therapeutic options, response to treatment, and prognosis are based on the diagnosis and classification of tumours into one of the different sub-types [184]. Resistance to treatment and recurrence of breast cancer eventually occurs in many patients leading to the need for combinational treatments, which are associated with an increase in adverse side effects, decreased quality of life and increased morbidity. Latent recurrence is prevalent, particularly in estrogen receptor α (ERα) breast cancers, and is associated with dormancy after treatment, as reviewed in [185]. Treatment options such as radiotherapy and chemotherapy induce tumour suppressor pathways, such as p53, to facilitate cell cycle arrest and cell death (apoptosis) [186-190]. Novel therapies that mimic p14ARF, a tumour suppressor and an upstream regulator of p53, are now in anti-cancer pre-clinical and clinical trials [144, 145]. Albeit, there is growing evidence to strongly suggest that re-expression of the p53 protein protects cells from apoptosis [186, 187]. Retrospective human breast cancer studies show tumours with functional p53 respond more poorly to some chemotherapeutic agents when compared to tumours with non-functional p53 [191-193]. Chemotherapy responses in mouse models with p53 show induction of growth arrest, and cellular senescence, but not cell death, resulting in minimal tumour regression and early relapse, hence supporting the findings of poorer responses to chemotherapy in the presence of p53 [187]. Prior studies have suggested that p53 binds to ER as a strategy to prevent apoptosis in ER+ breast cancers [112, 121, 126]. Our laboratory has demonstrated that activation of the

p53-p21 pathway by p14ARF, in addition to rapid induction of cell cycle arrest, initiated a change in cellular metabolism consistent with a metabolically active senescence-like phenotype most likely to be important in cell survival and recurrence [95]. In our studies, the cancer cells maintained cell viability, and a sub-set of these cells retained the ability to proliferate [27, 95]. Dormant and senescent cells may be more resistant to cancer treatments so the more we understand about the behaviour of these cells, the more likely we will be able to understand how cancers develop resistance to current treatments and, importantly, how they recur after treatment.

To gain an understanding of the proteomic fluctuations occurring in breast cancer cells post p14ARF-p53-p21 expression, we employed stable isotope labelling of amino acids in cell culture (SILAC) and tandem mass spectrometry techniques (LC-MS/MS) [194]. This technology allowed the direct comparison of the cellular proteome of breast cancer cells pre- and post-activation of the p53 pathway. From the broad based proteomic changes detected, we describe a unique snapshot profile analysis of the differential regulation of the annexin and S100A calcium binding associated protein family members through p14ARF-p53-p21 activation in breast cancer cells. This family of proteins are important regulators of normal cellular function, including cell division, growth regulation and apoptosis [195]. The conserved core calcium/membrane binding unit of these proteins has been described as a means to peripherally tether proteins to membranes, potentially to enable the annexins to organize membranes, thus promoting membrane segregation, vesicle fusion and vesicle trafficking in a calcium dependent manner. Conversely, the unique N-terminus of the individual annexins allows functional diversity [195]. Annexins are consistently deregulated in cancer

[196] and particular annexins have been associated with different cancer types and as potential clinical biomarkers [196, 197]. However, the literature on dysregulation of annexin protein expression in breast cancer is contentious. Deregulation of individual annexins and S100A proteins have been associated with malignant transformation [198-202], tumour invasion [203-205], metastasis, angiogenesis and drug resistance [196, 206, 207], the effect being dependent on breast cancer sub-type.

This report identifies changes in the annexin and associated S100A family in breast cancer, brought about by p14ARF-p53-p21-activation. Given that individual annexins and S100A proteins have been implicated in cancer initiation and progression, and modulation of calcium signalling has been demonstrated to change sensitivity of chemotherapeutic agents to apoptotic signals[208], we further investigated how the combined overexpression of annexins/S100A proteins, as identified in this study, may contribute to treatment resistance and breast cancer recurrence and metastasis. In principle, we have explored the paradigm of how modulation of calcium regulators through p53 activation may impact on therapeutic options.

4.2 Materials and Methods

4.2.1 Cell lines and culture

MCF-7 breast cancer epithelial cells (American Type Culture Collection (ATCC) HTB-22) and U2OS osteosarcoma cells (ATCC HTB-96) were stably transfected with p14ARF using the LacSwitch™ inducible vector system as previously described [152, 153]. MCF-7p14ARF and U2OSp14ARF cells were selected based on hygromycin B (hB) and Geneticin (G418) resistance respectively. Cells were maintained in hB (200 mg/ml) and G418 (200 mg/ml) to ensure selection of inducible p14ARF. Expression of p14ARF was induced in both cell lines using 5mM tissue culture grade Isopropyl β-D-1-thiogalactopyranoside (IPTG) (Promega) dissolved in phosphate buffered saline (PBS). Cells were routinely cultured in Dulbecco's Modified Eagle Medium (DMEM, high glucose), with 10% (v/v) foetal bovine serum (FBS). All cell lines were routinely tested for mycoplasma (Lonza MycoAlert).

4.2.2 SILAC and LC-MS/MS methodology

The method for SILAC metabolic triple labelling has been described previously [155]. Labelled amino acids, dialyzed foetal bovine serum (FBS), and lysine and arginine-free media (SILAC media) were purchased from Silantes GmbH. Sequencing grade modified porcine trypsin (Promega) was used for all cell passages in labelled medium.

Cells were cultured in SILAC media supplemented with 10% dialyzed FBS and either 'light', unlabelled lysine and arginine; 'medium' lysine-4 ($^{2}H_4$-lysine) and arginine-6 ($^{13}C_6$-L-arginine); or 'heavy' lysine-8 ($^{13}C_6$ $^{15}N_2$-L-lysine) and arginine-10 ($^{13}C_6$ $^{15}N_4$-L-arginine). Proteins were metabolically labelled in their respective

SILAC medium for a minimum of 6 doubling times and stable amino acid incorporation was verified by LC-MS/MS analysis prior to treatments and demonstrated approximately 96% incorporation of labelled amino acids (data not shown). Cells cultured in 'medium' and 'heavy' SILAC medium were treated with 5 mM IPTG to induce p14ARF and cells were harvested for protein isolation at 24 h and 72 h respectively. Cells cultured in 'light' SILAC medium were treated with PBS (vehicle) and did not express p14ARF (method outlined in Fig. 4.1).

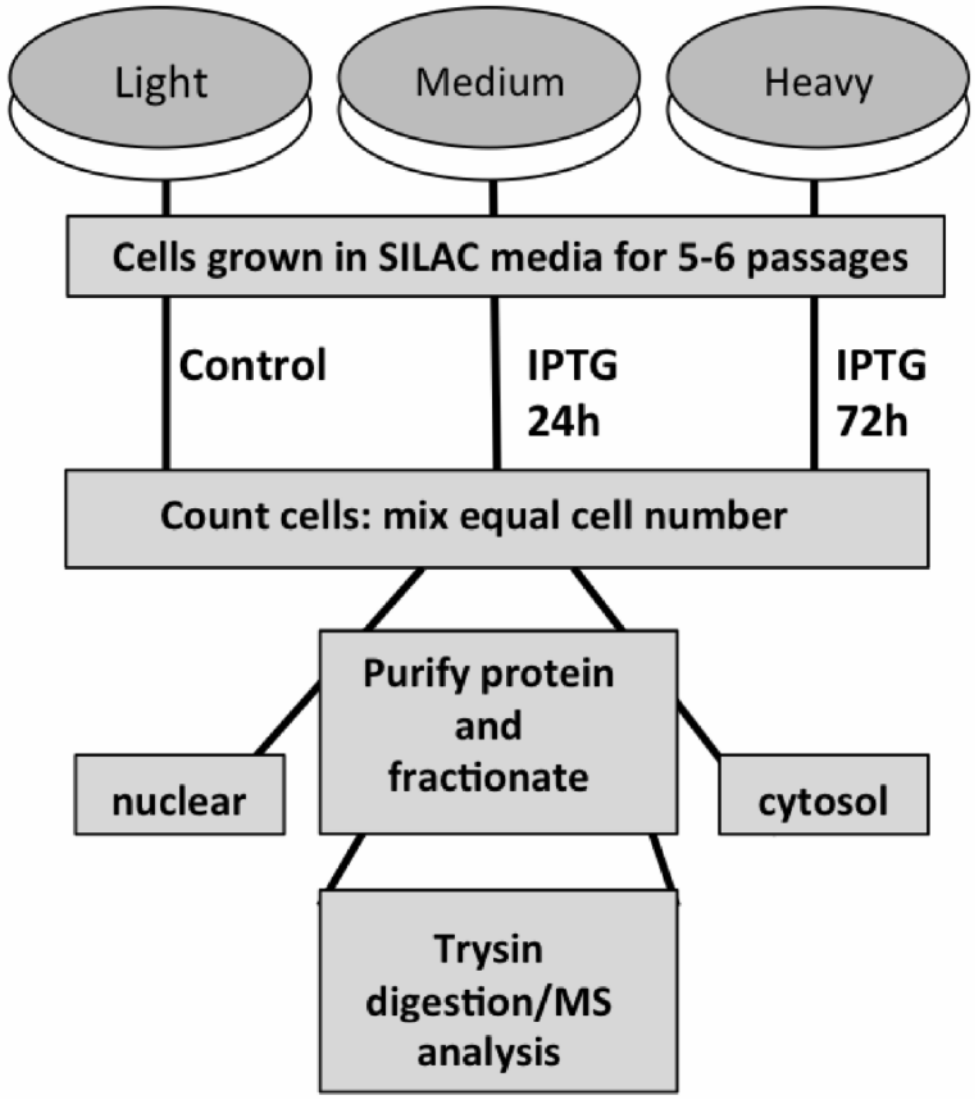


Figure 4.1. Triple labelling SILAC for proteomic analysis pre- and post p14ARF-p53-p21 activation. MCF-7 cells were split and triple-labelled with three differentially labelled ('light', 'medium', and 'heavy') media formulations as previously described[155]. Proteins were metabolically labelled for a minimum of 6 doublings in lysine- and arginine-free DMEM medium containing 10% ($^{v}/_{v}$) dialyzed FBS and supplemented with either: (a) 'light', unlabelled lysine and arginine; (b) 'medium' lysine-4 ($^{2}H_4$-lysine) and arginine-6 ($^{13}C_6$-L-arginine); or (c) 'heavy' lysine-8 ($^{13}C_6$ $^{15}N_2$-L-lysine) and arginine-10 ($^{13}C_6$ $^{15}N_4$-L-arginine). Cells cultured in 'medium' and 'heavy' medium were treated with 5mM IPTG for 24 h and 72 h respectively to induce p14ARF expression. Cells cultured in 'light' isotopic medium were treated with PBS. On harvesting, cells were counted, and

equal numbers of cells were combined at a 1:1:1 ratio. Lysates were fractionated into nuclear and cytoplasmic fractions for better peptide coverage. Cell lysates were separated by electrophoresis and in-gel tryptic digestion was carried out prior to analysis by high-resolution mass spectrometry [155]. Treated cells were harvested, counted and equal numbers of cells were combined from the different SILAC labelled cells in a 1:1:1 ratio and protein extracted. The extracted protein underwent quantitative proteomic analysis by tryptic digestion followed by tandem mass spectrometry (LC MS/MS) [155].

4.2.3 Data analysis

To generate a high confidence list of proteins, biological duplicate experiments were performed with the triple labelling strategy, with each biological replicate subsequently being subjected to mass spectrometric analysis twice, producing technical replicates. Mass spectrometric data was processed using MaxQuant software (version 1.0.13.13). MS/MS spectra were searched with the MASCOT search engine against the decoy IPI-human database (forward and reverse sequences) with a peptide and protein false discovery rate of 0.01 as described previously[155]. After identifications at the 1% false discovery rate (FDR) threshold were made, identified proteins were filtered. For inclusion into the filtered dataset, proteins had to be present in both sets of biological replicates and observed at least twice in technical replicates in duplicate experiments. The STRING database [209], in conjunction with GeneMania [210], was used to analyse the p53/p21/annexin/S100A network associated biological effects. *In silico* pathway-based exploratory multivariate analysis, analysing associations between the differential annexin regulation seen and treatment outcomes using available patient data from 4142 breast cancer patients with a mean follow up of 69 months, was performed using the Kaplan-Meier Plotter (KMPlot) for breast cancer [211].

4.2.4 Protein analysis and western blot

Protein isolation and western blot analysis were performed as described previously [95]. Primary antibodies used were p53 (DO-7, Dako, CA, USA), p21 (c-19, Santa Cruz), ANXA A1, ANXA A2 (Becton Dickinson) and β-actin (Abcam),

followed by mouse secondary conjugated antibody (Abcam). Protein abundance was quantified by image analysis using the Kodak image station 4000 MM.

4.2.5 Immunofluorescence microscopy

MCF-7p14ARF and U2OSp14ARF cells were cultured on glass coverslips in 6-well plates for 24 h and then treated with 5mM IPTG for 72 h. Cells were fixed in freshly thawed 4% paraformaldehyde for 10 min at 37 ^{0}C, washed with PBS then permeabilized by the addition of cold acetone for 3–5 min at -20 ^{0}C. Cells were then blocked with 2% (v/v) BSA and 0.1% (v/v) PBS for 1 h at RT and labelled with primary antibodies overnight. Primary antibodies were Ki67 (1:400, Abcam, Sapphire) and p14ARF (1:300, Zymed-DKSH). Cells were washed with PBS at RT with gentle rocking for 1 h prior to incubation for 1 h at RT with secondary antibodies. Alexa fluor 568 conjugated anti-mouse IgG (1:500), Alexa fluor 488 conjugated anti-mouse IgG (1:500) and the nuclear stain Hoechst 33342 (trihydrochloride trihydrate 10mg/mL solution in water) (1:1000) were purchased from Invitrogen. Coverslips containing cells were washed and mounted on slides with glycerol based mounting medium. Slides were viewed on a Nikon A1 scanning confocal microscope. Objective specifications were: 60x, oil planApo, 1.40 N/A Perfect Focus System and Differential Interference Contrast (DIC). DAPI (EX 340-380 nm), GFP-HQ (EX 420-440 nm) and Texas Red (EX 542-580 nm) fluorescent filter cubes were used.

4.2.6 RT-qPCR analysis

RNA was extracted using RNAzol (Molecular Research Centre Inc., Cincinnati, OH, USA). RNA (1µg) was reverse transcribed using the High-Capacity cDNA Reverse Transcription Kit (Life Technologies). Quantitative RT-PCR reactions

were performed in triplicate in 96-well MicroAmp Fast Optical plates (Applied Biosystems) in a QuantStudio 12K Flex System (Applied Biosystems), using pre-designed and optimized TaqMan gene expression assays (Applied Biosystems). TaqMan Gene Expression Assays used were ANXA1, Hs00167549_m1; ANAX2, Hs01561520_m1; ANXA5, Hs00996187_m1, ANXA6, Hs00XXX_m1 and normalized to GAPDH (Hs02758991_g1) expression. Fold change in expression was calculated by the $2^{-\Delta\Delta Ct}$ method [156].

4.3 Results

4.3.1 Differential regulation of the expression of the annexin/S100A protein family post p14ARF-p53-p21 activation

We have previously reported that activation of the p14ARF-p53 pathway in MCF-7 cells leads to cell cycle arrest, without inducing apoptosis, and, additionally, induces a metabolically active senescent-like phenotype [95]. To further explore the underlying mechanisms that lead to cell cycle arrest and metabolic/phenotypic changes we used SILAC LC-MS/MS methodology to determine the proteomic profile of MCF-7 cells post activation of p14ARF-p53 at 24 h and 72 h. Re-expression of p14ARF had no effect on the estrogen response in these cells (Fig.4.2 inset). Mass spectrometric data processed with MaxQuant software using a stringent filtered dataset, as described in materials and methods, identified 1265 differentially regulated proteins in duplicate experiments. Only proteins identified in biological duplicates in this triple labelling experiment were included to ensure a high confidence list. Linear regression analysis performed on the 1265 proteins demonstrated a strong correlation coefficient value for the 24 h and 72 h data (0.79 and 0.72 respectively using the two independent datasets) (Fig. 4.2). Most of the proteins did not show a significant difference in expression (Fig. 4.2: 0.7:1.3 ratio). A ratio of <0.7 (downregulated) and >1.3 (upregulated) was considered to be significantly different[212]. Among the top 50 upregulated proteins, annexins A1, A2, A4, A6, S100A10, S100A11 and S100A13 were significantly upregulated at 24 h ($P<0.05$) and 72 h ($P<0.05$). Annexin A9 was upregulated at 72 h only ($P<0.05$). The expression of annexins

A5 (an important calcium-dependent regulator of apoptosis), A7, A11, S100A6 and S100A14 remained unchanged at both time points. The SILAC LC-MS/MS analysis of the annexin family and S100A associated proteins is listed in Suppl. Table 4.1.

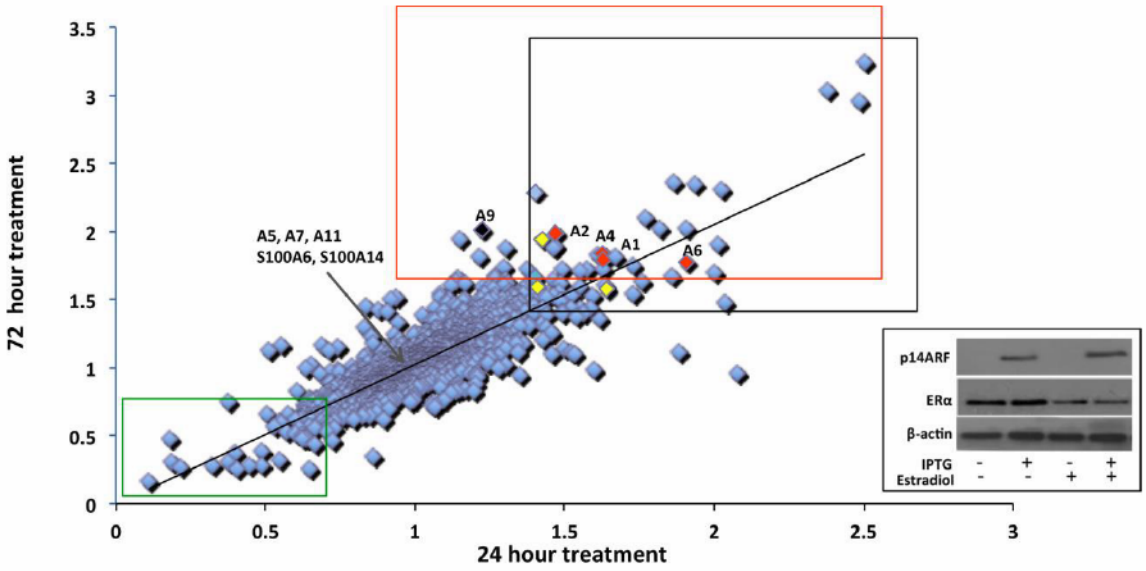


Figure 4.2. Linear regression analysis of Annexin and S100A protein expression 24 h and 72 h post p14ARF-p53-p21 activation. MCF-7 cells were treated with IPTG (5mM) to induce the p14ARF-p53 signalling pathway. A filtered set of 1265 proteins was analysed for two independent biological experiments with technical replicates at 24 h and 72 h post activation. The correlation coefficient value for the 24 h and 72 h data for biological duplicate experiments showed a strong correlation (0.79 and 0.72 respectively). The black box highlights proteins significantly over-expressed p<0.05) post p14ARF-p53-p21 activation at 24 h and maintained at 72 h. The green box highlights proteins significantly downregulated at 24 h and maintained at 72 h post treatment. The red box highlights proteins significantly upregulated at 72 h. The red cubes represent annexin proteins (A1, A2, A4, A6) significantly upregulated at 24 h and maintained at 72 h; the black cube represents annexin A9 significantly upregulated at 72 h (P<0.05). Yellow cubes represent S100A10, S100A11 and S100A13 proteins significantly upregulated at 24 h and maintained at 72 h. Annexins A5, A7, A11, S100A6 and S100A14 are expressed and not regulated (between ratios 0.8–1.1). Inset: Western blot shows the expression of p14ARF and ER status in MCF-7 cells pre- and post IPTG and β-estradiol treatment at 24 h.

4.3.2 Annexin peptide sequences detected by SILAC LC-MS/MS map to unique N-terminal regions of annexin proteins

There is a high degree of sequence similarity among the annexin protein family members. The annexin proteins retain a conserved core structural region, containing a Ca^{2+} binding site, and responsible for the Ca^{2+}-dependent binding of the proteins to phospholipids, however, individual annexin family members possess unique N-terminal domains, a feature underscoring the functional diversity of individual annexins[195]. Annexin peptides identified by SILAC LC-MS/MS analysis (Table 4.1) were mapped to the annexin protein sequences using the Clustal Omega and sequence coverage of the annexins ranged from approximately 12–50% (Table 4.1). The alignment of the annexin sequences listed in the SILAC LC-MS/MS data demonstrated the positioning of peptides to the N-terminal region, which contains amino acid sequences unique to individual annexin family members (Fig. 4.3). No overlap of the annexin peptides, as identified by SILAC/MS/MS, was observed confirming the unique identification and differential regulation of individual annexin family members through the activation of p14ARF-p53-p21.

Table 4.1: SILAC data showing differential expression of the Annexins and associated S100A proteins at 24 and 72 hours post p14ARF induction.

ID	Protein	24h Ratio M/L	72h Ratio H/L	Peptides	Sequence Coverage (%)
IPI00218918	**A1**	1.6	1.8	14	49.7
IPI00418169	**A2**	1.5	2.0	35	71.7
IPI00793199	**A4**	1.6	1.8	7	24.9
IPI00329801	**A5**	1.1	1.1	17	44.4
IPI00221226	**A6**	1.9	1.8	19	13.1
IPI00002460	**A7**	1.1	1.2	5	12.3
IPI00008714	**A9**	1.2	2.0	6	20.3
IPI00414320	**A11**	0.9	1.2	5	10.6
IPI00395627	**S100A6**	0.8	0.8	6	33.8
IPI00183695	**S100A10**	1.4	1.9	3	32.0
IPI00013895	**S100A11**	1.4	1.6	9	63.8
IPI00016179	**S100A13**	1.6	1.6	12	28.6
IPI00010214	**S100A14**	0.99	1	4	46.2

A1-A11 = Annexins A1-A11; S100A = S100A calcium binding protein. Grey highlights indicate no significant regulation at 24 h post p14ARF induction (significance threshold ≥ 1.4).

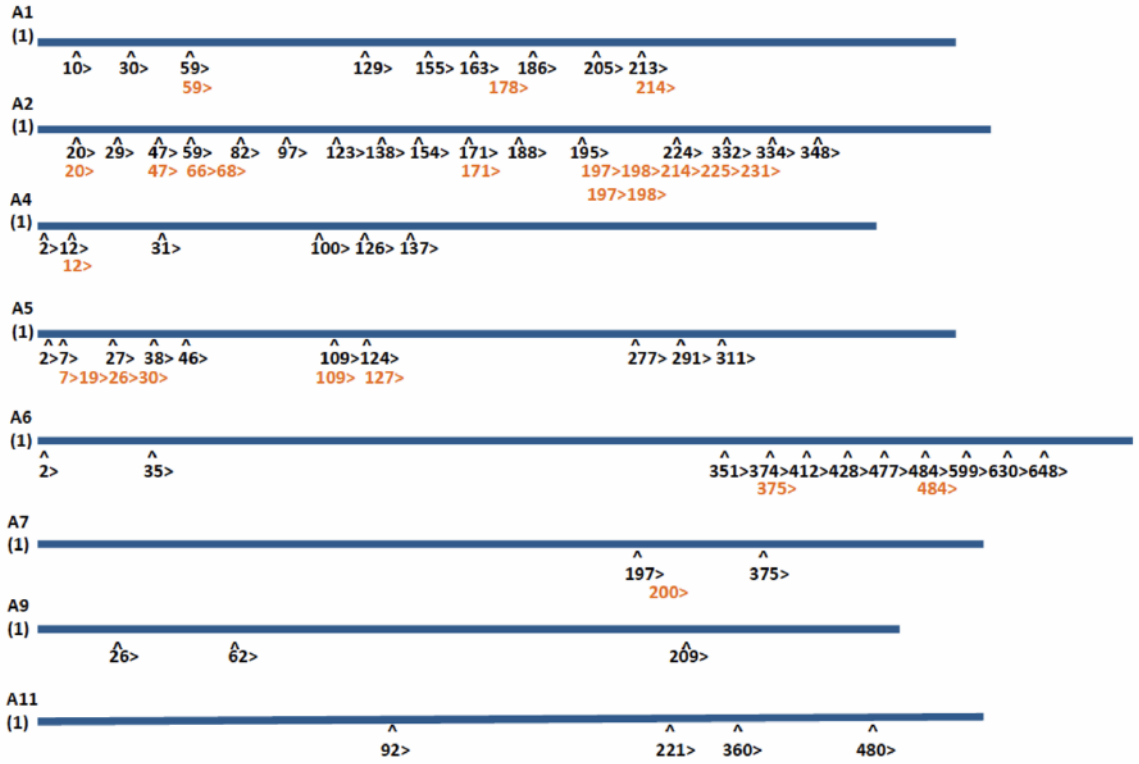


Figure 4.3. Alignment of annexin peptides identified by MaxQuant with the annexin protein sequences. Unique annexin peptide sequences identified by SILAC-based mass spectrometric analysis were aligned to the N-terminal region of annexins A1, A2, A4, A5, A6, A7, A9, and A11. The number 1 represents the start “M” (methionine) codon, or first amino acid of the protein. Each arrow identifies a unique peptide identified by SILAC LC/MS/MS. The numbers in black indicate the start of the peptide and the orange numbers indicate the overlap of different peptide sequences.

4.3.3 Differential regulation of annexin expression in MCF-7 cells post p14ARF-p53 activation occurs at the transcriptional level

To determine if the changes in the annexin protein expression observed were reflected at the transcription level, RT-qPCR was performed at 15h post-p14ARF-p53 induction using specific annexin Taqman probes. The results showed significant upregulation of ANXA1, ANXA2 and ANXA6 ($P<0.01$) mRNA expression, whereas ANXA5 expression remained unchanged (Fig. 4.4). This is consistent with the SILAC protein quantitation data, which showed upregulation of A1, A2 and A6 proteins with no change in the A5 protein level (Table 1.1).

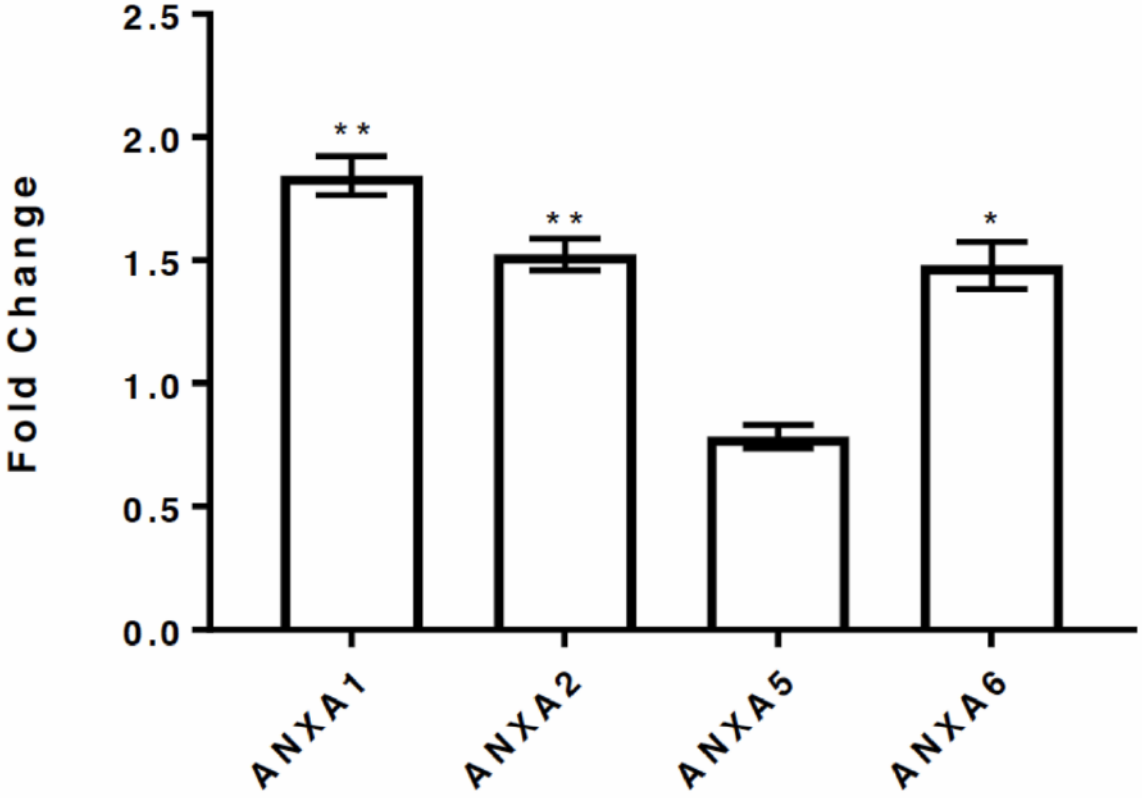


Figure 4.4. Differential regulation of Annexin A1, A2, A5 and A6 expression at the transcriptional level in MCF-7 breast cancer cells. p14ARF expression was induced by the addition of 5mM IPTG for 15h. Quantitation of ANXA1, ANXA2, ANXA5 and ANXA6 expression was analysed at 15h post p14ARF induction using the Taqman fast master mix and pre-optimized primer and probe sets. Data were normalized to levels of the reference gene glyceraldehyde-3-phosphate dehydrogenase (GAPDH). Data have been expressed as fold change in expression post p14ARF induction by IPTG at the 15h time point relative to control ($2^{-\Delta\Delta Ct}$). Experiments were performed in duplicate in which each set of experiments contained technical triplicates. Statistical differences between groups were determined using a two tailed, paired t-test. *$p < 0.02$, **$p < 0.003$ respectively.

4.3.4 Functional significance of alterations in the p53-p21-annexin network signaling

As we have strong evidence implicating p53 in the control of annexin and S100A protein expression, we sought to determine how changes in the expression of this family of proteins could influence cell physiology. Using the STRING (v10) database we first searched for strength of the interactions between TP53 (p53) and CDKN1A (p21) and the 13 annexin and S100A proteins. The predicted interactome scores for the protein-protein interactions are shown in the score ladder in Table 4.2. Unsurprisingly, there is a strong relationship between TP53 and CDKN1A as shown in the score ladder (Table 4.2), with a very high score of 0.999 (the highest predictive score being 1.0). ANXA1, ANXA2 and ANXA4 directly and strongly interact with TP53 with scores of 0.871, 0.946 and 0.867 respectively. Although ANXA5 is the annexin protein most commonly associated with p53 function, the predicted interactome scores for both TP53 and CDKN1A revealed a lower score of 0.744. ANXA6 and ANXA9 did not reveal direct interaction with TP53 and CDKN1A (Fig. 4.5A). Therefore, the prediction from the STRING analysis demonstrated that not all the ANXAs/S100A family interacted directly with TP53 or CDKN1A.

Table 4.2. p53/p21/annexin/S100A interactome scores for the protein to protein interactions from STRING database.

Protein 1	Protein 2	Accession for protein 1	Accession for protein 2	Score
TP53	CDKN1A	ENSP00000269305	ENSP00000244741	0.999
S100A10	ANXA2	ENSP00000357799	ENSP00000346032	0.999
CDKN1A	TP53	ENSP00000244741	ENSP00000269305	0.999
ANXA2	S100A10	ENSP00000346032	ENSP00000357799	0.999
S100A11	ANXA1	ENSP00000271638	ENSP00000257497	0.983
ANXA1	S100A11	ENSP00000257497	ENSP00000271638	0.983
TP53	ANXA2	ENSP00000269305	ENSP00000346032	0.946
ANXA2	TP53	ENSP00000346032	ENSP00000269305	0.946
TP53	S100A6	ENSP00000269305	ENSP00000357708	0.93
S100A6	TP53	ENSP00000357708	ENSP00000269305	0.93
TP53	ANXA1	ENSP00000269305	ENSP00000257497	0.871
ANXA1	TP53	ENSP00000257497	ENSP00000269305	0.8
TP53	ANXA4	ENSP00000269305	ENSP00000377833	0.8
ANXA4	TP53	ENSP00000377833	ENSP00000269305	0.8
S100A6	ANXA11	ENSP00000357708	ENSP00000265447	0.8
ANXA11	S100A6	ENSP00000265447	ENSP00000357708	0.8
S100A6	ANXA2	ENSP00000357708	ENSP00000346032	0.7
ANXA2	S100A6	ENSP00000346032	ENSP00000357708	0.7
TP53	ANXA5	ENSP00000269305	ENSP00000296511	0.7
ANXA5	TP53	ENSP00000296511	ENSP00000269305	0.7

Note: The highest predictive score is 1.0.

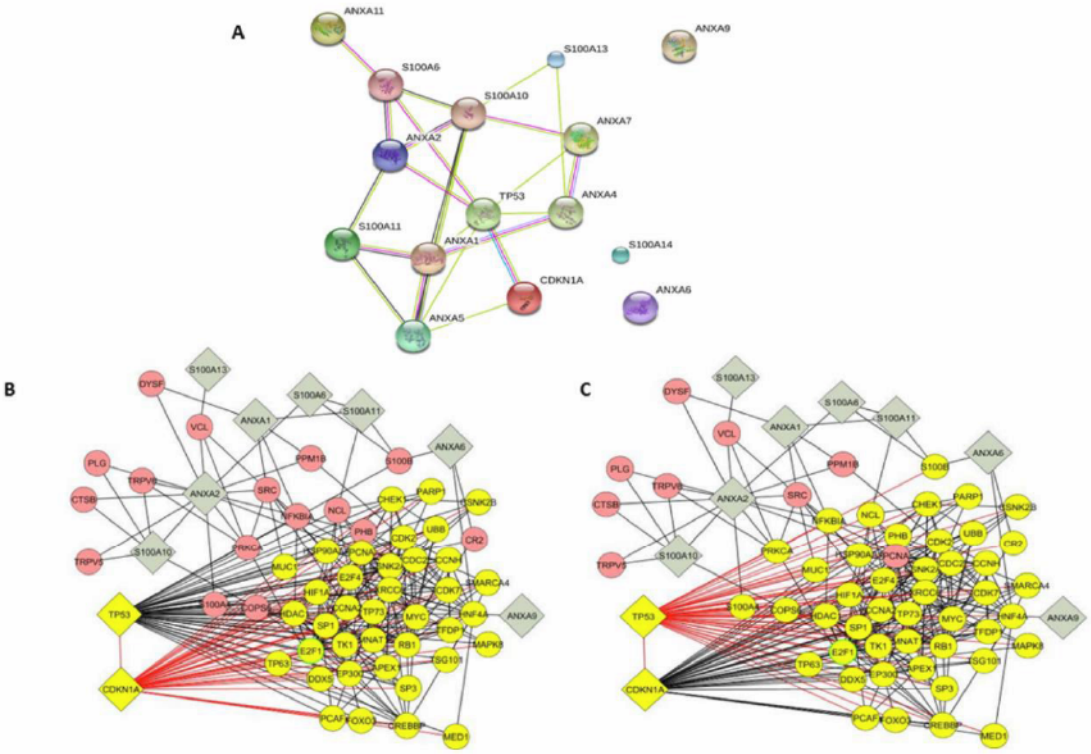


Figure 4.5. Schematic representation of the p53/p21/annexin/S100A interactome. TP53 and CDNK1A, and their association with ANXA A1, A2, A4, A5, A6, A7, A9, A11 and S100A -6, -10, -11, -13 and -14 were analysed using the STRING database (v10.0) and the Cytoscape Mimi PLUGIN. **A.** Each node represents all the proteins produced by a single protein-coding gene locus, whereby a small node signifies a protein of unknown 3D structure and a large node denotes a protein where some 3D structure is known or predicted. Coloured nodes indicate query proteins and first shell interactors. Coloured edges (lines) represent interactions between proteins: light blue—known interactions from curated databases; purple—experimentally determined interactions; green—predicted interactions between gene neighbourhood; red—gene fusions; dark blue—gene co-occurrence; light green–represents text mining; black—co-expression; grey—protein homology. **B.** and **C.** Highlighted in yellow are the direct common interactions between CDNK1A and TP53. The annexins and S100A interactions are highlighted in grey. Linkages were analysed using two methods. **B.** TP53 interactions: black lines, CDKN1A red lines. **C.** TP53 red lines and CDKN1A black lines (summarized in Suppl. Table 4.2).

Further, we used the Cytoscape platform to determine the TP53 and CDKN1A and annexin interactive functions. These are predicted functions drawn from known interactions from curated databases or have been experimentally determined. Functional analysis showed TP53 and CDKN1A share many common interactions as distinctly shown in Fig.4.5B and 4.5C, and Suppl. Table 4.2. Again, using this program, we show a close association between all the ANXAs/S100A and TP53 and CDKN1A with only 2–3 degrees of freedom (Fig. 4.5B and 4.5C). Specifically, these are illustrated by CR2 and HNF4A, which directly interact with TP53 and CDKN1A and directly interact with ANXA6, however ANXA6 does not directly interact with either TP53 or CDKN1A (Fig. 4.5B and 4.5C and Suppl. Table 4.2). Similarly, ANXA9 directly interacts with HNF4A by not CDKN1A or TP53. The full gene description, function and processes of the p53-p21-annexin/S100A interactome are presented in Suppl. Table 4.2.

4.3.5 Predicted changes in cellular dynamics associated with annexin/S100A expression post p53 activation

The annexins are calcium-dependent phospholipid binding proteins and Metscape analysis of the annexin/S100A families identified in this report showed similar and compensatory functions of the family members as outlined in Table 4.3. The annexin family members and the S100A binding proteins have shared protein domains and the GeneMANIA program was used to predict potential degeneracy, or substitution through alternative physical interaction, co-localization and genetic interactions (Table 4.4). Changes in annexin binding or interacting partners lead to changes or alterations in cellular function, dependent upon the annexin in question. An example from this report is that of annexin A2,

predicted to physically interact with both S100A10 and S100A6. However, p53 activation leads to a preferential increase in A2 and S100A10 levels, therefore, in the absence of increases in any of the other A2 binding proteins, A2 would preferentially bind to S100A10. Consequently, the formation of increased levels of the A2/S100A10 complex will promote the cellular functions mediated by this complex, which is to bind to cytoskeletal components associated with intracellular fusion [213]. Annexin A4, also upregulated through p53 activation, is also associated with membrane fusion [214]. Whether A4 and A2/S100A10 are complementary or compensatory mechanisms is yet to be shown.

Table 4.3: Annexin protein function analysed using the MetScape Plugin in Cytoscape.

Protein	Functions
A1	Calcium-dependent phospholipid binding, phospholipid binding, lipid binding, extracellular organelle, extracellular vesicle exosome, extracellular membrane-bounded organelle, lipase inhibitor activity, vesicle fusion.
A2	Calcium-dependent phospholipid binding, phospholipid binding, lipid binding, extracellular organelle, extracellular vesicle exosome, extracellular membrane-bounded organelle, vesicle fusion.
A4	Calcium-dependent phospholipid binding, phospholipid binding, lipid binding, lipase inhibitor activity, calcium ion binding.
A5	Calcium-dependent phospholipid binding, phospholipid binding, lipid binding, extracellular organelle, extracellular vesicle exosome, extracellular membrane-bounded organelle, lipase inhibitor activity.
A6	Calcium-dependent phospholipid binding, phospholipid binding, lipid binding, extracellular organelle, extracellular vesicle exosome, extracellular membrane-bounded organelle.
A7	Calcium dependent protein binding, lipid binding.
A9	Phospholipid binding.
A11	Calcium dependent protein binding.
S100A6	Calcium dependent protein binding, calcium ion binding, regulation of fibroblast proliferation, ruffle.
S100A10	No independent function listed
S100A11	Ruffle
S100A13	Calcium ion binding

Grey shading denotes no change in annexin and S100A protein expression.

Table 4.4: Cytoscape (GeneMANIA) analysis of overexpression of Annexins and associated S100A partners defining the physical interactions; co-localisation and genetic interactions post p14ARF induction.

Protein	Physical interaction	Co-localise	Genetic interactions
A1	S100A11	S100A11, A11	A2
A2	S100A10, S100A6	NO	A1
A4	NO	A9	A5, A11
A5	NO	S100A10	A4
A6	NO	NO	NO
A7	S100A10	NO	NO
A9	NO	A4	NO
A11	S100A6	A1, S100A11	A4, A11
S100A10	A2 and A7	A10	A2
S100A11	A1	A1, A11	NO
S100A13	NO	NO	NO

All annexin and associated S100A proteins are co-expressed. Annexins have shared protein domains and the S100A proteins have shared protein domains. Physical interactions, co-localization and genetic interaction analysis was completed using Cytoscape GenMANIA plugin. Grey shading highlights proteins that are not regulated by ARF-p53.

4.3.6 Regulation of annexin expression is cell type specific

To determine if annexin expression was regulated by p53 in other cell types, we examined the effects of p53 activation in two distinct and functionally different cell lines, U2OS, an osteosarcoma cell line and MCF-7 breast cancer cells. Immunofluorescence microscopy showed P14ARF expression in the nucleolus in both cell lines post IPTG treatment (Fig. 4.6A and 4.6B). p14ARF expression correlates with downregulation of the proliferation marker Ki-67 in the same cells (Fig. 4.6A and 4.6B). We compared annexin A1 and A2 protein expression, both of which are important regulators of normal breast cell physiology [213, 215, 216], breast cancer progression and are associated with more aggressive and invasive cancer phenotypes [205]. Using specific annexin (A1 and A2) antibodies, we detected p14ARF-p53 induced upregulation of A1 and A2 proteins in MCF-7 cells (Fig. 4.6C) but no significant change in these protein levels was observed in the U2OS p14ARF cells. Interestingly, higher basal levels of A1 and A2 were detected in U2OS cells compared to MCF-7 cells (Fig. 4.6C). Activation of p14ARF-p53-p21 was confirmed by western blot analysis of p53 and p21 in the same experiments (Fig. 4.6C). This lack of annexin regulation by p53 in U2OS cells was also confirmed at the transcriptional level by RT-qPCR analysis (Fig. 4.6D). Differential annexin regulation was unique to MCF-7 cells and not a common feature of other cell types. This adds further evidence that regulation of annexin expression by p14ARF-p53 is strongly associated with specific annexin-mediated cell functions. Interestingly, one common feature of both cell lines (U2OS and MCF-7) was that calcium dependent apoptosis through annexin A5 was not regulated by p53 at either the transcriptional or translational level.

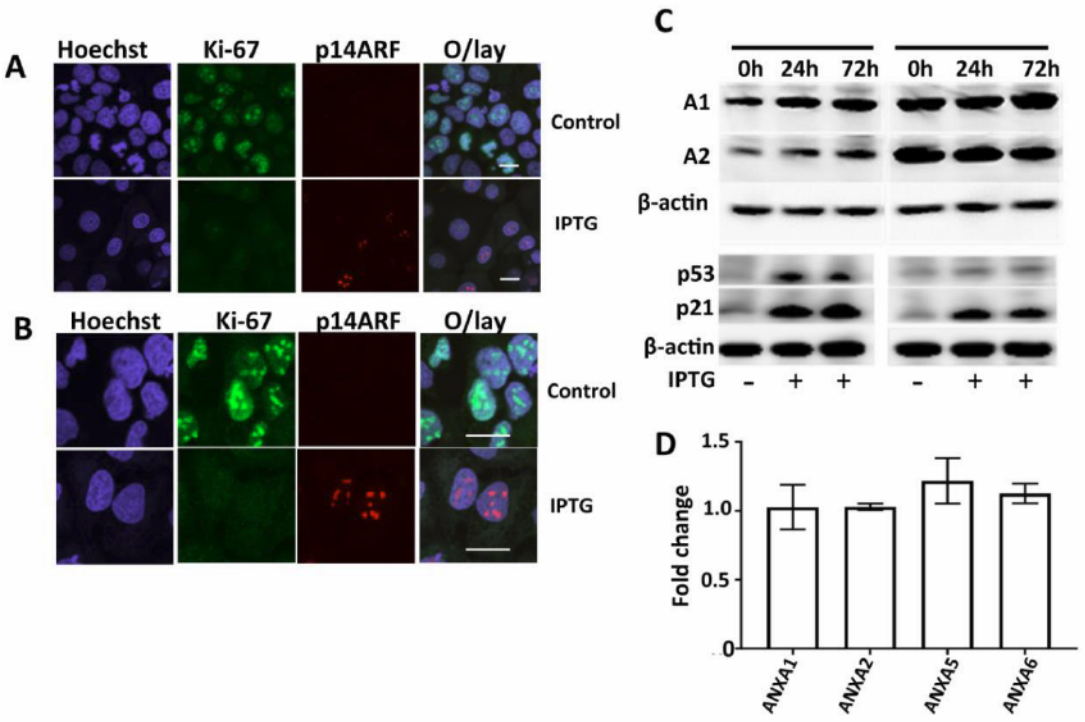


Figure 4.6. Differential regulation of Annexin A1, A2, A5 by p14ARF-p53 occurs in MCF-7 but not in U2OS osteosarcoma cells. p14ARF expression was induced in MCF-7p14ARF and U2OSp14ARF cells by the addition of 5mM IPTG at 15h 24 h and 72 h, PBS was added to control cells. Expression and localization of p14ARF expression in **A.** U2OS cells, **B.** MCF-7 pre- and post IPTG induction using immunofluorescence microscopy. **C.** Top panel shows a representative western blot analysis of annexin A1 and A2 protein expression in MCF-7 and U2OS cells at 24 h and 72 h time points after p14ARF induction. β-actin was used as a loading control. The MCF-7p14ARF and U2OSp14ARF protein samples shown are from the same western blot. Bottom panel, p21, a p53 transcriptional target, was used to confirm p53 activation in the cell lysates. β-actin was used as a loading control. **D.** Gene expression of p14ARF was induced by the addition of 5mM IPTG for 15 h in U2OSp14ARF cells. Vehicle control contained PBS in place of IPTG. Transcriptional regulation of ANXA1, ANXA2, ANXA5 and ANXA6 was analysed at 15h post p14ARF induction using RT-qPCR. Data were normalized to the reference gene glyceraldehyde-3-phosphate dehydrogenase (GAPDH). Data have been expressed as fold change in expression post p14ARF induction relative to the control ($2^{-\Delta\Delta Ct}$). Experiments

were performed in duplicate in which each set of experiments contained technical triplicates. Statistical differences between groups were determined using a two tailed, paired t-test.

4.3.7 Association between p53 induced annexin-S100A overexpression and treatment outcomes in breast cancer: Analysis by individual protein expression status

Dysregulation of the expression of individual annexins has been associated with breast cancer development and poor prognosis, and modulation of calcium signalling by p53 has been associated with lack of sensitivity to chemotherapy and radiotherapy [196, 198, 203, 217-221]. Pre-clinical validation of prognostic gene candidates in a large independent cohort is a prerequisite for the development of robust biomarkers. To evaluate the potential prognostic value of elevated annexin/S100A protein levels, as identified in this study, we performed a meta-analysis using a publicly available breast cancer patient mRNA expression database (accessed from the website *Kmplot.com*) [211]. The available breast cancer patient data from the Kaplan Meier website, which consists of 4142 patients with a mean follow up of 69 months, was categorized in treatment sub-groups as indicated in Fig. 4.7A and the number of patients in each cohort is also provided. Cohorts were also compared to a filtered sub-set of patients with ER+/p53 status (Fig. 4.7B), to determine if patients harbouring p53 had a better or poorer prognosis. We aimed to assess how p53 induced upregulation of annexin/S100A would affect the following clinical outcomes: Relapse Free Survival (RFS), Distant Metastasis Free Survival (DMFS), and Overall Survival (OS), both in untreated and treated ER+ (luminal A) breast cancer patients. The first set of Kaplan-Meier plot analyses were conducted to determine how elevated expression of individual annexins and S100A family

members (i.e. ANXA1 ANXA2 ANXA4 ANXA6 ANXA9 S100A10 S100A11 S100A13) would influence response of ER+ patient cohorts to conventional treatments (Fig. 4.7A). Associations between individual annexin/S100A expression data and predicted clinical outcome were categorized according to patient treatment regimes of (A) combined endocrine therapy and chemotherapy (Endo/C), (B) tamoxifen therapy (Tam), (C) chemotherapy alone (Chemo), (D) endocrine therapy alone (Endo), (E) combined tamoxifen and chemotherapy (Tam+C) and (F) untreated (UNTR). All finding and associations are summarized in Fig. 6.7. For simplicity, the predicted survival data has been portrayed as a heat chart whereby the green bars represent a positive prognosis; a negative prognosis by the pink bars and a neutral or non-significant outcome represented the yellow bars (Fig. 4.7).

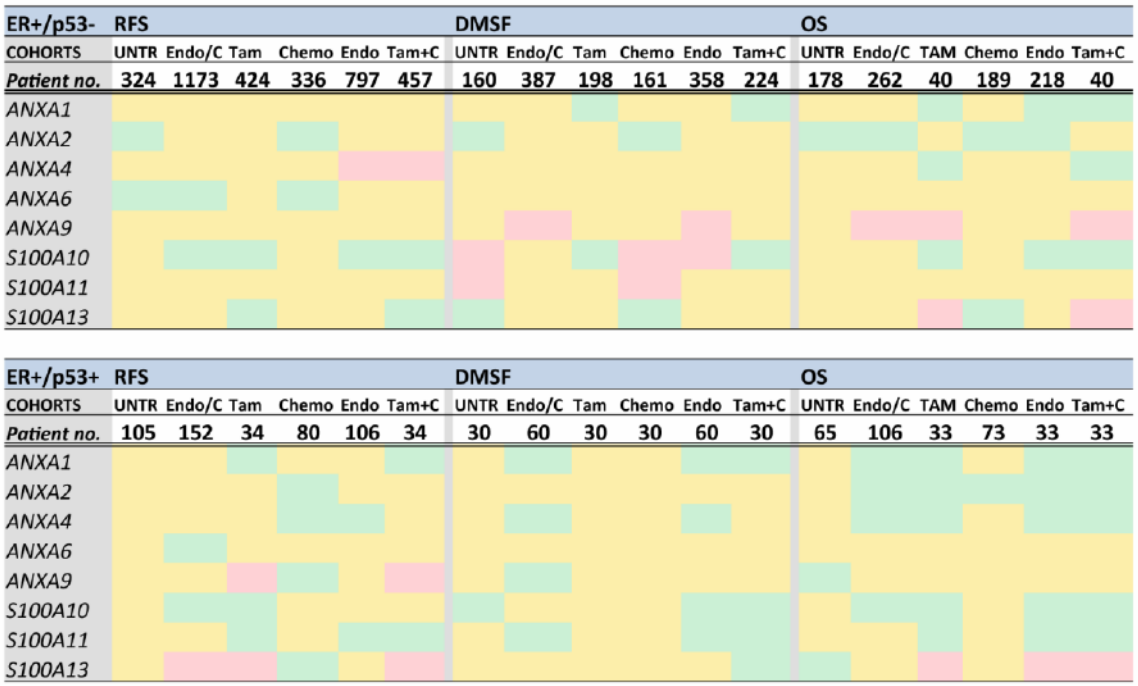


Figure 4.7. The effect of p53 and individual upregulated annexins on patient prognosis. Kaplan-Meier analysis [211] was used to predict breast cancer patient survival (RFS, DMSF and OS) post p53 induction and upregulation of individual annexins: ANXA1, ANXA2, ANXA4, ANXA6, ANXA9 and S100A10, S100A11 and S100A13. A comparison was made between ER+ patients (A), and a sub-set of patients with ER+/p53 (B). A hazard ratio of 95% confidence intervals and the log-rank P-value ($P<0.05$) was determined for differences in survival for each treatment option outcome and the results are represented as a heat chart: green = positive prognosis; pink = negative prognosis and yellow neutral (the median was used as a cut off). The number of patients in each treatment sample is shown. Abbreviations: RFS = Relapse free survival; DMFS = Distant metastasis free survival; OS = Overall survival; UNTR = untreated; Endo = endocrine; Tam = Tamoxifen, C and chemo = chemotherapy.

Using the Kaplan-Meier plot for breast cancer treatment outcome, there were distinct differences in how patients responded to specific therapies dependent on their annexin gene expression profile (Fig. 4.7). In general, a more positive DMSF and overall outcome was predicted in the sub-set of patients where tumours were documented as expressing ER+/p53. With reference to Fig. 4.7A, only expression of annexin A9, and S100A13 predicted poor overall survival when endocrine therapies were used for treatment. In the sub-set of patients that expressed ER+/p53, only S100A13 was shown to be a predictor of poor overall survival (Fig. 4.7B).

4.3.7.1 Association of p53 induced annexin-S100A overexpression and breast cancer treatment outcome: Analysis by combined annexin expression status

To determine whether cluster analysis of the differentially regulated annexins and S100A genes (Fig. 4.8A) would confer any concessionary changes on patient prognostic outcome, we used an unbiased combinational approach, which assessed treatment outcome based on the overall (combined) annexin and S100A overexpression profile in ER+ breast cancer patients (Fig. 4.8B). In comparison to the analysis of individual annexins, the first observation was that, overall, patient prognosis was significantly improved when all upregulated gene expression changes (annexin + S100A) were taken into account, and this was independent of treatment regime (compare Figs 4.7 and 4.8B). The most striking difference was when the ER+/p53+ sub-group was analysed with the same parameters. Significantly improved outcomes (RFS, DMSF and OS) were observed with tamoxifen treatment alone, or when tamoxifen was included in the treatment regime (compare Fig. 4.8B, 4.8C, 4.8D and 4.8E). Representative

Kaplan-Meier plots comparing the difference in ER+ patient outcome (Fig. 4.8D) with the ER+/p53+ (Fig. 4.8E) patient subset when patients are treated with endo+chemo whereby a significant improvement in time to relapse is observed in the presence of p53.

A

Affymetrix ID	Gene ID
201012_at	ANXA1, LPC1, ANX1
201590_x_at	ANXA2, ANX2L4, CAL1H, LPC2D, ANX2, LIP2
201301_s_at	ANXA4, ANX4
200982_s_at	ANXA6, ANX6
210085_s_at	ANXA9, ANX31
200872_at	S100A10, CAL1L, 42C, CLP11, ANX2LG, P11
200660_at	S100A11, S100C
	S100A13

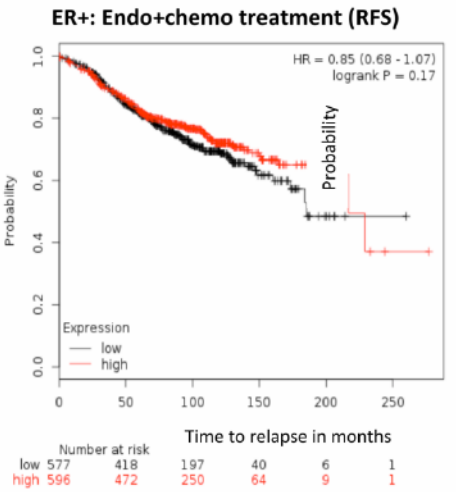
B

ER+	RFS		DMSF		OS	
Treatment	Patient no.	P-value	Patient no.	P-value	Patient no.	P-value
Untreated	324	0.26	160	0.14	178	0.25
Endo+chemo	1173	0.3	387	0.3	262	0.06
Tam	424	0.39	198	0.16	40	0
Chemo	336	0.19	161	0.14	189	0.23
Endo	797	0.48	358	0.27	218	0.07
Tam+chemo	457	0.1	224	0.08	40	0

C

ER+/p53wt+	RFS		DMSF		OS	
Treatment	Patient no.	P-value	Patient no.	P-value	Patient no.	P-value
Untreated	72	0.12	30	0.16	65	0.11
Endo+chemo	152	0.011	60	0.041	106	0.001
Tam	34	0.0024	30	0.049	33	0.001
Chemo	80	0.099	30	0.16	73	0.18
Endo	106	0.0041	60	0.04	98	0.001
Tam+chemo	34	0.0024	30	0.049	33	0.001

D



E

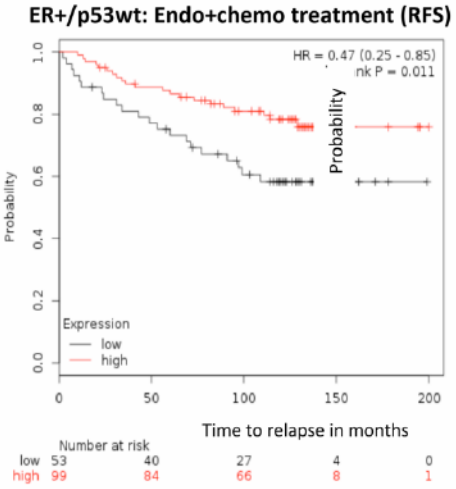


Figure 4.8. Effect of p53 and all upregulated annexins and S100A genes (annexin expression profile) on ER+ patient prognosis. Kaplan-Meier analysis [211] was used to predict breast cancer patient survival (RFS, DMSF and OS) post p53 and upregulation of all combined annexins/S100A genes (Fig. 4.8A). A comparison was made between ER+ patients (B), and a sub-set of patients with ER+/p53 (C). A hazard ratio with 95% confidence intervals and the log-rank P-value (P<0.05) was determined for differences in survival for each treatment option outcome and the results are represented as a heat chart: green = positive prognosis; pink = negative prognosis and yellow neutral (the median was used as a cut off). The number of patients in each treatment sample is shown. (D) and (E) show comparative representative Kaplan-Meier plots of

relapse free survival (RFS) for ER+ (D) and ER+/p53+ (E) patients treated with Endo + chemo therapies. The x-axis shows the number survival months from diagnosis. The red line represents patients with high annexin/S100A expression, and the black line represents patients with low annexin/S100A expression.

4.4 Discussion

Approximately two-thirds of all breast cancers harbour the p53 protein. Contrary to a long-held belief that favourable chemotherapy outcome is dependent upon p53-mediated apoptosis [222], some reports suggest a less favourable outcome for p53 breast cancers [126, 187]. Our previous studies have demonstrated that p53 induces a viable, metabolically active senescence-like cellular phenotype which supports the paradigm that p53 may be protective against apoptosis in breast cancer cells [27, 95]. This has been partly explained by the concept that p53 interacts with ER to protect cells against apoptosis, yet how p53 activity hinders chemotherapy response is not clear. In order to accurately predict clinical response, we need to understand the cellular changes occurring in response to activation of the p53 pathway. Regulating calcium signalling is essential for mammary gland function and deregulation of calcium homeostasis is associated with cancer pathophysiology. It has been difficult to determine how these calcium-dependent multi-faceted annexin proteins are regulated due to the sequence similarity of the annexin family of proteins and their compensatory functions within the cell. However, using SILAC LC-MS/MS methodology, we could identify unique peptides within the N-terminal region of the individual annexin proteins and show how p53 regulates the expression of members of this protein family. Our bioinformatic analysis of p53-induced upregulation of protein expression showed a strong association between ANXAs/S100A and either TP53 (p53) or CDKN1A (p21). This aligns with previous findings showing that p53 transcriptional regulation of p21 is a link to its pro-survival function and is opposed to the A5 induced cell death, reviewed in Clarke et al, 2015 [223]. These findings

support a renewed study of p53 as a central regulator of normal cellular function and pathophysiology. This report is the first to demonstrate p14ARF-p53 as a key central orchestrator of the annexin/S100A family of calcium regulators in favour of pro-survival functions in the breast cancer cell, in contrast to the activation of the canonical annexin A5 pro-apoptotic response usually associated with this tumour suppressor function. In the two cell lines studied, the annexin A5 pro-apoptotic pathway was not activated by p14ARF-p53.

The annexins A1, A2, A4, A6 and A9, and annexin binding proteins S100A10, S100A11 and S100A13 were in the top 50 proteins upregulated by p14ARF/p53, as evidenced by SILAC-based analysis. Although the function(s) of each annexin is not clearly defined, annexin-Ca^{2+} regulation is unquestionably important in a wide range of both intra- and extracellular functions that require interaction with the acidic phospholipids of the intracellular compartment of all membranes and Ca^{2+} signalling [195].

4.4.1 Annexins in normal physiology and breast cancer

The annexin A2/S100A10 complex, the abundance of which is increased by p53 activation, plays a role in membrane organization, membrane trafficking, in promoting ion conductance across membranes [195], and in calcium redistribution from bone to breast [224-226]. Annexin A4 has recently been shown to be involved in plasma membrane remodelling, through regulation of the actin cytoskeleton, and in cellular cholesterol homeostasis [227]. The role of annexin A6 as a membrane organizer is further supported by a recent study [228]. These observations are consistent with the changes we have observed in the architectural reorganization of the cytoskeleton of MCF-7 cells post

p14ARF/p53/p21 activation [27], suggesting annexin regulation via this pathway may be a normal cellular process in breast physiology.

Aberrant calcium signalling is often linked to each of the hallmarks of cancer cells [229]. In this report we highlight how differential changes in annexin and S100A expression may impact on signalling pathways and potentially lead to the activation or inhibition of downstream and/or compensatory cellular mechanisms, dependent upon the direction of expression change. Annexin and S100A deregulation has been associated with tumour invasion and metastasis, angiogenesis and drug resistance [196, 206, 207]. Loss of annexin A1 has been associated with malignant transformation in ER+ breast cancer[198], and, conversely, recent reports associate high annexin A1 expression with cellular invasion in ER- [203]. Increases in annexin A2 and S100A11 are associated with cell viability and increased invasiveness through their ability to maintain plasma membrane integrity [230] and promote epithelial-mesenchymal transition [205]. Dysregulation of individual annexin expression is associated with cancer development and treatment outcomes and it has been suggested that considering the expression of individual annexins may provide useful diagnostic and prognostic biomarkers [196]. Furthermore, modulation of calcium signalling has been demonstrated to change sensitivity of chemotherapeutic agents to apoptotic signals. This led to our further investigation of the impact of the differential regulation of annexin expression by p53 on patient treatment outcomes.

4.4.2 The ER-p53-annexin expression profile and treatment outcomes

To address how increases in the expression of individual annexins (A1, A2, A4, A6 and A9) and S100A binding partners (S100A10, S100A11 and S100A13), and combinations of thereof, could influence treatment outcomes, we performed a meta-analysis (biomarker assessment) based on 4142 breast cancer samples using the Kaplan-Meier plot database for breast cancer (available online) [211]. This is the first biomarker analysis directly comparing patient treatment outcomes using expression data of each individual annexin and then combining the expression date of all annexins and S100A binding proteins (i.e. an annexin expression profile) in a specific sub-set of breast cancer patients (ER^+p53^+) within a larger cohort. Overall, ER^+ patient prognosis was more favourable when p53 was present and was associated with increased RFS, DMSF and OS. The exception to this was upregulation of annexin A9 and S100A13, which were associated with poor RFS and RFS/OS respectively, and, interestingly, this was only in patients who had undergone endocrine treatments. The most favourable prognosis and survival odds were observed when all the upregulated annexins and S100A proteins were taken into account together as an expression profile or signature, and a comparison was made between ER^+p53^- patient tumours and ER^+p53^+ tumours. In general, all tumours responded more positively when p53 was expressed independent of treatment regime. The most striking observation was that of ER^+p53^+ tumours with the expression profile of upregulated annexin A1, A2, A4, A6, A9 and S100A, A11 and A13, which showed great benefit from tamoxifen intervention alone, and, it was further shown, that additional treatment with chemotherapy would have no added beneficial effect. *In conclusion*, this

study ascribes to p53 the functions of a key organizer of calcium metabolism in breast cancer cells through the differential regulation of expression of the annexins, which are important calcium regulators. We have shown that p53 mediates pro-survival signalling in breast cancer cells and does not induce the canonical annexin A5 apoptotic pathway as previously thought. Although we, and others, have shown that reactivation of the canonical p14ARF-p53 pathway does not induce apoptosis in our studies, this does not necessarily relate to resistance to either chemotherapy or endocrine therapies. In our retrospective studies using a freely available breast cancer database, induction of p53 and overexpression of annexins associated with pro-survival functions is not associated with resistance to endocrine therapy. However, p53 induced overexpression of annexins, with consequent cellular phenotypic alterations appears to influence treatment outcomes in breast cancer. Importantly, prognosis/treatment outcome prediction is modified by whether one considers single genes individually or combines the gene expression profiles of various genes. Combining expression data of many genes is therefore the way forward to getting best /most accurate prognostic/treatment outcome information.

Acknowledgments

Nikki Alling for making the MCF-7p14ARF cell lines, her dedication, excitement and believing in this project.

Chapter Five

p14ARF-p53-p21: Reprogramming metabolic regulation and function in breast cancer

5.1 Introduction

5.1.1 Overview of the p14ARF-p53 pathway

The p53 transcription factor is well characterised for its anti-cancer role and is one of the most extensively studied tumour suppressor proteins preventing cancer development [30-33]. Upon DNA damage or oncogenic signaling, p53 is stabilised within the nucleus, thus inducing genes associated with cell cycle progression, DNA repair, senescence or apoptosis [32, 37, 231, 232]. Mutations in TP53 are common in approximately 50% of all cancers, however only 30% of breast cancers are associated with TP53 mutations or deletions of this gene, leaving the remaining 70% with WT p53 [113], which makes reactivation of p53 in breast cancer a good target for breast cancer treatments [163]. This is particularly relevant for hormone responsive breast cancers where a large majority of tumours harbour WT p53 [113, 114]. A targeted protein for p53 reactivation is p14ARF, which blocks the ubiquitination of p53 by the ubiquitin-protein lysate, human double minute 2 (hdm2) [165], preventing p53 degradation thus stabilizing p53 expression [166, 233-235].

Additionally, the cellular roles of p53 extend beyond its role in cancer prevention whereby p53 plays a key role in normal breast development and function [164]. In 2001, O'Malley and colleagues proposed ample precedent to the complex role of hormonal regulation of p53 expression in both normal mammary gland development as well as in tumourigenesis [236], thus providing a hypothesis for the p53 paradigm in normal breast development and function and extending to the contradictory and evasive role p53 plays in breast cancer progression and protection.

Most studies have used DNA damaging agents (radiation, chemotherapeutics) or mimetics of p14ARF, such as nutlin-3a, to explore p53 reactivation in breast cancer [126, 145, 237]. Other studies have used retroviruses or adenovirus to reactivate p14ARF-p53 and the main focus of these studies has been revisiting cell cycle arrest and cell death [238]. To understand the process of reactivating the p53 pathway in breast cancer cells, an inducible vector system whereby physiologically relevant expression of p14ARF is induced in the same cellular background as control is used [27, 95, 153]. Previous studies in our laboratory, exploring the paradigm of p14ARF in the activation of the p53 pathway in breast cancer demonstrated a metabolically active, differentiated, senescence-like (dormant) phenotype [27, 95]. Some of the features included an increase in cell size (cytoplasmic and nuclear), a more structural cellular skeletal architecture and a significant increase in viable mitochondrial biomass (Fig. 5.2) [27]. Thus, activation of the p14ARF-p53-p21 pathway initiated a change in cellular metabolism consistent with a differentiated phenotype with an increase in mitochondrial activity, most likely to be important in cell survival and recurrence [95]. This led to the hypothesis that the breast cancer cell retains a 'functional memory", and, by reactivating this pathway, we could mimic some of the functions of p53.

5.1.2 Cancer metabolism and metabolic reprogramming

Cancer is the uncontrolled growth and division of cells in which cell cycle regulatory checkpoints have been lost [239]. As in normal cells, cell division requires an increase in energy [240], in cancer, metabolic pathways and nutrient uptake mechanisms are reprogrammed to fulfil the requirements of the uncontrolled cell proliferation characteristic of cancer cells [240-243]. As

discussed in *section 1.2.3*, the 'Warburg Effect' is a characteristic of all proliferating cells where cancer cells exhibit have a shift in energy production from oxidative phosphorylation, occurring in the mitochondria, to a predominance of glycolysis in the cytoplasm [91-93]. It is therefore not surprising that glucose transporters have been shown to be overexpressed in cancer cells [244, 245].

5.1.3 The role of p53 in cellular metabolism and metabolic switch

Alterations in cellular metabolism are one of the well characterised hallmarks of cancer [246], however, we still do not fully appreciate the importance of the metabolic changes occurring in normal and cancer cells and how these changes may lead to tumourigenesis. It is only in the last 9 years that p53 has been identified as a co-ordinator of the mitochondrial respiratory and cytosolic glycolytic pathways of cellular energy generation, [247]. Of interest, p53 is associated with the suppression of cytoplasmic glycolysis and enhancement of the mitochondrial oxidative phosphorylation [248].

In normal metabolism, Saleem and Hood (2013) demonstrated that in skeletal muscle, levels of p53 in the mitochondria are usually low, but upon acute exercise p53 translocates to the mitochondria. This accumulation of p53 in the mitochondria was shown to induce oxidative respiration [249]. Further to this, p53 has been shown to supress glycolysis and when p53 is mutated or defective, as occurs in many cancers of various types, glycolytic metabolism is increased [250]. In addition, p53 physically interacts with the mitochondrial transcription factor A (TFAM) [251], which enhances the binding of TFAM to mitochondrial DNA (mtDNA), thus enhancing mtDNA transcription [249].

In 2011, work in our laboratory showed that induction of p14ARFexpression and p53 reactivation in MCF-7 breast cancer epithelial cells did not lead to cellular apoptosis but instead, the cells remained viable, were metabolically active and demonstrated an increase in mitochondrial biomass [95]. This chapter describes work that was conducted to further explore the mechanisms underlying the metabolic changes occurring in the breast cancer epithelial cells post p53 activation and focuses on the role of p53 in regulating mitochondria and mitochondrial dynamics.

5.1.4 Mitochondrial Dynamics

Sustaining metabolic homeostasis not only relies on the activity of tumour suppressor proteins such as p53, but also on the regulation of mitochondria and mitochondrial function. This includes the regulation of mitochondrial size, number and shape through fusion and fission events and intracellular transportation [252, 253]. These mechanisms, known as mitochondrial dynamics, ensure optimal mitochondrial bioenergetic function to accommodate the energy demands of the cell [254, 255]. Mitochondrial dynamics have been observed to be influenced by p53 [95, 256, 257], however, this is yet to be explored in breast cancer models.

Mitochondrial morphology is intimately linked to mitochondrial functional state [252, 254, 255] with mitochondrial fission and fusion being critical balancing events in the maintenance of mitochondrial function when cells are exposed to a wide array of metabolic and environmental stresses [254, 255, 258]. This includes maintaining mitochondria biomass, number, biogenesis and degradation (Fig. 5.1). When fission is unopposed, mitochondrial fragmentation occurs, and is associated with excess glucose abundance, severe stress, cellular death and

impaired oxidative phosphorylation (OXPHOS). However, fission has also been observed to be vital in the generation of new mitochondria (mitochondrial biogenesis) alongside a quality control process to remove old defective mitochondria, ensuring proper mitochondrial function (Fig. 5.1) [254, 255].

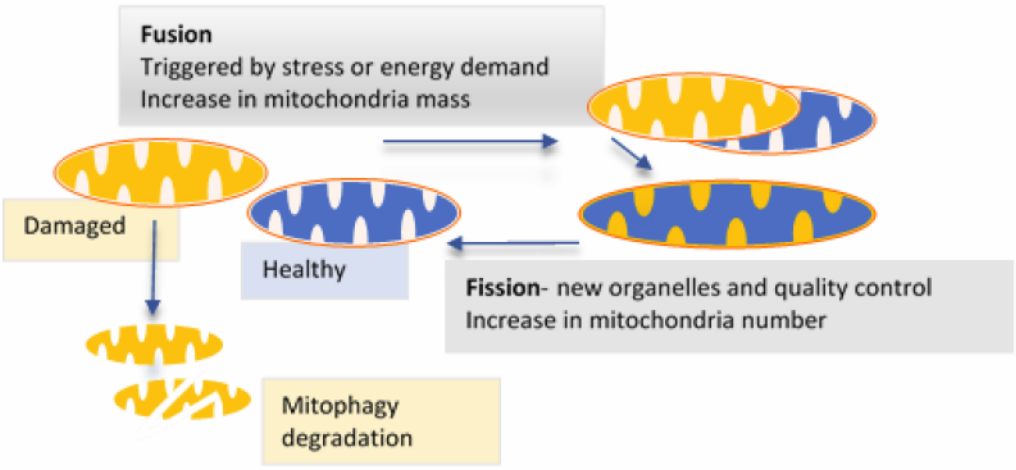


Figure 5.1 The mitochondrial fission-fusion cycle sustaining mitochondrial function, number and genetic health. Under stressful or energy demanding conditions, mitochondria undergo fusion to complement damaged (yellow) and healthy (blue) mitochondria. This allows a mixing of constituents alongside increasing membrane surface area, which optimizes bioenergetic functioning. An imbalance between fission and fusion – for instance greater fission – leads to mitochondrial fragmentation and may increase the number of mitochondria if mitophagy does not eliminate mitochondria. Conversely, more fusion is seen to form large tubular networks. The biogenesis of mitochondria occurs to increase mitochondrial biomass or to compensate for mitochondrial degradation. Thus, imbalances between mitochondrial fission, fusion, biogenesis and degradation appear to regulate mitochondrial number, shape, size and biomass [255, 259]. Mitochondrial fission has been associated with sensitizing cells to apoptosis during highly stressful conditions and with environments of nutrient excess. However, fission has also been implicated in the "house-keeping" of mitochondria to produce new mitochondria (blue) and remove old/damaged mitochondria.

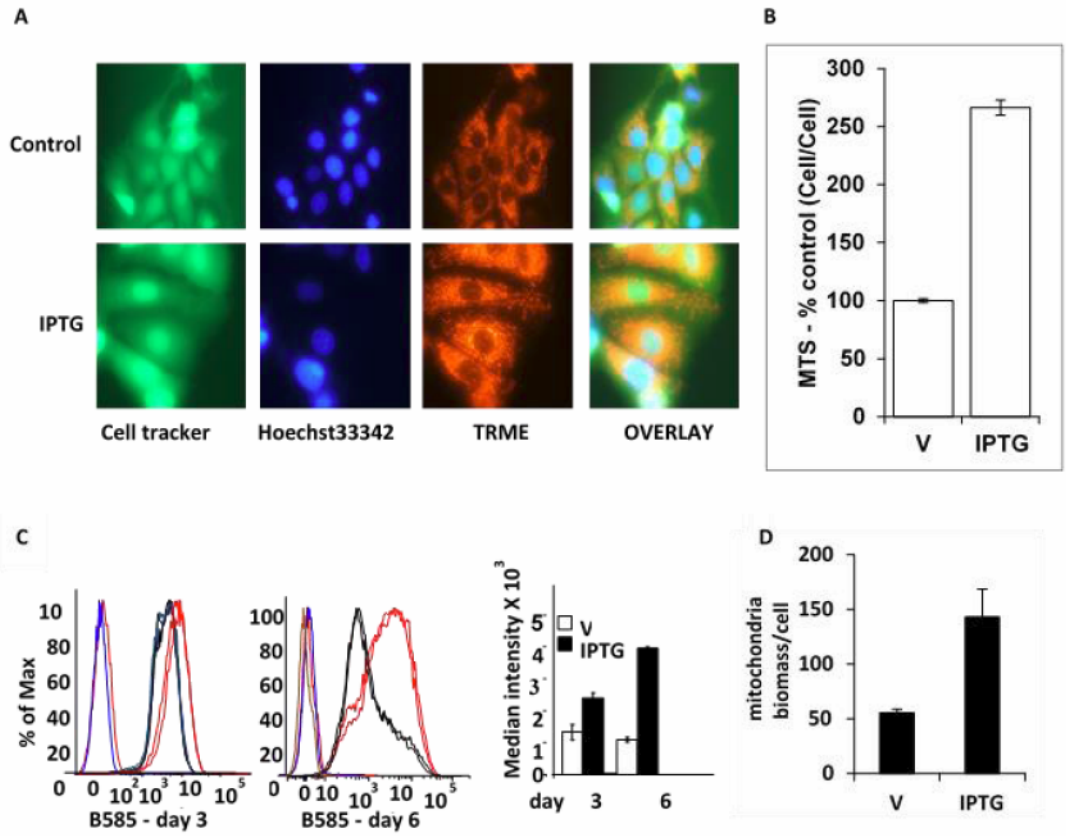


Figure 5.2. Increase in mitochondria activity, viability and biomass without loss of membrane potentiality post p14ARF-p53 activation. (A) Immunofluorescent images 72 h post p14ARF-p53 induction with IPTG (5 mM) and vehicle (control) PBS. Live cells were incubated with TMRE, Cell tracker and Hoechst 33342. Legend: blue – Hoechst 33342; red – TRME; green – Cell tracker. (B) Mitochondrial assay (MTS) showed a 2.5-fold increase in activity at 3 days post p14ARF induction. V = vehicle (control), IPTG – P14ARF induction. p14ARF-p53 was induced for 3 and 6 days with 5 mM IPTG or vehicle (control). (C) No loss of membrane integrity was evident using TMRE in Flow Cytometric assays. (D) Mitochondria measured by HCA and counted using BD Attovision™ software showed an average 3-fold increase in mitochondria biomass per cell post p14ARF activation. V = vehicle (control), IPTG – P14ARF induction [95].

5.2 Methods

5.2.1 Cell culture

Cells were seeded at a density of 2.0 x 10^5 cells/mL in DMEM for 24 h. IPTG (5mM) and PBS (control) were added to cells for 24 h and 72 h, respectively. Cells were harvested by washing twice in cold PBS then adding 150 µL of lysis buffer with protease inhibitors (PI) for 3 mins each wash. Cells were scraped from the monolayer and transferred to a 1.5 mL Eppendorf tube. Cell lysates were centrifuged for 10 min and the supernatant transferred to a new Eppendorf tube. Cell were centrifuged at 12000 g at 4 ^{0}C and samples were kept on ice at all times. Protein was quantitated using the Quick Start™ Bradford Kit 2 according to the manufacturer's instructions. Protein samples were stored at -80 ^{0}C until required for use.

5.2.2 Western blotting

Denaturing polyacrylamide gel electrophoresis was performed by adding 10 µg of total protein to 25% (v/v) NuPAGE®LDS Sample Buffer (4x), 10% (v/v) NuPAGE®Reducing Agent (10x) and dH_2O, then incubating at 85 ^{0}C for 3 min, followed by centrifugation for 2 min. Proteins were separated on NuPAGE®Novex®Bis-Tris gels using MES SDS Running Buffer and SeeBlue® Plus2 Pre-Stained Standard as a reference ladder. The proteins were then transferred onto PVDF membranes for 1 h in Western blot transfer buffer using the Invitrogen Western blot transfer system. Protein transfer was verified by staining the membrane with Ponceau S. PVDF membranes were soaked in blocking solution for 2 h (with gentle agitation) at RT and washed twice. PVDF membranes were incubated in the appropriate primary antibody for 2 h on a

MACSmix™ tube rotator at room temperature then washed. The membranes were incubated with secondary α-mouse HRP for 1 h at RT then washed every 10 min for 1 h. The membranes were visualised using Amersham ECL reagents (1:1 ratio) and protein abundance quantified by image analysis using the Kodak image station 4000 MM. To prepare the loading control, PVDF membranes were stripped by placing in boiled stripping buffer for 7 min, repeating three times with fresh stripping buffer each time, then washed three times by incubating for 10 min each time followed by blocking with 0.2% (v/v) FCS in PBST for 2 h. Membranes were probed with mouse β-actin secondary conjugated antibody for 1 h then visualised as described above. PBST was used in all washing steps.

5.2.3 RNA extraction and Real-time quantitative polymerase chain reaction (RT-qPCR)

MCF-7p14ARF and U2OSp14ARF cells were seeded at 2.0 x 10^5 cells/mL in DMEM for 24 h. Test cells and control cells were then treated with 5 mM IPTG and PBS respectively for 6 h and 15 h. Centrifugation at all steps was performed at 12000 g at 4 ^{0}C and samples were always kept on ice.

5.2.3.1 RNA extraction and quality control

RNA was harvested by washing cells with cold PBS, adding RNAzol®RT, at 500 mL per well and scraping cells before pipetting into an Eppendorf tube. Cells in RNAzol®RT were frozen at -20 ^{0}C. RNA was extracted by adding 40% (v/v) RNase/DNase free water to the lysate, centrifuging at 12000 g for 15 min and transferring 75% of the supernatant to a fresh vial. 0.5% (v/v) 4-bromoanisole (BAN) was added to the supernatant, the mixture was shaken for 15 sec and store for 3-5 min at room temperature followed by centrifugation at 12000 g for

10 min. The RNA-containing supernatant was transferred to a new vial and 75% (v/v) Isopropanol was then added to the supernatant and incubated overnight at -20 ^{0}C to increase the RNA yield.

The RNA was collected as a pellet after centrifugation for 15 min (at RT) and washed twice with 75% (v/v) ethanol to completely remove any residue supernatant. The pellet was dried at 37 ^{0}C until it became clear and resuspended in 20 µL RNase/DNase free water by pipetting slowly up and down, then heating the samples 55 ^{0}C for no more than 5 min. RNA samples were stored at -80 ^{0}C until required.

The quality of RNA was assessed and total RNA concentration was measured at 260 nm using the NanoDrop 1000 Spectrophotometer (Thermo Fisher Scientific, DE, USA).

5.2.3.2 cDNA Synthesis

RNA (400ng) was reverse transcribed using the High Capacity cDNA Reverse Transcription kit according to the manufacturer's instructions. The following reagents were used to prepare Reverse Transcriptase (RT) master mix per reaction: 2.0 µL of 10 x RT Buffer, 0.8 µL of 100 mM dNTP, 1.0 µL of RNase Inhibitor, 2.0 µL of 10 x RT Random Primers, 0.5 µL of MultiScribe™ RT and 9.7 µL RNase/DNase free water. 4 µL of pure RNA (400ng) was added to 16 µL of RT master mix and centrifuged briefly. Reverse transcription was performed at 37 ^{0}C for 120 min. As soon as reverse transcription was completed, cDNA was diluted (1:4) in RNase/DNase free water and stored at -20 ^{0}C until required.

5.2.4 Immunofluorescence microscopy

5.2.4.1 Cell fixation and immunofluorescence staining

Transfected MCF-7p14ARF cells were seeded at $1x10^5$ cells on glass coverslips in 6-well plates for 24 h, in a 37 ^{0}C, 5% CO_2 incubator. Following seeding, 5 mM IPTG was added to induce p14ARF and PBS (vehicle) added to the control wells for 24 h and 72 h. Cells were washed three times in warm PBS followed by fixation by the addition of 1 mL of freshly thawed 4 % paraformaldehyde (PFA) and incubation at 37 ^{0}C for 30 min at RT. Following incubation, cells were washed with warm PBS then permeabilised with 0.2% Triton for 10 min at RT. Cells were washed with PBS and blocked with 2% (v/v) BSA in 0.1% (v/v) Triton for 1 hour at RT. Cells were washed with PBS and incubated with tubulin primary antibody (1:50) in 1% BSA plus Tween 20 overnight at 4 ^{0}C. Cells were washed three times in PBS leaving the first wash for 1 h. Secondary antibodies (1:500) conjugated to Alexa fluor 568, Alexa fluor 488, plus GFP booster (1:500) and Hoechst 33342 (trihydrochloride trihydrate 10mg/mL solution in water) (1:1000) containing 1% BSA plus Tween 20 (0.25 v/v) were incubated at RT for 1 h. Coverslips containing the cells were washed three times with PBS and mounted by adding n-propyl-gallate (npg). Slides were placed onto coverslips cells side down then sealed with nail polish. Slides were then viewed on OMX super resolution microscope.

5.2.4.2 OMX microscopy and analysis

3D Structured Illumination imaging was performed on the prepared sample using a DeltaVision OMX SR imaging system (GE Healthcare, Issaquah, WA, USA). Solid-state lasers provided wide-field illumination and images were captured

using a × 60 1.4 numerical aperture UPlanSApo objective (Olympus, Toyko, Japan), standard filter sets and three scientific CMOS 512 × 512 pixel 15-bit cameras (pco.edge, PCO AG, Kelheim, Germany). Interference patterns were generated by interfering light beams [157] and samples were sectioned using a 125 nm Z-step size. Raw 3-phase images were then reconstructed to extract finer detail using the Gustafsson algorithms [158, 159]. Images were captured and processed using AcquireSR and SoftWorX software (GE Healthcare). Light sources used were 405 and 488 nm lasers and emission Filters: DAPI (405 EX / 419-465 EM) and EGFP (488 EX / 500-550 EM).

IMARIS x64 (9.0.0) was used to find the number of mitochondria per cell using the 'Surface' module by thresholding for DAPI to find surface 1 (nucleus) and EGFP signal to find surface 2 (mitochondria) then the number of detected surfaces was counted in the selected region of interest.

5.3 Results and Discussion

5.3.1 p14ARF upregulates TFAM but not Cytochrome C

Given p53 has been demonstrated to positively increase mitochondria dynamics, effects of two key regulatory proteins that are associated with p53-mediated regulation of mitochondrial function were investigated in our breast cancer model. Cytochrome C, located mainly in the inner mitochondrial membrane [260], is associated with p53-mitochondrial mediated cell death [260, 261]. On the other hand transcriptional factor A, mitochondrial (TFAM) is a positive regulator of mitochondrial activity [262]. TFAM is a DNA binding protein that is transcribed in the nucleus and translocates to the mitochondria where it activates two of the major promoters of mitochondrial-DNA (mt-DNA) [263].

Both cytochrome C and TFAM pre- and post p14ARF-p53 induction were visualised by immunofluorescent staining in MCF-7p14ARF cells and representative images are shown in Fig. 5.3 and TFAM videos (attached). Cytochrome C, which is associated with p53 mediated cell death did not change in intensity in the pre- and post- images of p14ARF-p53 activation (Fig. 5.3A). Alternatively, a significant increase in TFAM was observed in the nucleus (the source of TFAM transcription and translation) and throughout the cytoplasm (Fig. 5.3B). A video showing the TFAM expression throughout the nucleus and cytoplasm can be found in the attached supplementary files. These results were very exciting both visually and conceptually, providing more evidence that p53 was very much associated with cell survival and the cells were functionally active post p14ARF-p53 activation.

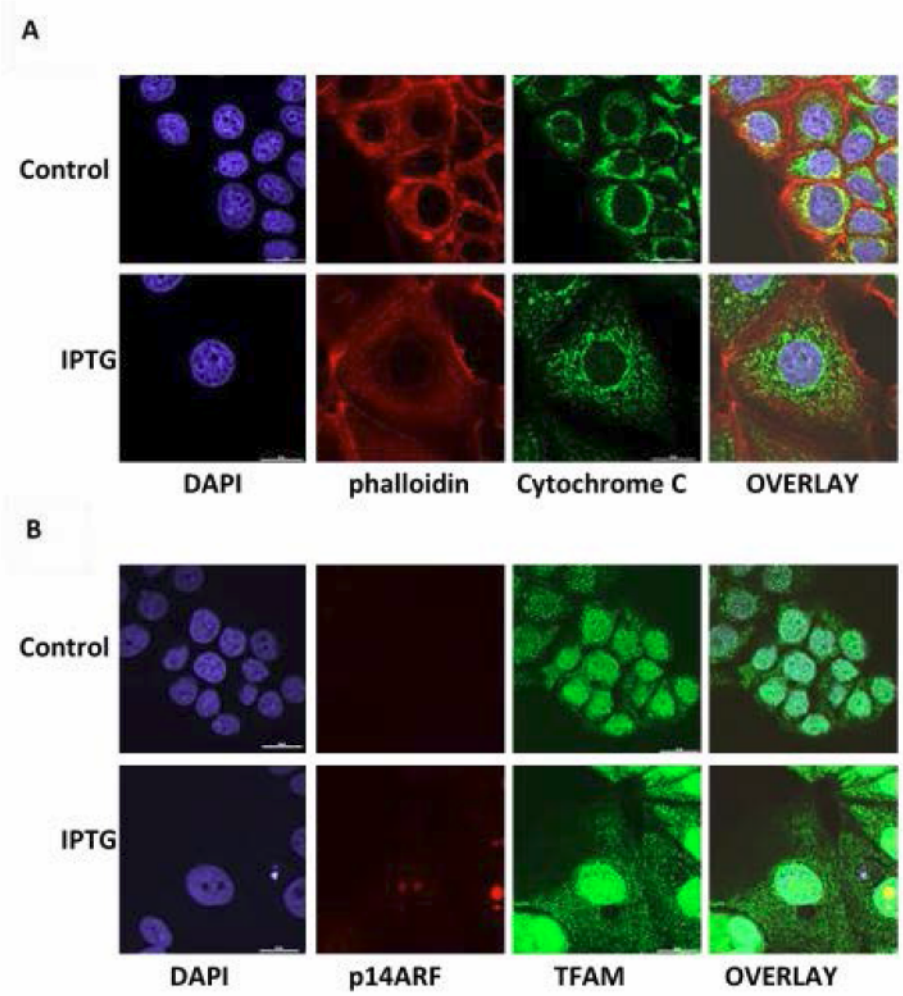


Figure 5.3. Upregulation of mitochondrial associated protein TFAM but not Cytochrome C post p14ARF-p53 activation. Expression of p14ARF was induced by the addition of 5mM IPTG at 72 h, vehicle control contained PBS in place of IPTG. (A) Immunofluorescent images 72 h post p14ARF-p53 induction with IPTG (5 mM) and control PBS. Legend: blue – DAPI; red -Phalloidin; green – Cytochrome C. (B) Immunofluorescent images 72 h post p14ARF-p53 induction with IPTG (5 mM) and control PBS. Legend: blue – DAPI; red – p14ARF; green – TFAM. Increases in TFAM in the nucleus and cytoplasm is associated with p14ARF-p53 activation. The bar represents 20μm.

5.3.2 Signalling pathways associated with metabolic reprogramming

Here we investigated the co-ordination of signalling pathways associated with p53-metabolic reprogramming in our MCF-7p14ARF breast cancer model. The uniqueness of SILAC used in this study was that it allowed the direct comparison of all proteins in the same cell, pre- and post-treatment at any given timepoint. Using the triple SILAC technique allowed us to analyse p53-mediated changes in metabolic signalling pathways over time. Here direct comparison of proteome profiling in our breast cancer cell model was performed comparing global protein expression in the vehicle-treated the cells with cells expressing p14ARF at 24 h and 72 h time-points post p53 activation. Only p53-mediated protein changes in MCF-7p14ARF at both time points were analysed using the GOstats analysis package in Bioconductor [264]. This allowed us to observe long-term, or more permanent, changes in signalling pathways involved in p53-mediated metabolic reprogramming in contrast to transitory changes.

5.3.2.1 Signalling pathways that are rapidly downregulated inhibit cell cycle progression, DNA repair and apoptosis

Our observations clearly showed that p53- mediated metabolic changes involved turning off all non-essential functions including the aforementioned DNA replication mechanism, and anti-intuitively, DNA repair mechanisms (Fig. 5.4). Interestingly, protein signalling pathways associated with apoptosis were either unchanged or downregulated (Fig. 5.4). The well characterised annexin associated with apoptosis was not regulated by p53, however the less known mitochondrial-associated protein, DNAJC15, whose expression is associated

with negative regulation of the mitochondrial respiratory chain was downregulated [183].

5.3.2.2 Signalling pathways that are upregulated are associated with metabolic functions

Long-term changes in the p53-mediated signalling pathways associated with upregulation of global cell proteins at 24 h and 72 h were very much centred on gross changes in the cellular metabolism. One of the most interesting findings of this study was the stimulation of the fatty acid oxidation (FAO) and an integral pathway of FAO, β-oxidation (Fig. 5.5). As mentioned, p53 has known roles in FAO to inhibit the hyperactivity of membrane synthesis in cancer and enhance OXPHOS, thus hindering the reliance on glycolysis [90]. p53 has also been shown to regulate fatty acid oxidation (FAO) by facilitating the transport of fatty acids into the mitochondria through the activation of carnitine palmitoyltransferase 1C (CPTC1) and by positively regulating the b-oxidation of fatty acids in response to nutrient stress [30]. This ability of p53 to increase FAO promotes NADH and $FADH_2$ production that enhances OXPHOS. As mentioned, cancer cells typically increase fatty acid uptake and synthesis to meet the demands of membrane biosynthesis and p53 has been shown to oppose this effect. Furthermore, membrane fusion and organelle reorganisation functions may correspond to organelles including mitochondria undergoing dynamic alterations post p14ARF-p53 activation.

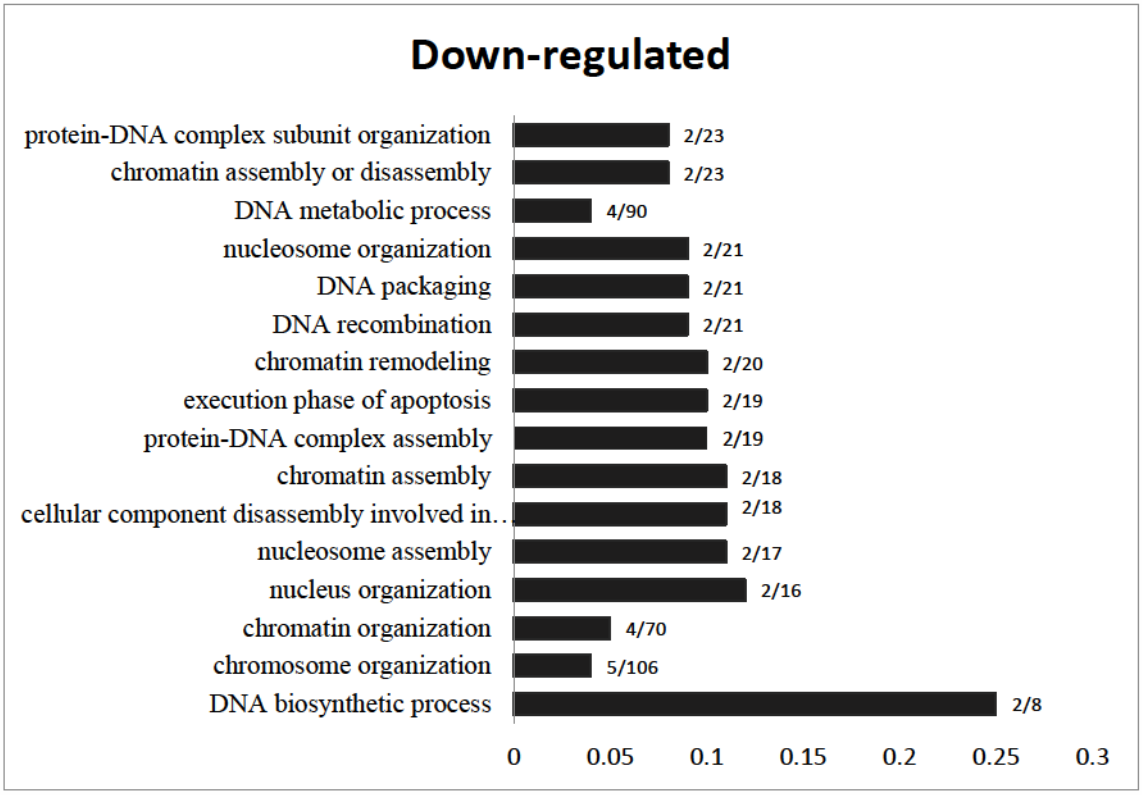


Figure 5.4 Gene ontology analysis of the top 50 down-regulated proteins post p53 activation in MCF-7 cells. Each horizontal bar represents the percentage of total genes for each gene ontology (GO) term which are present in the list of the bottom 50 down-regulated proteins post p14ARF-p53 activation. The first number next to each bar represents the gene count, and the second number represents the total number of genes associated with that GO term. GO terms were obtained from the GO Central GO terms for *Homo sapiens*. All associations are valid at $P < 0.05$. GO term analysis was performed using GOstats package in Bioconductor [264].

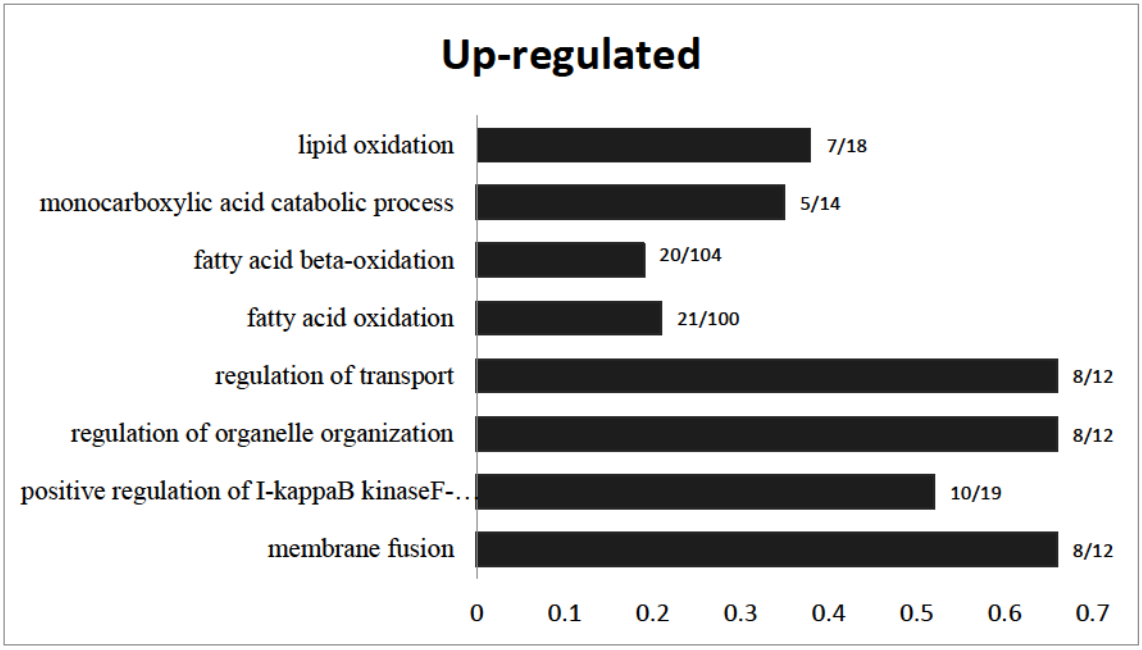


Figure 5.5 Gene ontology (GO) analysis of the top 50 upregulated proteins post p53 activation in MCF-7 cells. Each horizontal bar represents the percentage of total genes for each GO term which are present in the list of top 50 up-regulated proteins post p14ARF-p53 activation. The first number next to each bar represents the gene count, and the second number represents the total number of genes associated with that GO term. GO terms were obtained from the GO Central GO terms for *Homo sapiens*. All associations are valid at $P < 6.1 \times 10^{-06}$. GO term analysis was performed using GOstats package in Bioconductor [264].

These studies placed p53 as the 'guardian of the proteome' and confirmed the rightful place of p53 as the 'guardian of cellular energy metabolism'.

5.3.3 p53-mediated mitochondrial relocation/distribution and regulation of mitochondrial size and shape

One of the unique observations from the p53-mediated proteomic changes was the importance of p53 in redirecting specific mitochondrial functions. From the literature (discussed in section 5.1.4), sustained metabolic homeostasis is very much reliant on the regulation of mitochondrial number and distribution, size and shape. These are also dictated by intracellular transportation and mitochondrial fission and fusion events. As previously mentioned, changes in mitochondrial dynamics ensures the energy demands within the cell are optimally met.

To-date there are no studies focusing on determining the mechanism(s) by which p53 directs mitochondrial organisation in the cell, in association with cellular function. Here we observed how p53 is involved in regulating mitochondrial re-distribution, size and shape. We employed super resolution microscopy (OMX) to observe, in detail, mitochondrial size and shape. In addition, redistribution of mitochondria post p14ARF-p53 activation was determined both by visualisation and by measuring the distance of individual mitochondria from the nucleus. using 3D imaging. As demonstrated in MCF-7 cells, before p14ARF-p53 induction, mitochondria are more tubular in structure (Fig. 5.6) and most of the mitochondria were very closely associated with the nucleus, indicating more communication between the mitochondria and the nucleus in these cells. Mitochondria are the powerhouse of a cell and most of the energy produced by the mitochondria is needed for cell proliferation and associated nuclear division [265]. Post p14ARF-

p53 activation, mitochondria were found to be more dispersed throughout the cytoplasm in the MCF-7 cells (Fig. 5.7). There was also an increase in the number of mitochondria (Fig 5.8 and Fig 5.9), as well as a change in their distribution, which is associated with the function of the cell. In the control MCF-7 cell, all mitochondria are found to be close to the nucleus, however, in the induced cells, mitochondrial distribution was clearly cytoplasmic (i.e. more spread out and further away from the nucleus). This change is likely due to changes in cellular function from cell proliferation, where more energy is needed for DNA replication and nuclear division, to the lesser energy demands of a non-proliferating cell.

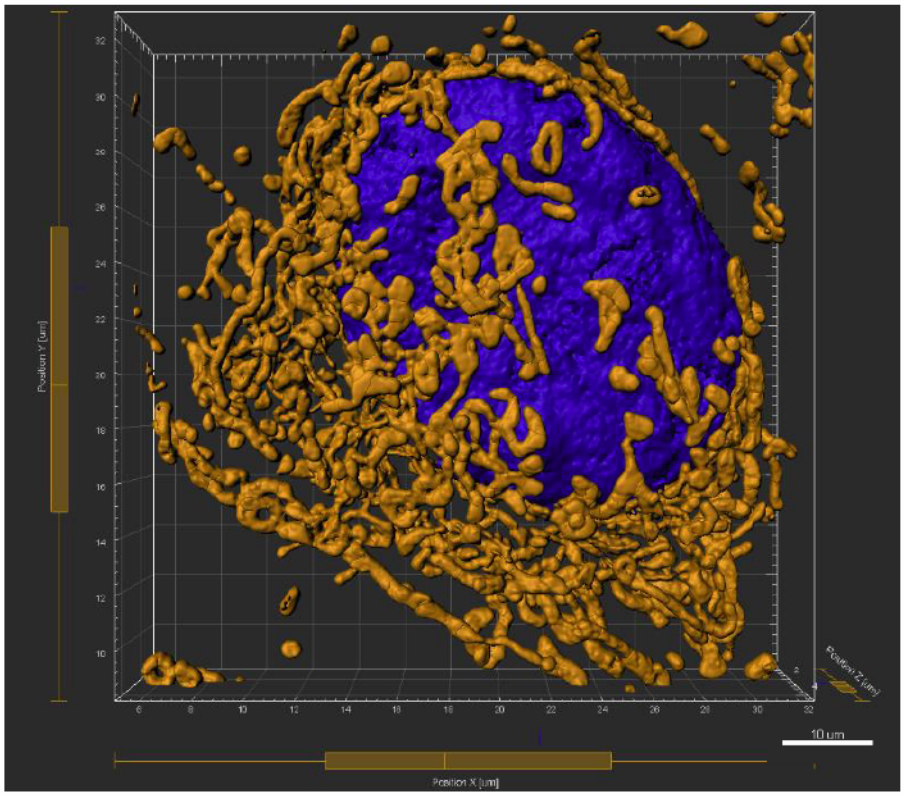


Figure 5.6. Visualisation of mitochondria in normal proliferating MCF-7 cells before p14ARF-p53 activation. Super resolution OMX microscopy and IMARIS x64 (9.0.0) image analysis was used to visualise the nucleus (blue) and the mitochondria (brown) of a normal proliferating MCF-7 cell. The bar represents 10 µm.

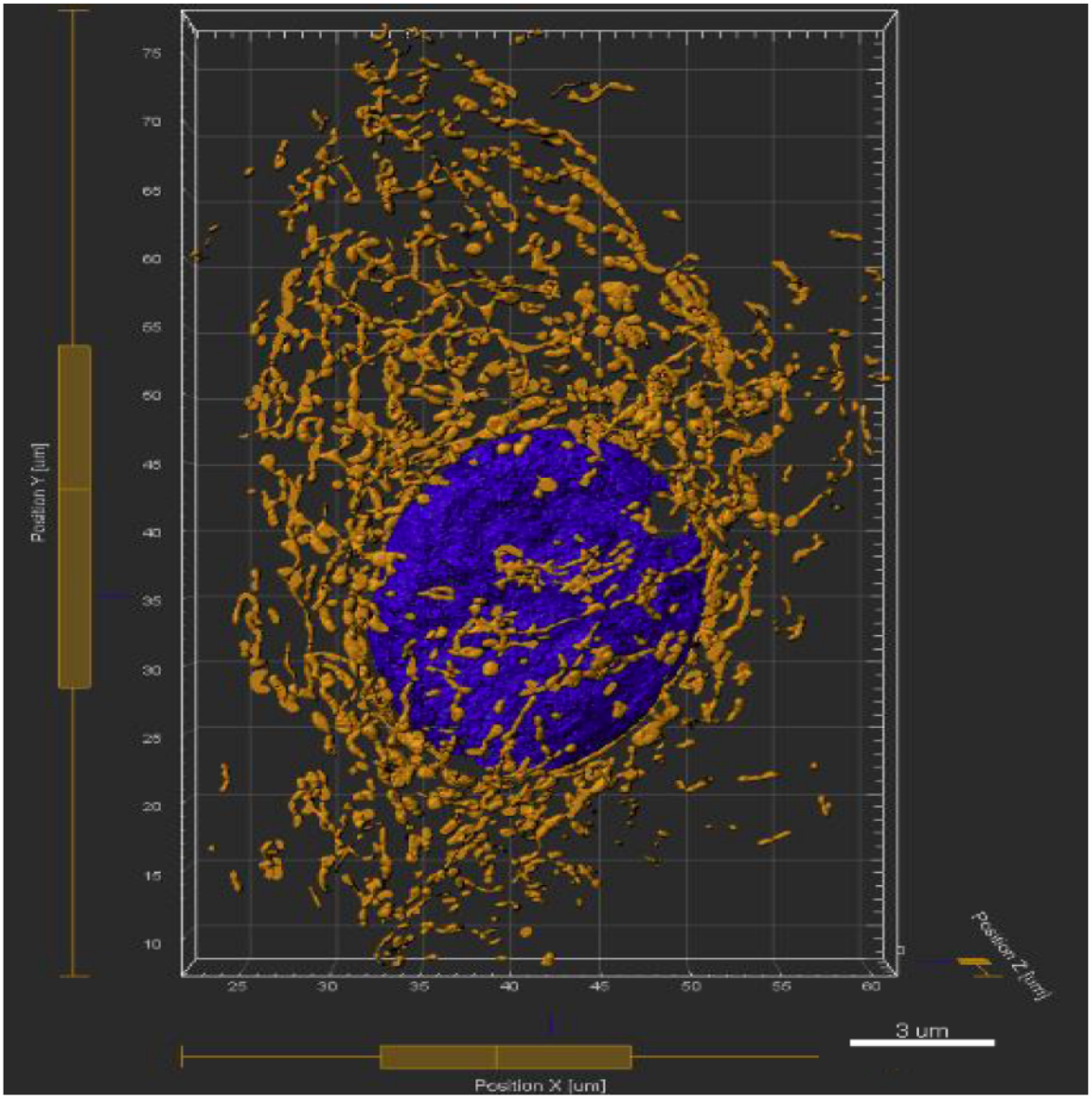


Figure 5.7. visualisation of mitochondria in non-proliferating MCF-7 cells after p14ARF-p53 activation. Expression of p14ARF was induced by the addition of 5 mM IPTG for 72 h. Super resolution OMX microscopy and IMARIS x64 (9.0.0) image analysis was used to visualise the nucleus (blue) and the mitochondria (brown) of MCF-7 cell after p14ARF-p53 activation. The bar represents 3 µm.

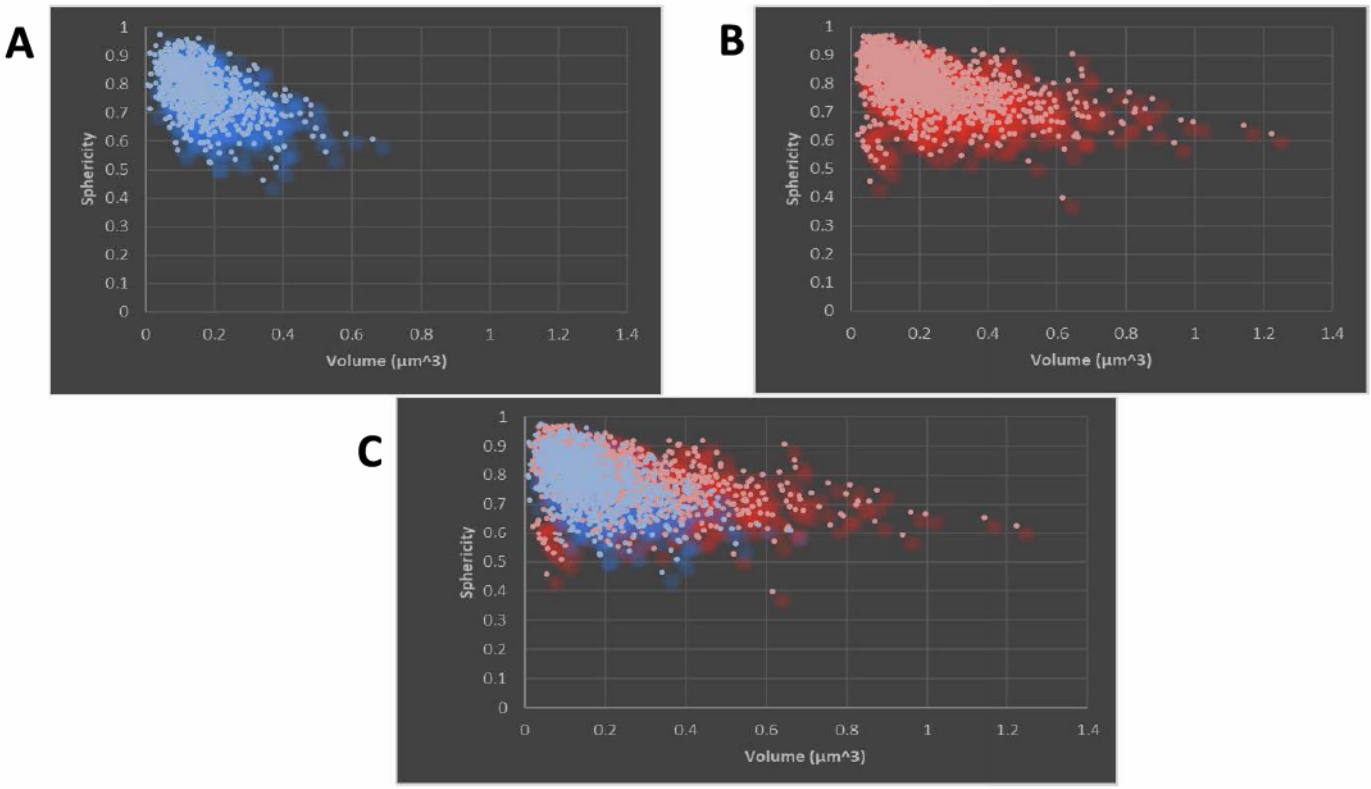


Figure 5.8. Mitochondrial volume and sphericity are increased post p14ARF activation. IMARIS x64 (9.0.0) was used to measure the volume and sphericity of mitochondria pre and post p14ARF activation. Volume (x-axis) was plotted versus Sphericity (y-axis) in excel. **A.** volume vs sphericity of mitochondria in MCF-7 cells pre p14ARF induction. **B.** volume vs sphericity of mitochondria in MCF-7 cells post p14ARF induction. **C.** Overlay of graphs **A** and **B.**

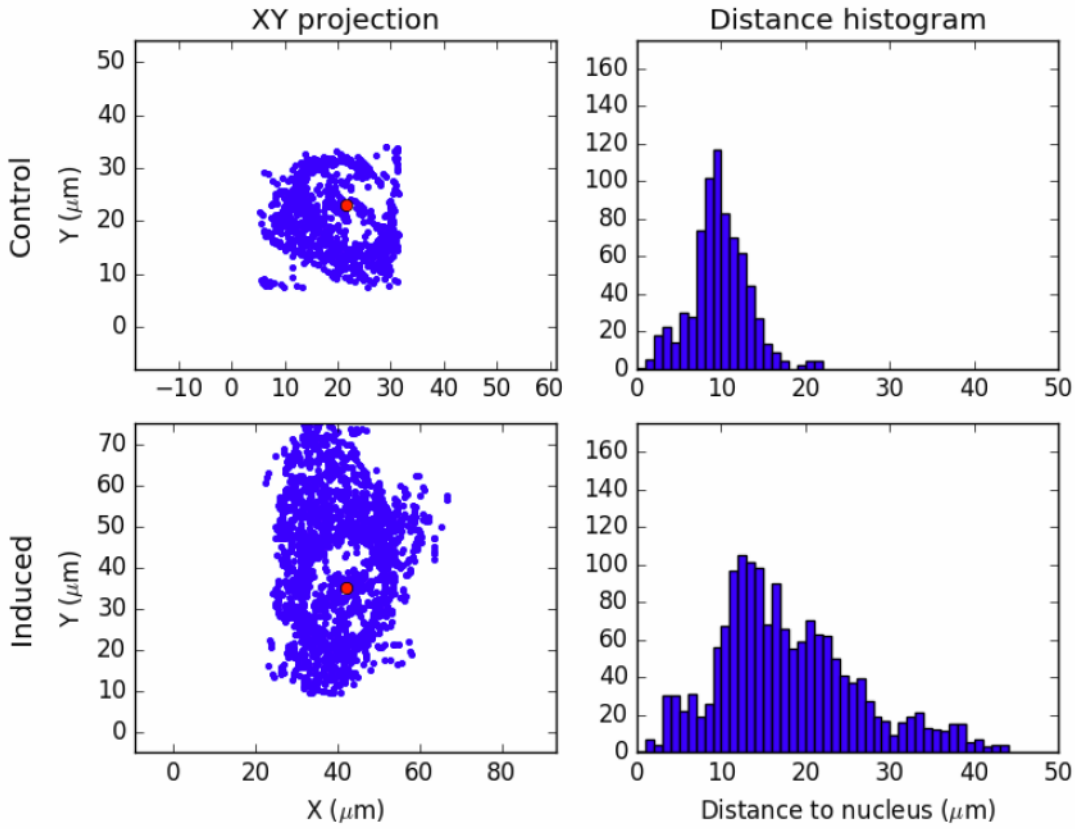


Figure 5.9. Mitochondria number and distance from the nucleus are increased post p14ARF activation. IMARIS X64 (9.0.0) was used to measure the distance of individual mitochondria from the nucleus of MCF-7 cells.

5.4 Conclusion

Altered cellular metabolism is a hallmark of cancer [91, 241-243, 266]. p53 is a key regulator of metabolic processes and metabolic programming [86-89]. Morphological and protein expression changes occurring in the mitochondria post p53 activation was investigated in this chapter and an increase in biomass, activity, and distribution of mitochondria was observed. In addition, mitochondria were more diverse in their shape post p14ARF induction and were dispersed throughout the cytoplasm. Upregulated proteins identified by SILAC analysis were mainly associated with mitochondria function.

Mitochondria were very closely associated with the nucleus pre- p53 activation (Fig. 5.6 and 5.9) and since mitochondria are the powerhouse of the cell, and these cells are cancer cells, they require all the energy provided by the mitochondria for their uncontrolled proliferation [130, 239, 240].

While p53 is associated with mitochondrial cell death (as discussed in Chapter 1 section 1.2) and preventing cancer, it also has a role in cell survival and function as shown in this chapter. Activation of the p53 pathway results in to cell cycle arrest, however, the unique protein changes and pathways being activated upon 'switching on' p53 are not those associated with cell death. This is clearly demonstrated in the results of this chapter where TFAM, a known transcriptional target of p53, which is important for the transcriptome and replication of mitochondria [267, 268], was increased both in the nucleus and cytoplasm (Fig. 5.3B), accompanied by global changes in proteins affecting the metabolic signalling pathways (Fig. 5.5), effected by changes in mitochondrial dynamics.

(Figs. 5.6, 5.8 and 5.9) Thus, p53 regulates mitochondrial DNA at the nuclear and mitochondrial cell compartments in these breast cancer cells [269].

Chapter Six

Concluding Remarks and Future Directions

Concluding Remarks

Breast cancer is one of the leading burdens of disease worldwide. Quality of life for women with breast cancer is reduced, and the cost to society emotionally and financially is huge. The majority of ERα positive breast cancers are treatable however acquired resistance, or recurrence of breast cancer is the major cause of morbidity.

P53 is a master protein that is important for normal mammary development and function and is switched off in the majority of cancers. One of the regulators of the p53 protein is p14ARF, which regulates p53 post-transcription, therefore regulation is not observed at the transcription level. In a mouse model, ARF is regulated by hormones in pregnancy, necessary for proliferation and cell death [28]. Loss of ARF is involved of breast cancer progression and reactivating p14ARF has been proposed as a targetable protein for breast cancer therapy. However too little is known about the consequences of activating this pathway.

Rationale for targeting p14ARF in the p53 pathway: Many breast cancer cells have lost expression of p14ARF, therefore allowing MDM2 ubiquitination of p53 destabilizing p53 expression. Reactivation of p14ARF has been proposed as a novel gene therapeutic approach to re-stabilising p53 expression. Alternatively, therapies that target MDM2 and MDMX, such as Nutlin 3A, again as a means of stabilising p53 are being trialled as a cancer therapy [144].

Problems associated with targeting p14ARF/p53 in breast cancer treatment: We have previously shown that breast cancer cells are still viable when the p14ARF-p53 pathway is reinitiated into breast cancers lacking p14ARF with p53-WT, as found in many post-menopausal breast cancers. The importance of

understanding this pathway is imperative to prevent recurrence or resistance with this type of treatment. This thesis explored the pathways initiated by p14ARF and explored the biology underlying potential resistance. At the start of this investigation, little was known about p14ARF-p53 and metabolism. Here we identified p14ARF-p53 as a game-changer in the contribution of p53 in the metabolism of breast cancer.

Most reports on overexpressing p14ARF systems show high levels of p14ARF and induce apoptosis. This system uses inducible low levels of p14ARF, more representative of the endogenous system. To determine if p14ARF was activated we always followed through and looked at p53 and p21 expression. In this system we did not see apoptosis, cells were still viable (the basis of this thesis). The system used expresses low levels of p14ARF, difficult to detect on a western, and more representative of what you may observe in the natural system.

This thesis raises concerns about reactivating p53 through p14ARF by exploring changes in downstream signalling and cell biology. The p14ARF-p53 tumour suppressor pathway is induced by environmental stress, leading to cell death/apoptosis or senescence, or, as mentioned reproductive hormones. Our laboratory has previously shown that activation of p53 through its upstream regulator p14ARF in our ERα positive breast cancer model did not produce the expected canonical effects i.e. apoptosis. Paradoxically, reactivation of p53 led to an increase in cell size, with cells remaining viable and showing an increase in mitochondrial biomass and mitochondrial viability [27, 95]. Therefore, the overall aim of the project was to define the role of the p14ARF-p53 in estrogen responsive breast cancer cells and the following were the experimental aims.

Aim one was to determine the global proteomic changes associated with p53 activation in breast cancer using a well characterised MCF-7 breast cancer luminal epithelial cell model. This was addressed by using SILAC and LC-MS/MS proteomics where 1265 differentially regulated proteins were identified after reactivation of p14ARF-p53 in ER+ breast cancer cells. From these proteins we found that specific downregulated proteins were associated with cell cycle arrest, DNA repair, and anti-apoptosis; and specific upregulated proteins were associated with differentiation and changes in cell metabolism.

Aim two was to characterise and validate novel p53 regulated proteins, and associated signalling pathways, detected by the proteomic analysis. Aim two was addressed by identifying from our SILAC dataset, a family of proteins, the annexin family and its associated S100 proteins, which were differentially regulated by activation of the p14-p53 pathway. This regulation of annexin protein expression was found to be cell type specific and this most probably equates with function since annexins are associated with calcium regulation. Using a free, well recognised software analysis program called Kaplan Meier (kmplot.com) we inferred that proteomic signature profiles may play a key role in determining treatment options.

Aim three was to examine the morphological and protein expression changes occurring in the mitochondria post p53 activation. Here we demonstrated unique p53-mediated effects on mitochondrial dynamics and function in hormone-dependent breast cancer cells. We showed how activation of the p14ARF-p53 has dramatic effects on the morphological, activity and protein expression changes in the mitochondria perceived by an increase in biomass, increase in activity, changes in distribution, sphericity, volume and distance from nucleus.

Thus, reactivation of p53 induced mitochondria associated cell survival and cell function and not mitochondria associated cell death in the breast cancer cell model.

In this thesis, we looked at the global proteomic changes that occur in breast cancer cells rather than a simplistic approach where we look at protein changes in isolation on Western blots. We looked at the whole cell proteome to observe is changes post activation of p53. p53 is a multifaceted master regulator of cellular dynamics. Most investigations use artificial chemical reagents and/or DNA damaging reagents to investigate p53 dynamics in cancer. Here, in this thesis, a natural upstream regulator (p14ARF) of p53 was used to investigate how activation of the p53-pathway affected not only the proteomic changes but how reactivation of one protein can dramatically change cell dynamics, especially observed in the metabolism. This work in this thesis provides a novel paradigm of p53 activation in hormone-dependent breast cancer cells, which may explain breast cancer survival after treatment and recurrence many years after seemingly successful treatment.

Future Directions

Mitochondrial isolation and SILAC analysis are still ongoing in our laboratory. This will provide insight to specific mitochondria proteins involved in the changes in mitochondria dynamics observed. Understanding the change in dynamics will provide insight on the basis of cell survival which may have implications in future therapy.

Supplementary Materials

Disclaimer: These files relate to chapters three and four. They are too large to be inserted into the thesis and are available in the zip file and on the USB drive provided. A PDF version of the thesis and two of my review papers are also included. The following materials can be found:

- **Supplementary table 3.1:** an excel workbook containing the filtered dataset of proteomic changes occurring at 24 h and 72 h which includes only proteins present in both sets of biological replicates and observed in technical replicates in duplicate experiments (Chapter 3).
- **Supplementary table 3.2A:** an excel workbook containing the results for the pathway analysis for Fig. 3.6A (Chapter 3).
- **Supplementary table 3.2B:** an excel workbook containing the results for the pathway analysis for Fig. 3.6B (Chapter 3).
- **Supplementary table 4.1:** an excel workbook containing the SILAC LC-MS/MS analysis of the annexin family and S100A associated proteins (Chapter 4).
- **Supplementary table 4.2:** an excel workbook containing full gene description, function and processes of the p53-p21-annexin/S100A interactome (Chapter 4).
- **TFAM pre p14ARF-p53 activation video**
- **TFAM post p14ARF-p53 activation video**

PDF file of the Thesis

References

1. Li, C., ed. *Breast Cancer Epidemiology*. 2009, Springer: New York, USA.
2. Ferlay, J., et al., *Cancer incidence and mortality worldwide: sources, methods and major patterns in GLOBOCAN 2012.* Int J Cancer, 2015. **136**(5): p. E359-86.
3. AIHW, *Cancer in Australia 2017*, in *Cancer series*. 2017.
4. Burton, R.C., et al., *Adjuvant therapy, not mammographic screening, accounts for most of the observed breast cancer specific mortality reductions in Australian women since the national screening program began in 1991.* Breast Cancer Res Treat, 2012. **131**(3): p. 949-55.
5. Ferlay, J., et al., *Cancer Incidence and Mortality Worldwide*. 2013, International Agency for Research on Cancer.
6. AIHW, *Breast Cancer in Australia An Overview* in *Cancer Series Number 71*, A.I.o.H.a. Welfare, Editor. 2012.
7. Roder, D.M., et al., *Age effects on survival from early breast cancer in clinical settings in Australia.* ANZ J Surg, 2012. **82**(7-8): p. 524-8.
8. McPherson, K., C.M. Steel, and J.M. Dixon, *ABC of breast diseases. Breast cancer-epidemiology, risk factors, and genetics.* BMJ, 2000. **321**(7261): p. 624-8.
9. Voduc, K.D., et al., *Breast cancer subtypes and the risk of local and regional relapse.* J Clin Oncol, 2010. **28**(10): p. 1684-91.
10. Guiu, S., et al., *Molecular subclasses of breast cancer: how do we define them? The IMPAKT 2012 Working Group Statement.* Ann Oncol, 2012. **23**(12): p. 2997-3006.
11. Slamon, D., et al., *Adjuvant trastuzumab in HER2-positive breast cancer.* N Engl J Med, 2011. **365**(14): p. 1273-83.
12. Binkley, J.M., et al., *Patient perspectives on breast cancer treatment side effects and the prospective surveillance model for physical rehabilitation for women with breast cancer.* Cancer, 2012. **118**(8 Suppl): p. 2207-16.
13. Kumar, N., et al., *Prevalence of molecular subtypes of invasive breast cancer: A retrospective study.* Med J Armed Forces India, 2015. **71**(3): p. 254-8.
14. Ali, S. and R.C. Coombes, *Endocrine-responsive breast cancer and strategies for combating resistance.* Nat Rev Cancer, 2002. **2**(2): p. 101-12.
15. Musgrove, E.A. and R.L. Sutherland, *Biological determinants of endocrine resistance in breast cancer.* Nat Rev Cancer, 2009. **9**(9): p. 631-43.
16. Liu, C.Y., et al., *Treatment for the endocrine resistant breast cancer: Current options and future perspectives.* J Steroid Biochem Mol Biol, 2017. **172**: p. 166-175.
17. Palmieri, C., et al., *Breast cancer: current and future endocrine therapies.* Mol Cell Endocrinol, 2014. **382**(1): p. 695-723.
18. Leal, F., et al., *Neoadjuvant endocrine therapy for resectable breast cancer: A systematic review and meta-analysis.* Breast, 2015. **24**(4): p. 406-12.
19. Mansouri S., et al., *Challenges of Endocrine Therapy in Breast Cancer*, in *Cancer Genetics and Psychotherapy.* , M.P. (eds), Editor. 2017, Springer, Cham.
20. Group, A.B.C.T. *Breast Cancer Trials*. 2018 22/02/2018]; Available from: https://www.breastcancertrials.org.au/current-clinical-trials.
21. Ozaki, A., T. Tanimoto, and S. Saji, *Palbociclib in Hormone-Receptor-Positive Advanced Breast Cancer.* N Engl J Med, 2015. **373**(17): p. 1672-3.
22. Turner, N.C., C. Huang Bartlett, and M. Cristofanilli, *Palbociclib in Hormone-Receptor-Positive Advanced Breast Cancer.* N Engl J Med, 2015. **373**(17): p. 1672-3.
23. Mangini, N.S., et al., *Palbociclib: A Novel Cyclin-Dependent Kinase Inhibitor for Hormone Receptor-Positive Advanced Breast Cancer.* Ann Pharmacother, 2015. **49**(11): p. 1252-60.

24. Lu, J., *Palbociclib: a first-in-class CDK4/CDK6 inhibitor for the treatment of hormone-receptor positive advanced breast cancer.* J Hematol Oncol, 2015. **8**: p. 98.
25. Turner, N.C., et al., *Palbociclib in Hormone-Receptor-Positive Advanced Breast Cancer.* N Engl J Med, 2015. **373**(3): p. 209-19.
26. Medicine, U.S.N.L.o., *ClinicalTrials.gov*. 2018.
27. McGowan, E.M., et al., *p14ARF Post-Transcriptional Regulation of Nuclear Cyclin D1 in MCF-7 Breast Cancer Cells: Discrimination between a Good and Bad Prognosis?* PLoS ONE, 2012. **7**(7): p. e42246.
28. McGowan, E.M., Y. Lin, and D. Hatoum, *Good guy or bad guy? The duality of wild-type p53 in breast cancer origin, treatment , and recurrence.* Cancers, 2018. **accepted**.
29. Lacroix, M., R.A. Toillon, and G. Leclercq, *p53 and breast cancer, an update.* Endocr Relat Cancer, 2006. **13**(2): p. 293-325.
30. Kruiswijk, F., C.F. Labuschagne, and K.H. Vousden, *p53 in survival, death and metabolic health: a lifeguard with a licence to kill.* Nat Rev Mol Cell Biol, 2015. **16**(7): p. 393-405.
31. Meek, D.W., *Tumour suppression by p53: a role for the DNA damage response?* Nat Rev Cancer, 2009. **9**(10): p. 714-23.
32. Braithwaite, A.W. and C.L. Prives, *p53: more research and more questions.* Cell Death Differ, 2006. **13**(6): p. 877-80.
33. Braithwaite, A.W., J.A. Royds, and P. Jackson, *The p53 story: layers of complexity.* Carcinogenesis, 2005. **26**(7): p. 1161-9.
34. Vousden, K.H. and C. Prives, *Blinded by the Light: The Growing Complexity of p53.* Cell, 2009. **137**(3): p. 413-31.
35. Levine, A.J. and M. Oren, *The first 30 years of p53: growing ever more complex.* Nat Rev Cancer, 2009. **9**(10): p. 749-58.
36. Lane, D.P., *Cancer. p53, guardian of the genome.* Nature, 1992. **358**(6381): p. 15-6.
37. Riley, T., et al., *Transcriptional control of human p53-regulated genes.* Nat Rev Mol Cell Biol, 2008. **9**(5): p. 402-12.
38. Gasco, M., S. Shami, and T. Crook, *The p53 pathway in breast cancer.* Breast Cancer Res, 2002. **4**(2): p. 70-6.
39. Stommel, J.M. and G.M. Wahl, *Accelerated MDM2 auto-degradation induced by DNA-damage kinases is required for p53 activation.* EMBO J, 2004. **23**(7): p. 1547-56.
40. Vogelstein, B., D. Lane, and A.J. Levine, *Surfing the p53 network.* Nature, 2000. **408**(6810): p. 307-10.
41. Oren, M., *Decision making by p53: life, death and cancer.* Cell Death Differ, 2003. **10**(4): p. 431-42.
42. He, G., et al., *Induction of p21 by p53 following DNA damage inhibits both Cdk4 and Cdk2 activities.* Oncogene, 2005. **24**(18): p. 2929-43.
43. Brooks, C.L. and W. Gu, *New insights into p53 activation.* Cell Res, 2010. **20**(6): p. 614-21.
44. Musgrove, E.A., et al., *Cyclin D as a therapeutic target in cancer.* Nat Rev Cancer, 2011. **11**(8): p. 558-72.
45. Abbas, T. and A. Dutta, *p21 in cancer: intricate networks and multiple activities.* Nat Rev Cancer, 2009. **9**(6): p. 400-14.
46. Oda, E., et al., *Noxa, a BH3-only member of the Bcl-2 family and candidate mediator of p53-induced apoptosis.* Science, 2000. **288**(5468): p. 1053-8.
47. Nakano, K. and K.H. Vousden, *PUMA, a novel proapoptotic gene, is induced by p53.* Mol Cell, 2001. **7**(3): p. 683-94.
48. Chipuk, J.E., et al., *Direct activation of Bax by p53 mediates mitochondrial membrane permeabilization and apoptosis.* Science, 2004. **303**(5660): p. 1010-4.
49. Chen, Z., et al., *Crucial role of p53-dependent cellular senescence in suppression of Pten-deficient tumorigenesis.* Nature, 2005. **436**(7051): p. 725-30.

50. Rufini, A., et al., *Senescence and aging: the critical roles of p53.* Oncogene, 2013. **32**(43): p. 5129-43.
51. Xue, W., et al., *Senescence and tumour clearance is triggered by p53 restoration in murine liver carcinomas.* Nature, 2007. **445**(7128): p. 656-60.
52. Qian, Y. and X. Chen, *Senescence regulation by the p53 protein family.* Methods Mol Biol, 2013. **965**: p. 37-61.
53. Itahana, K., et al., *A role for p53 in maintaining and establishing the quiescence growth arrest in human cells.* J Biol Chem, 2002. **277**(20): p. 18206-14.
54. Liu, Y., et al., *p53 regulates hematopoietic stem cell quiescence.* Cell Stem Cell, 2009. **4**(1): p. 37-48.
55. Korotchkina, L.G., et al., *The choice between p53-induced senescence and quiescence is determined in part by the mTOR pathway.* Aging (Albany NY), 2010. **2**(6): p. 344-52.
56. Aguirre-Ghiso, J.A., *Models, mechanisms and clinical evidence for cancer dormancy.* Nat Rev Cancer, 2007. **7**(11): p. 834-46.
57. Mathew, R., V. Karantza-Wadsworth, and E. White, *Role of autophagy in cancer.* Nat Rev Cancer, 2007. **7**(12): p. 961-7.
58. Levy, J.M.M., C.G. Towers, and A. Thorburn, *Targeting autophagy in cancer.* Nat Rev Cancer, 2017. **17**(9): p. 528-542.
59. Maycotte, P. and A. Thorburn, *Targeting autophagy in breast cancer.* World J Clin Oncol, 2014. **5**(3): p. 224-40.
60. Okamoto, K. and N. Kondo-Okamoto, *Mitochondria and autophagy: critical interplay between the two homeostats.* Biochim Biophys Acta, 2012. **1820**(5): p. 595-600.
61. Tasdemir, E., et al., *Regulation of autophagy by cytoplasmic p53.* Nat Cell Biol, 2008. **10**(6): p. 676-87.
62. Maiuri, M.C., et al., *Autophagy regulation by p53.* Curr Opin Cell Biol, 2010. **22**(2): p. 181-5.
63. Proskuryakov, S.Y., A.G. Konoplyannikov, and V.L. Gabai, *Necrosis: a specific form of programmed cell death?* Exp Cell Res, 2003. **283**(1): p. 1-16.
64. Baumann, K., *Cell death: multitasking p53 promotes necrosis.* Nat Rev Mol Cell Biol, 2012. **13**(8): p. 480-1.
65. Galluzzi, L., et al., *Molecular mechanisms of regulated necrosis.* Semin Cell Dev Biol, 2014. **35**: p. 24-32.
66. Vanden Berghe, T., et al., *Regulated necrosis: the expanding network of non-apoptotic cell death pathways.* Nat Rev Mol Cell Biol, 2014. **15**(2): p. 135-47.
67. Su, Z., et al., *Cancer therapy in the necroptosis era.* Cell Death Differ, 2016. **23**(5): p. 748-56.
68. Wu, W., P. Liu, and J. Li, *Necroptosis: an emerging form of programmed cell death.* Crit Rev Oncol Hematol, 2012. **82**(3): p. 249-58.
69. Chan, F.K., N.F. Luz, and K. Moriwaki, *Programmed necrosis in the cross talk of cell death and inflammation.* Annu Rev Immunol, 2015. **33**: p. 79-106.
70. Li, T., et al., *Tumor suppression in the absence of p53-mediated cell-cycle arrest, apoptosis, and senescence.* Cell, 2012. **149**(6): p. 1269-83.
71. Gnanapradeepan, K., et al., *The p53 Tumor Suppressor in the Control of Metabolism and Ferroptosis.* Front Endocrinol (Lausanne), 2018. **9**: p. 124.
72. Dixon, S.J., et al., *Ferroptosis: an iron-dependent form of nonapoptotic cell death.* Cell, 2012. **149**(5): p. 1060-72.
73. Galluzzi, L., J.M. Bravo-San Pedro, and G. Kroemer, *Ferroptosis in p53-dependent oncosuppression and organismal homeostasis.* Cell Death Differ, 2015. **22**(8): p. 1237-8.
74. Chen, Z., et al., *Crucial role of p53-dependent cellular senescence in suppression of Pten-deficient tumorigenesis.* Nature, 2005. **436**(7051): p. 725-730.

75. Xue, W., *Senescence and tumour clearance is triggered by p53 restoration in murine liver carcinomas.* Nature, 2007. **445**: p. 656-660.
76. Itahana, K., et al., *A Role for p53 in Maintaining and Establishing the Quiescence Growth Arrest in Human Cells.* Journal of Biological Chemistry, 2002. **277**(20): p. 18206-18214.
77. Karrison, T.G., D.J. Ferguson, and P. Meier, *Dormancy of Mammary Carcinoma After Mastectomy.* Journal of the National Cancer Institute, 1999. **91**(1): p. 80-85.
78. Tryfonidis, K., et al., *Endocrine treatment in breast cancer: Cure, resistance and beyond.* Cancer Treat Rev, 2016. **50**: p. 68-81.
79. Aguirre-Ghiso, J.A., *Models, mechanisms and clinical evidence for cancer dormancy.* Nature reviews. Cancer, 2007. **7**(11): p. 834-846.
80. Muller, C. and A. Leutz, *Chromatin remodeling in development and differentiation.* Curr Opin Genet Dev, 2001. **11**(2): p. 167-74.
81. Levine, A.J., *The p53 protein plays a central role in the mechanism of action of epigentic drugs that alter the methylation of cytosine residues in DNA.* Oncotarget, 2017. **8**(5): p. 7228-7230.
82. Levine, A.J. and S.L. Berger, *The interplay between epigenetic changes and the p53 protein in stem cells.* Genes Dev, 2017. **31**(12): p. 1195-1201.
83. Tovy, A., et al., *p53 is essential for DNA methylation homeostasis in naive embryonic stem cells, and its loss promotes clonal heterogeneity.* Genes Dev, 2017. **31**(10): p. 959-972.
84. Jerry, D.J., K.A. Dunphy, and M.J. Hagen, *Estrogens, regulation of p53 and breast cancer risk: a balancing act.* Cell Mol Life Sci, 2010. **67**(7): p. 1017-23.
85. Barton, M., J. Santucci-Pereira, and J. Russo, *Molecular pathways involved in pregnancy-induced prevention against breast cancer.* Front Endocrinol (Lausanne), 2014. **5**: p. 213.
86. Vousden, K.H. and K.M. Ryan, *p53 and metabolism.* Nat Rev Cancer, 2009. **9**(10): p. 691-700.
87. Liu, J., et al., *Tumor suppressor p53 and its mutants in cancer metabolism.* Cancer Lett, 2015. **356**(2 Pt A): p. 197-203.
88. Berkers, Celia R., et al., *Metabolic Regulation by p53 Family Members.* Cell Metabolism. **18**(5): p. 617-633.
89. Matoba, S., et al., *p53 regulates mitochondrial respiration.* Science, 2006. **312**(5780): p. 1650-3.
90. Kruiswijk, F., C.F. Labuschagne, and K.H. Vousden, *p53 in survival, death and metabolic health: a lifeguard with a licence to kill.* Nature reviews Molecular cell biology, 2015. **16**(7): p. 393-405.
91. Hsu, P.P. and D.M. Sabatini, *Cancer cell metabolism: Warburg and beyond.* Cell, 2008. **134**(5): p. 703-7.
92. Koppenol, W.H., P.L. Bounds, and C.V. Dang, *Otto Warburg's contributions to current concepts of cancer metabolism.* Nat Rev Cancer, 2011. **11**(5): p. 325-337.
93. Vander Heiden, M.G., L.C. Cantley, and C.B. Thompson, *Understanding the Warburg effect: the metabolic requirements of cell proliferation.* Science, 2009. **324**(5930): p. 1029-33.
94. Hatoum, D. and E.M. McGowan, *Recent advances in the use of metformin: can treating diabetes prevent breast cancer?* Biomed Res Int, 2015. **2015**: p. 548436.
95. McGowan, E.M., et al., *Evaluation of Cell Cycle Arrest in Estrogen Responsive MCF-7 Breast Cancer Cells: Pitfalls of the MTS Assay.* PLoS ONE, 2011. **6**(6): p. e20623.
96. Hatoum, D., et al., *Annexin/S100A Protein Family Regulation through p14ARF-p53 Activation: A Role in Cell Survival and Predicting Treatment Outcomes in Breast Cancer.* PLoS One, 2017. **12**(1): p. e0169925.

97. Ryan, K.M., *p53 and autophagy in cancer: guardian of the genome meets guardian of the proteome.* Eur J Cancer, 2011. **47**(1): p. 44-50.
98. Aylon, Y. and M. Oren, *The Paradox of p53: What, How, and Why?* Cold Spring Harb Perspect Med, 2016. **6**(10).
99. Levine, A.J., et al., *The p53 family: guardians of maternal reproduction.* Nat Rev Mol Cell Biol, 2011. **12**(4): p. 259-65.
100. Gomes, A.S., et al., *p53 and glucose metabolism: an orchestra to be directed in cancer therapy.* Pharmacol Res, 2018. **131**: p. 75-86.
101. Itahana, Y. and K. Itahana, *Emerging Roles of p53 Family Members in Glucose Metabolism.* Int J Mol Sci, 2018. **19**(3).
102. Parrales, A. and T. Iwakuma, *p53 as a Regulator of Lipid Metabolism in Cancer.* Int J Mol Sci, 2016. **17**(12).
103. Hainaut, P., *p53 in metabolism, aging and cancer.* Ann Dermatol Venereol, 2014. **141**(12 Suppl): p. S200-1.
104. Jiang, P., W. Du, and X. Yang, *p53 and regulation of tumor metabolism.* J Carcinog, 2013. **12**: p. 21.
105. Sen, N., Y.K. Satija, and S. Das, *p53 and metabolism: old player in a new game.* Transcription, 2012. **3**(3): p. 119-23.
106. Fields, J., et al., *How does p53 regulate mitochondrial respiration?* IUBMB Life, 2007. **59**(10): p. 682-4.
107. Ma, W., et al., *A pivotal role for p53: balancing aerobic respiration and glycolysis.* J Bioenerg Biomembr, 2007. **39**(3): p. 243-6.
108. Cheung, E.C. and K.H. Vousden, *The role of p53 in glucose metabolism.* Curr Opin Cell Biol, 2010. **22**(2): p. 186-91.
109. Lin, T. and Y. Lin, *p53 switches off pluripotency on differentiation.* Stem Cell Res Ther, 2017. **8**(1): p. 44.
110. Zhang, M., et al., *Synergistic Rescue of Nonsense Mutant Tumor Suppressor p53 by Combination Treatment with Aminoglycosides and Mdm2 Inhibitors.* Front Oncol, 2017. **7**: p. 323.
111. Bykov, V.J.N., et al., *Targeting mutant p53 for efficient cancer therapy.* Nat Rev Cancer, 2018. **18**(2): p. 89-102.
112. Sayeed, A., et al., *Estrogen receptor alpha inhibits p53-mediated transcriptional repression: implications for the regulation of apoptosis.* Cancer Res, 2007. **67**(16): p. 7746-55.
113. Bertheau, P., et al., *TP53 status and response to chemotherapy in breast cancer.* Pathobiology, 2008. **75**(2): p. 132-9.
114. Bertheau, P., et al., *p53 in breast cancer subtypes and new insights into response to chemotherapy.* Breast, 2013. **22 Suppl 2**: p. S27-9.
115. Miller, L.D., et al., *An expression signature for p53 status in human breast cancer predicts mutation status, transcriptional effects, and patient survival.* Proc Natl Acad Sci U S A, 2005. **102**(38): p. 13550-5.
116. Geisler, S., et al., *TP53 gene mutations predict the response to neoadjuvant treatment with 5-fluorouracil and mitomycin in locally advanced breast cancer.* Clin Cancer Res, 2003. **9**(15): p. 5582-8.
117. Avery-Kiejda, K.A., et al., *The relative mRNA expression of p53 isoforms in breast cancer is associated with clinical features and outcome.* Carcinogenesis, 2014. **35**(3): p. 586-96.
118. Benz, C.C., *Impact of aging on the biology of breast cancer.* Crit Rev Oncol Hematol, 2008. **66**(1): p. 65-74.

119. Yamamoto, M., et al., *p53 accumulation is a strong predictor of recurrence in estrogen receptor-positive breast cancer patients treated with aromatase inhibitors.* Cancer Sci, 2014. **105**(1): p. 81-8.
120. Konduri, S.D., et al., *Mechanisms of estrogen receptor antagonism toward p53 and its implications in breast cancer therapeutic response and stem cell regulation.* Proc Natl Acad Sci U S A, 2010. **107**(34): p. 15081-6.
121. Liu, W., et al., *Estrogen receptor-alpha binds p53 tumor suppressor protein directly and represses its function.* J Biol Chem, 2006. **281**(15): p. 9837-40.
122. Liu, W., et al., *Disruption of estrogen receptor alpha-p53 interaction in breast tumors: a novel mechanism underlying the anti-tumor effect of radiation therapy.* Breast Cancer Res Treat, 2009. **115**(1): p. 43-50.
123. Holst, F., et al., *Estrogen receptor alpha (ESR1) gene amplification is frequent in breast cancer.* Nat Genet, 2007. **39**(5): p. 655-60.
124. Fernandez-Cuesta, L., et al., *Estrogen levels act as a rheostat on p53 levels and modulate p53-dependent responses in breast cancer cell lines.* Breast Cancer Res Treat, 2011. **125**(1): p. 35-42.
125. Berger, C.E., et al., *p53, a target of estrogen receptor (ER) alpha, modulates DNA damage-induced growth suppression in ER-positive breast cancer cells.* J Biol Chem, 2012. **287**(36): p. 30117-27.
126. Bailey, S.T., et al., *Estrogen receptor prevents p53-dependent apoptosis in breast cancer.* Proc Natl Acad Sci U S A, 2012. **109**(44): p. 18060-5.
127. Lu, W. and B.S. Katzenellenbogen, *Estrogen Receptor-beta Modulation of the ERalpha-p53 Loop Regulating Gene Expression, Proliferation, and Apoptosis in Breast Cancer.* Horm Cancer, 2017. **8**(4): p. 230-242.
128. Yi, Y., et al., *p19ARF determines the balance between normal cell proliferation rate and apoptosis during mammary gland development.* Mol Biol Cell, 2004. **15**(5): p. 2302-11.
129. Sharpless, N.E., et al., *Loss of p16Ink4a with retention of p19Arf predisposes mice to tumorigenesis.* Nature, 2001. **413**(6851): p. 86-91.
130. Salazar-Roa, M. and M. Malumbres, *Fueling the Cell Division Cycle.* Trends Cell Biol, 2017. **27**(1): p. 69-81.
131. Carr-Wilkinson, J., et al., *High Frequency of p53/MDM2/p14ARF Pathway Abnormalities in Relapsed Neuroblastoma.* Clin Cancer Res, 2010. **16**(4): p. 1108-18.
132. D'Amico, M., et al., *The inhibitor of cyclin-dependent kinase 4a/alternative reading frame (INK4a/ARF) locus encoded proteins p16INK4a and p19ARF repress cyclin D1 transcription through distinct cis elements.* Cancer Res, 2004. **64**(12): p. 4122-30.
133. Masuda, S., *Breast cancer pathology: the impact of molecular taxonomy on morphological taxonomy.* Pathol Int, 2012. **62**(5): p. 295-302.
134. Shan, M., et al., *P16 and p53 play distinct roles in different subtypes of breast cancer.* PLoS One, 2013. **8**(10): p. e76408.
135. Clark, P.A., S. Llanos, and G. Peters, *Multiple interacting domains contribute to p14ARF mediated inhibition of MDM2.* Oncogene, 2002. **21**(29): p. 4498-507.
136. Michael, D. and M. Oren, *The p53-Mdm2 module and the ubiquitin system.* Semin Cancer Biol, 2003. **13**(1): p. 49-58.
137. Sherr, C.J. and F. McCormick, *The RB and p53 pathways in cancer.* Cancer Cell, 2002. **2**(2): p. 103-12.
138. Inoue, K. and E.A. Fry, *Aberrant splicing of the DMP1-ARF-MDM2-p53 pathway in cancer.* Int J Cancer, 2016. **139**(1): p. 33-41.
139. Sherr, C.J., *Divorcing ARF and p53: an unsettled case.* Nat Rev Cancer, 2006. **6**(9): p. 663-73.

140. Eymin, B., et al., *p14ARF induces G2 arrest and apoptosis independently of p53 leading to regression of tumours established in nude mice.* Oncogene, 2003. **22**(12): p. 1822-35.
141. Qi, Y., et al., *p19ARF directly and differentially controls the functions of c-Myc independently of p53.* Nature, 2004. **431**(7009): p. 712-7.
142. Yarbrough, W.G., et al., *Human tumor suppressor ARF impedes S-phase progression independent of p53.* Cancer Res, 2002. **62**(4): p. 1171-7.
143. Silva, J., et al., *Concomitant expression of p16INK4a and p14ARF in primary breast cancer and analysis of inactivation mechanisms.* J Pathol, 2003. **199**(3): p. 289-97.
144. Burgess, A., et al., *Clinical Overview of MDM2/X-Targeted Therapies.* Front Oncol, 2016. **6**: p. 7.
145. Crane, E.K., et al., *Nutlin-3a: A Potential Therapeutic Opportunity for TP53 Wild-Type Ovarian Carcinomas.* PLoS One, 2015. **10**(8): p. e0135101.
146. Patton, J.T., et al., *Levels of HdmX expression dictate the sensitivity of normal and transformed cells to Nutlin-3.* Cancer Res, 2006. **66**(6): p. 3169-76.
147. Shangary, S. and S. Wang, *Small-molecule inhibitors of the MDM2-p53 protein-protein interaction to reactivate p53 function: a novel approach for cancer therapy.* Annu Rev Pharmacol Toxicol, 2009. **49**: p. 223-41.
148. Ho, G.H., et al., *Genetic alterations of the p14ARF -hdm2-p53 regulatory pathway in breast carcinoma.* Breast Cancer Res Treat, 2001. **65**(3): p. 225-32.
149. Ali, S., L. Buluwela, and R.C. Coombes, *Antiestrogens and their therapeutic applications in breast cancer and other diseases.* Annu Rev Med, 2011. **62**: p. 217-32.
150. Soule, H.D., et al., *A human cell line from a pleural effusion derived from a breast carcinoma.* J Natl Cancer Inst, 1973. **51**(5): p. 1409-16.
151. Niforou, K.M., et al., *The proteome profile of the human osteosarcoma U2OS cell line.* Cancer Genomics Proteomics, 2008. **5**(1): p. 63-78.
152. McGowan, E.M. and C.L. Clarke, *Effect of overexpression of progesterone receptor A on endogenous progestin-sensitive endpoints in breast cancer cells.* Mol Endocrinol, 1999. **13**(10): p. 1657-71.
153. Gallagher, S., R.F. Kefford, and H. Rizos, *Enforced expression of p14ARF induces p53-dependent cell cycle arrest but not apoptosis.* Cell Cycle, 2005. **4**(3): p. 465-72.
154. Packer, L.M., et al., *Gene expression profiling in melanoma identifies novel downstream effectors of p14ARF.* Int J Cancer, 2007. **121**(4): p. 784-90.
155. Yagoub, D., et al., *Sphingosine kinase 1 isoform-specific interactions in breast cancer.* Mol Endocrinol, 2014. **28**(11): p. 1899-915.
156. Livak, K.J. and T.D. Schmittgen, *Analysis of relative gene expression data using real-time quantitative PCR and the 2(-Delta Delta C(T)) Method.* Methods, 2001. **25**(4): p. 402-8.
157. Strauss, M.P., et al., *3D-SIM super resolution microscopy reveals a bead-like arrangement for FtsZ and the division machinery: implications for triggering cytokinesis.* PLoS Biol, 2012. **10**(9): p. e1001389.
158. Gustafsson, M.G., et al., *Three-dimensional resolution doubling in wide-field fluorescence microscopy by structured illumination.* Biophys J, 2008. **94**(12): p. 4957-70.
159. Schermelleh, L., et al., *Subdiffraction multicolor imaging of the nuclear periphery with 3D structured illumination microscopy.* Science, 2008. **320**(5881): p. 1332-6.
160. Kinzler, K.W. and B. Vogelstein, *Cancer therapy meets p53.* N Engl J Med, 1994. **331**(1): p. 49-50.
161. Gottlieb, E. and K.H. Vousden, *p53 regulation of metabolic pathways.* Cold Spring Harb Perspect Biol, 2010. **2**(4): p. a001040.

162. Silwal-Pandit, L., et al., *TP53 mutation spectrum in breast cancer is subtype specific and has distinct prognostic relevance.* Clin Cancer Res, 2014. **20**(13): p. 3569-80.
163. Lu, J., et al., *Reactivation of p53 by MDM2 Inhibitor MI-77301 for the Treatment of Endocrine-Resistant Breast Cancer.* Mol Cancer Ther, 2016. **15**(12): p. 2887-2893.
164. Medina, D., et al., *Mechanisms of hormonal prevention of breast cancer.* Ann N Y Acad Sci, 2001. **952**: p. 23-35.
165. Chen, J., J. Lin, and A.J. Levine, *Regulation of transcription functions of the p53 tumor suppressor by the mdm-2 oncogene.* Mol Med, 1995. **1**(2): p. 142-52.
166. Agrawal, A., et al., *Regulation of the p14ARF-Mdm2-p53 pathway: an overview in breast cancer.* Exp Mol Pathol, 2006. **81**(2): p. 115-22.
167. Llanos, S., et al., *Stabilization of p53 by p14ARF without relocation of MDM2 to the nucleolus.* Nat Cell Biol, 2001. **3**(5): p. 445-52.
168. Bates, S., et al., *p14ARF links the tumour suppressors RB and p53.* Nature, 1998. **395**(6698): p. 124-5.
169. Brooks, S.C., E.R. Locke, and H.D. Soule, *Estrogen receptor in a human cell line (MCF-7) from breast carcinoma.* J Biol Chem, 1973. **248**(17): p. 6251-3.
170. Barnes, D. and G. Sato, *Growth of a human mammary tumour cell line in a serum-free medium.* Nature, 1979. **281**(5730): p. 388-9.
171. Comsa, S., A.M. Cimpean, and M. Raica, *The Story of MCF-7 Breast Cancer Cell Line: 40 years of Experience in Research.* Anticancer Res, 2015. **35**(6): p. 3147-54.
172. PRIDE, *PRIDE Archive - proteomics data repository*. 2018.
173. Gatlin, C.L., et al., *Protein identification at the low femtomole level from silver-stained gels using a new fritless electrospray interface for liquid chromatography-microspray and nanospray mass spectrometry.* Anal Biochem, 1998. **263**(1): p. 93-101.
174. Vizcaino, J.A., et al., *2016 update of the PRIDE database and its related tools.* Nucleic Acids Res, 2016. **44**(22): p. 11033.
175. Yeh, G.C., et al., *The effect of pyrroline-5-carboxylic acid on nucleotide metabolism in erythrocytes from normal and glucose-6-phosphate dehydrogenase-deficient subjects.* J Biol Chem, 1984. **259**(9): p. 5454-8.
176. Stelzer, C., et al., *Expression profile of Papss2 (3'-phosphoadenosine 5'-phosphosulfate synthase 2) during cartilage formation and skeletal development in the mouse embryo.* Dev Dyn, 2007. **236**(5): p. 1313-8.
177. Cai, K., et al., *Human Mitochondrial Ferredoxin 1 (FDX1) and Ferredoxin 2 (FDX2) Both Bind Cysteine Desulfurase and Donate Electrons for Iron-Sulfur Cluster Biosynthesis.* Biochemistry, 2017. **56**(3): p. 487-499.
178. Kwiatkowski, D.J., *Functions of gelsolin: motility, signaling, apoptosis, cancer.* Curr Opin Cell Biol, 1999. **11**(1): p. 103-8.
179. Whitfield, M.L., et al., *Common markers of proliferation.* Nat Rev Cancer, 2006. **6**(2): p. 99-106.
180. Sahebjam, S., et al., *Ki 67 is a major, but not the sole determinant of Oncotype Dx recurrence score.* Br J Cancer, 2011. **105**(9): p. 1342-5.
181. Vanyushin, B.F., *Enzymatic DNA methylation is an epigenetic control for genetic functions of the cell.* Biochemistry (Mosc), 2005. **70**(5): p. 488-99.
182. Kastan, M.B. and J. Bartek, *Cell-cycle checkpoints and cancer.* Nature, 2004. **432**(7015): p. 316-23.
183. Hatle, K.M., et al., *MCJ/DnaJC15, an endogenous mitochondrial repressor of the respiratory chain that controls metabolic alterations.* Mol Cell Biol, 2013. **33**(11): p. 2302-14.
184. Stingl, J. and C. Caldas, *Molecular heterogeneity of breast carcinomas and the cancer stem cell hypothesis.* Nat Rev Cancer, 2007. **7**(10): p. 791-9.

185. Clarke, R., J.J. Tyson, and J.M. Dixon, *Endocrine resistance in breast cancer--An overview and update.* Mol Cell Endocrinol, 2015. **418 Pt 3**: p. 220-34.
186. Xia, L., A. Paik, and J.J. Li, *p53 activation in chronic radiation-treated breast cancer cells: regulation of MDM2/p14ARF.* Cancer Res, 2004. **64**(1): p. 221-8.
187. Jackson, J.G., et al., *p53-mediated senescence impairs the apoptotic response to chemotherapy and clinical outcome in breast cancer.* Cancer Cell, 2012. **21**(6): p. 793-806.
188. Kaufmann, S.H. and W.C. Earnshaw, *Induction of apoptosis by cancer chemotherapy.* Exp Cell Res, 2000. **256**(1): p. 42-9.
189. Balmer, M.T., et al., *Doxorubicin and 5-fluorouracil induced accumulation and transcriptional activity of p53 are independent of the phosphorylation at serine 15 in MCF-7 breast cancer cells.* Cancer Biol Ther, 2014. **15**(8): p. 1000-12.
190. Pistritto, G., et al., *Apoptosis as anticancer mechanism: function and dysfunction of its modulators and targeted therapeutic strategies.* Aging (Albany NY), 2016. **8**(4): p. 603-19.
191. Lehmann-Che, J., et al., *[Exquisite sensitivity of TP53 mutant breast cancers to dose-dense chemotherapy].* Med Sci (Paris), 2007. **23**(11): p. 1021-3.
192. Bertheau, P., et al., *Exquisite sensitivity of TP53 mutant and basal breast cancers to a dose-dense epirubicin-cyclophosphamide regimen.* PLoS Med, 2007. **4**(3): p. e90.
193. Bertheau, P., et al., *Effect of mutated TP53 on response of advanced breast cancers to high-dose chemotherapy.* Lancet, 2002. **360**(9336): p. 852-4.
194. Ong, S.E. and M. Mann, *A practical recipe for stable isotope labeling by amino acids in cell culture (SILAC).* Nat Protoc, 2006. **1**(6): p. 2650-60.
195. Gerke, V. and S.E. Moss, *Annexins: from structure to function.* Physiol Rev, 2002. **82**(2): p. 331-71.
196. Mussunoor, S. and G.I. Murray, *The role of annexins in tumour development and progression.* J Pathol, 2008. **216**(2): p. 131-40.
197. Ahn, S.H., et al., *Differential expression of annexin I in human mammary ductal epithelial cells in normal and benign and malignant breast tissues.* Clin Exp Metastasis, 1997. **15**(2): p. 151-6.
198. Yom, C.K., et al., *Clinical significance of annexin A1 expression in breast cancer.* J Breast Cancer, 2011. **14**(4): p. 262-8.
199. Ang, E.Z., et al., *Annexin-1 regulates growth arrest induced by high levels of estrogen in MCF-7 breast cancer cells.* Mol Cancer Res, 2009. **7**(2): p. 266-74.
200. Cao, Y., et al., *Loss of annexin A1 expression in breast cancer progression.* Appl Immunohistochem Mol Morphol, 2008. **16**(6): p. 530-4.
201. Bhardwaj, A., et al., *Annexin A1 Preferentially Predicts Poor Prognosis of Basal-Like Breast Cancer Patients by Activating mTOR-S6 Signaling.* PLoS One, 2015. **10**(5): p. e0127678.
202. Sobral-Leite, M., et al., *Annexin A1 expression in a pooled breast cancer series: association with tumor subtypes and prognosis.* BMC Med, 2015. **13**: p. 156.
203. Okano, M., et al., *Upregulated Annexin A1 promotes cellular invasion in triple-negative breast cancer.* Oncol Rep, 2015. **33**(3): p. 1064-70.
204. Sharma, M.R., et al., *Angiogenesis-associated protein annexin II in breast cancer: selective expression in invasive breast cancer and contribution to tumor invasion and progression.* Exp Mol Pathol, 2006. **81**(2): p. 146-56.
205. Wang, T., et al., *Anxa2 binds to STAT3 and promotes epithelial to mesenchymal transition in breast cancer cells.* Oncotarget, 2015. **6**(31): p. 30975-92.
206. Hu, H., J. Zhao, and M. Zhang, *Expression of Annexin A2 and Its Correlation With Drug Resistance and Recurrence of Bladder Cancer.* Technol Cancer Res Treat, 2016. **15**(6): p. NP61-NP68.

207. Jaiswal, J.K. and J. Nylandsted, *S100 and annexin proteins identify cell membrane damage as the Achilles heel of metastatic cancer cells.* Cell Cycle, 2015. **14**(4): p. 502-9.
208. Roderick, H.L. and S.J. Cook, *Ca2+ signalling checkpoints in cancer: remodelling Ca2+ for cancer cell proliferation and survival.* Nat Rev Cancer, 2008. **8**(5): p. 361-75.
209. Szklarczyk, D., et al., *STRING v10: protein-protein interaction networks, integrated over the tree of life.* Nucleic Acids Res, 2015. **43**(Database issue): p. D447-52.
210. Zuberi, K., et al., *GeneMANIA prediction server 2013 update.* Nucleic Acids Res, 2013. **41**(Web Server issue): p. W115-22.
211. Gyorffy, B., et al., *An online survival analysis tool to rapidly assess the effect of 22,277 genes on breast cancer prognosis using microarray data of 1,809 patients.* Breast Cancer Res Treat, 2010. **123**(3): p. 725-31.
212. Mann, M., *Functional and quantitative proteomics using SILAC.* Nat Rev Mol Cell Biol, 2006. **7**(12): p. 952-8.
213. van de Graaf, S.F., et al., *Functional expression of the epithelial Ca(2+) channels (TRPV5 and TRPV6) requires association of the S100A10-annexin 2 complex.* EMBO J, 2003. **22**(7): p. 1478-87.
214. Piljic, A. and C. Schultz, *Annexin A4 self-association modulates general membrane protein mobility in living cells.* Mol Biol Cell, 2006. **17**(7): p. 3318-28.
215. Harder, T. and V. Gerke, *The subcellular distribution of early endosomes is affected by the annexin II2p11(2) complex.* J Cell Biol, 1993. **123**(5): p. 1119-32.
216. Benaud, C., et al., *AHNAK interaction with the annexin 2/S100A10 complex regulates cell membrane cytoarchitecture.* J Cell Biol, 2004. **164**(1): p. 133-44.
217. Liu, Y., H.K. Myrvang, and L.V. Dekker, *Annexin A2 complexes with S100 proteins: structure, function and pharmacological manipulation.* Br J Pharmacol, 2015. **172**(7): p. 1664-76.
218. Wang, C.Y. and C.F. Lin, *Annexin A2: its molecular regulation and cellular expression in cancer development.* Dis Markers, 2014. **2014**: p. 308976.
219. Deng, S., et al., *Annexin A1, A2, A4 and A5 play important roles in breast cancer, pancreatic cancer and laryngeal carcinoma, alone and/or synergistically.* Oncol Lett, 2013. **5**(1): p. 107-112.
220. Hedhli, N., et al., *The annexin A2/S100A10 system in health and disease: emerging paradigms.* J Biomed Biotechnol, 2012. **2012**: p. 406273.
221. Cmoch, A., et al., *S100A proteins in propagation of a calcium signal in norm and pathology.* Postepy Biochem, 2012. **58**(4): p. 429-36.
222. Giorgi, C., M. Bonora, and P. Pinton, *Inside the tumor: p53 modulates calcium homeostasis.* Cell Cycle, 2015. **14**(7): p. 933-4.
223. Gurpinar, E. and K.H. Vousden, *Hitting cancers' weak spots: vulnerabilities imposed by p53 mutation.* Trends Cell Biol, 2015. **25**(8): p. 486-95.
224. Menaa, C., et al., *Annexin II increases osteoclast formation by stimulating the proliferation of osteoclast precursors in human marrow cultures.* J Clin Invest, 1999. **103**(11): p. 1605-13.
225. Takahashi, S., et al., *Cloning and identification of annexin II as an autocrine/paracrine factor that increases osteoclast formation and bone resorption.* J Biol Chem, 1994. **269**(46): p. 28696-701.
226. Theill, L.E., W.J. Boyle, and J.M. Penninger, *RANK-L and RANK: T cells, bone loss, and mammalian evolution.* Annu Rev Immunol, 2002. **20**: p. 795-823.
227. Arii, Y., K. Butsusihta, and S. Fukuoka, *Role of calcium-binding sites in calcium-dependent membrane association of annexin A4.* Biosci Biotechnol Biochem, 2015. **79**(6): p. 978-85.
228. Alvarez-Guaita, A., et al., *Evidence for annexin A6-dependent plasma membrane remodelling of lipid domains.* Br J Pharmacol, 2015. **172**(7): p. 1677-90.

229. Stewart, T.A., K.T. Yapa, and G.R. Monteith, *Altered calcium signaling in cancer cells.* Biochim Biophys Acta, 2015. **1848**(10 Pt B): p. 2502-11.
230. Jaiswal, J.K., et al., *S100A11 is required for efficient plasma membrane repair and survival of invasive cancer cells.* Nat Commun, 2014. **5**: p. 3795.
231. Bieging, K.T., S.S. Mello, and L.D. Attardi, *Unravelling mechanisms of p53-mediated tumour suppression.* Nat Rev Cancer, 2014. **14**(5): p. 359-70.
232. Menendez, D., A. Inga, and M.A. Resnick, *The expanding universe of p53 targets.* Nat Rev Cancer, 2009. **9**(10): p. 724-37.
233. Agrawal, A., et al., *Regulation of the p14ARF-Mdm2-p53 pathway: An overview in breast cancer.* Experimental and Molecular Pathology, 2006. **81**(2): p. 115-122.
234. Llanos, S., et al., *Stabilization of p53 by p14ARF without relocation of MDM2 to the nucleolus.* Nat Cell Biol, 2001. **3**(5): p. 445-452.
235. Bates, S., et al., *p14ARF links the tumour suppressors RB and p53.* Nature, 1998. **395**(6698): p. 124-125.
236. Sivaraman, L., et al., *p53 is a potential mediator of pregnancy and hormone-induced resistance to mammary carcinogenesis.* Proc Natl Acad Sci U S A, 2001. **98**(22): p. 12379-84.
237. Das, M. and S.K. Sahoo, *Epithelial cell adhesion molecule targeted nutlin-3a loaded immunonanoparticles for cancer therapy.* Acta Biomater, 2011. **7**(1): p. 355-69.
238. Huang, Y., et al., *Enhanced tumor suppression by a p14ARF/p53 bicistronic adenovirus through increased p53 protein translation and stability.* Cancer Res, 2003. **63**(13): p. 3646-53.
239. Williams, G.H. and K. Stoeber, *The cell cycle and cancer.* J Pathol, 2012. **226**(2): p. 352-64.
240. DeBerardinis, R.J., et al., *The Biology of Cancer: Metabolic Reprogramming Fuels Cell Growth and Proliferation.* Cell Metabolism. **7**(1): p. 11-20.
241. Pavlova, N.N. and C.B. Thompson, *The Emerging Hallmarks of Cancer Metabolism.* Cell Metab, 2016. **23**(1): p. 27-47.
242. Cairns, R.A. and T.W. Mak, *The current state of cancer metabolism.* Nat Rev Cancer, 2016. **16**(10): p. 613-614.
243. Cairns, R.A., I.S. Harris, and T.W. Mak, *Regulation of cancer cell metabolism.* Nat Rev Cancer, 2011. **11**(2): p. 85-95.
244. Hay, N., *Reprogramming glucose metabolism in cancer: can it be exploited for cancer therapy?* Nat Rev Cancer, 2016. **16**(10): p. 635-649.
245. Szablewski, L., *Expression of glucose transporters in cancers.* Biochimica et Biophysica Acta (BBA) - Reviews on Cancer, 2013. **1835**(2): p. 164-169.
246. Hanahan, D. and R.A. Weinberg, *Hallmarks of cancer: the next generation.* Cell, 2011. **144**(5): p. 646-74.
247. !!! INVALID CITATION !!! [85, 242].
248. Shen, L., et al., *The fundamental role of the p53 pathway in tumor metabolism and its implication in tumor therapy.* Clin Cancer Res, 2012. **18**(6): p. 1561-7.
249. Saleem, A. and D.A. Hood, *Acute exercise induces tumour suppressor protein p53 translocation to the mitochondria and promotes a p53-Tfam-mitochondrial DNA complex in skeletal muscle.* J Physiol, 2013. **591**(Pt 14): p. 3625-36.
250. Kondoh, H., et al., *Glycolytic enzymes can modulate cellular life span.* Cancer Res, 2005. **65**(1): p. 177-85.
251. Yoshida, Y., et al., *P53 physically interacts with mitochondrial transcription factor A and differentially regulates binding to damaged DNA.* Cancer Res, 2003. **63**(13): p. 3729-34.
252. Westermann, B., *Bioenergetic role of mitochondrial fusion and fission.* Biochimica et Biophysica Acta (BBA) - Bioenergetics, 2012. **1817**(10): p. 1833-1838.

253. Westermann, B., *Mitochondrial fusion and fission in cell life and death.* Nat Rev Mol Cell Biol, 2010. **11**(12): p. 872-84.
254. Wai, T. and T. Langer, *Mitochondrial Dynamics and Metabolic Regulation.* Trends in Endocrinology & Metabolism. **27**(2): p. 105-117.
255. Youle, R.J. and A.M. van der Bliek, *Mitochondrial fission, fusion, and stress.* Science, 2012. **337**(6098): p. 1062-5.
256. Wang, W., et al., *Mitofusin-2 is a novel direct target of p53.* Biochem Biophys Res Commun, 2010. **400**(4): p. 587-92.
257. Saleem, A., P.J. Adhihetty, and D.A. Hood, *Role of p53 in mitochondrial biogenesis and apoptosis in skeletal muscle.* Physiol Genomics, 2009. **37**(1): p. 58-66.
258. Zamponi, N., et al., *Mitochondrial network complexity emerges from fission/fusion dynamics.* Sci Rep, 2018. **8**(1): p. 363.
259. Seo, A.Y., et al., *New insights into the role of mitochondria in aging: mitochondrial dynamics and more.* J Cell Sci, 2010. **123**(Pt 15): p. 2533-42.
260. Garrido, C., et al., *Mechanisms of cytochrome c release from mitochondria.* Cell Death Differ, 2006. **13**(9): p. 1423-33.
261. Yang, J., et al., *Prevention of apoptosis by Bcl-2: release of cytochrome c from mitochondria blocked.* Science, 1997. **275**(5303): p. 1129-32.
262. Larsson, N.G., et al., *Mitochondrial transcription factor A is necessary for mtDNA maintenance and embryogenesis in mice.* Nat Genet, 1998. **18**(3): p. 231-6.
263. Larsson, N.G., G.S. Barsh, and D.A. Clayton, *Structure and chromosomal localization of the mouse mitochondrial transcription factor A gene (Tfam).* Mamm Genome, 1997. **8**(2): p. 139-40.
264. Falcon, S. and R. Gentleman, *Using GOstats to test gene lists for GO term association.* Bioinformatics, 2007. **23**(2): p. 257-8.
265. Siekevitz, P., *Powerhouse of the cell.* Scientific American, 1957. **197**(1): p. 14.
266. Martinez-Outschoorn, U.E., et al., *Cancer metabolism: a therapeutic perspective.* Nat Rev Clin Oncol, 2016. **advance online publication**.
267. Shadel, G.S., *Expression and maintenance of mitochondrial DNA: new insights into human disease pathology.* Am J Pathol, 2008. **172**(6): p. 1445-56.
268. Park, J.Y., et al., *p53 improves aerobic exercise capacity and augments skeletal muscle mitochondrial DNA content.* Circ Res, 2009. **105**(7): p. 705-12, 11 p following 712.
269. Park, J.H., et al., *p53 as guardian of the mitochondrial genome.* FEBS Lett, 2016. **590**(7): p. 924-34.